THE MEASUREMENT OF TEMPERATURE DEPENDENT THERMAL NEUTRONS IN WATER USING A CRYSTAL DETECTOR.

by

Robert Gordon Bennett

LIBRARY
NAVAL POSTGRADUATE SCHOOL
MONTEREY, CALIF. 93940

United States
Naval Postgraduate School

THESIS

THE MEASUREMENT OF TEMPERATURE DEPENDENT
THERMAL NEUTRONS IN WATER USING A CRYSTAL DETECTOR

by

Robert Gordon Bennett

December 1970

This document has been approved for public release and sale; its distribution is unlimited.

T137261

The Measurement of Temperature Dependent Thermal Neutrons in Water Using a Crystal Detector

by

Robert Gordon Bennett
Lieutenant Commander, United States Navy
B.S., Purdue University, 1963

Submitted in partial fulfillment of the
requirements for the degree of

MASTER OF SCIENCE IN MECHANICAL ENGINEERING

from the

NAVAL POSTGRADUATE SCHOOL
December 1970

B377
C.1

STGRADUATE SCHOOL
, CALIF. 93940

ABSTRACT

This research was concerned with the temperature dependence of thermal neutron flux. In view of the excellent neutron detection capability exhibited by the Lithium Iodide Europium enriched crystal this phosphor was utilized for the investigation. A miniature crystal (4mm x 4mm) and a flexible light pipe combination were used to determine the neutron spatial distribution as a function of temperature using a Pu-Be source in a light-water medium.

A separate experimental investigation, with Indium foils and activation analysis, was used to determine the temperature dependence of thermal neutron flux under the same experimental conditions as the crystal.

A theoretical analysis was also conducted using Two-Group theory to obtain an expression for thermal flux with spatial and temperature dependent parameters.

The results of the research indicates that the thermal neutron flux is temperature dependent in the region of temperature investigated (77° - 168° F). The experimental results verify the increasing trend of flux magnitude with increasing temperature, as predicted by the Two-Group solution.

TABLE OF CONTENTS

I. INTRODUCTION 6

II. THEORY 7

A. TWO-GROUP DIFFUSION THEORY 7

B. TEMPERATURE DEPENDENCE OF NEUTRON AGE 11

C. TEMPERATURE DEPENDENCE OF SCATTERING CROSS SECTION . . . 13

D. TEMPERATURE DEPENDENCE OF DIFFUSION LENGTH 17

E. TEMPERATURE DEPENDENCE OF DIFFUSION COEFFICIENT 17

F. SUMMARY OF THEORETICAL ANALYSIS 22

III. EXPERIMENTAL DATA WITH INDIUM FOILS 26

A. DESCRIPTION OF EXPERIMENT USING INDIUM FOILS 26

B. DETERMINATION OF SATURATED ACTIVITIES 31

C. DETERMINATION OF RELAXATION LENGTH 34

D. DETERMINATION OF MIGRATION AREA, AGE AND DIFFUSION LENGTH 35

E. DISCUSSION OF EXPERIMENTAL RESULTS 37

IV. EXPERIMENTAL DATA WITH CRYSTAL 62

A. DISCUSSION OF CRYSTAL DETECTOR 62

B. DETERMINATION OF CRYSTAL 63

C. DESCRIPTION OF EXPERIMENT 68

D. DISCUSSION OF RESULTS OF CRYSTAL EXPERIMENTAL DATA . . . 69

E. SOFT GAMMA INFLUENCE AND MULTICHANNEL ANALYZER ANALYSIS OF DATA 77

V. COMPARISON OF THEORETICAL AND EXPERIMENTAL RESULTS 80

A. THEORETICAL VERSUS INDIUM FOIL DATA 80

B. THEORETICAL VERSUS CRYSTAL DATA 84

IV. CONCLUSIONS 90

APPENDIX A - COMPUTER PROGRAM 1 FOR EVALUATION AND COMPARISON OF THEORETICAL DATA 91

APPENDIX B - COMPUTER PROGRAM 2 FOR THEORETICAL PLOT OF DIFFUSION LENGTH, AGE DIFFUSION COEFFICIENT AND SCATTERING CROSS SECTION 95

APPENDIX C - COMPUTER PROGRAM 3 FOR THEORETICAL FLUX PLOT 97

APPENDIX D - COMPUTER PROGRAM 4 FOR EVALUATION OF SATURATED ACTIVITY 100

APPENDIX E - COMPUTER PROGRAM 5 FOR DETERMINATION OF MIGRATION AREA, AGE AND DIFFUSION LENGTH 107

APPENDIX F - COMPUTER PROGRAM 6 FOR FLUX PLOT FROM INDIUM FOIL 111

APPENDIX G - COMPUTER PROGRAM 7 FOR FLUX PLOT FROM CRYSTAL DETECTOR DATA 112

BIBLIOGRAPHY 118

INITIAL DISTRIBUTION LIST 119

FORM DD 1473 120

ACKNOWLEDGEMENT

A deep sense of appreciation is expressed for the continued guidance and inspiration given to this researcher during the period of investigation by my thesis advisor Professor Dong Nguyen. Gratitude is also expressed to my wife Marion who provided moral support during periods of frustration and who assisted in the preparation of the final draft.

I. INTRODUCTION

The use of a crystal for neutron detection has normally been limited to large crystals which are directly connected to a photo-multiplier tube. Optimum performance with a crystal is reportedly obtained when the crystal is maintained at near liquid nitrogen temperature [1]. In that no information was available for usage of the crystal under the desired temperature range (77° to 168° F) the effect of temperature change upon the crystal's detection capability had to be determined.

The LiI(Eu) crystal as per Price [2] and Murray [3] was first proposed as a neutron detector during the mid 1950's. Because of the high absorption cross section, the crystal has a high detection efficiency and should be suitable under different experimental conditions in pulsed neutron research dealing with small size media and fast decaying neutron fields. The Boron Trifluoride filled gaseous detector can also be manufactured in small sizes; however, the efficiency remains much less than the LiI(Eu) detector. In addition the BF_3 requires a minimum length of signal lead between the detector and the preamplifier; whereas, the light pipe and crystal combination provide considerable flexibility.

The indium foil activation analysis method is well established, but extremely time consuming in the ultimate determination of the thermal neutron flux.

The purpose of the research was to investigate the temperature dependence of thermal neutron flux using the crystal detector. The results of the crystal data are to be compared with a theoretical analysis and additional experimental data obtained by the indium foil activation method.

II. THEORY

A. TWO GROUP DIFFUSION THEORY

The object of this theoretical analysis was to develop an expression for neutron flux with temperature dependent parameters for comparison with data obtained from experimental phases of the investigation. The analysis considers a point source in an infinite medium of water. Neutrons (are born) at the source with high energies. The average neutron energy is 4.3 Mev for Pu-Be source. As a result of collisions with the water molecules the neutrons are either absorbed or moderated with an energy loss. The steady-state neutron flux was investigated with energy and position as variables. A two group method of analysis [1] utilizing the steady-state diffusion equation was used to develop an expression for the neutron flux. Group 1 neutrons (Fast Neutrons) are categorically those neutrons with energies greater than 1 ev and Group 2 neutrons (Thermal Neutrons) are those neutrons with energies less than 1 ev. The diffusion equation for Group 1 can be expressed as follows where D is the diffusion coefficient, Σ_T is the total scattering cross section, and ϕ is the flux with energy and position dependence.

$$D_1(E)\nabla^2\phi_1(r,E) - \Sigma_T(E)\phi_1(r,E) + \int_{1\ ev}^{\infty} \Sigma_s(E' \rightarrow E)\phi_1(r,E')dE' = 0 \qquad (1)$$

Equation (1) can be simplified by assuming that the flux is separable in space and energy and replacing $\phi(r,E)$ by $F(r)X(E)$. Integrating all the terms in equation (1) with respect to energy over the limits of the Group 1 neutrons results in the following:

$$\nabla^2 F_1(r)\int_{1\,ev}^{\infty} D_1(E)X_1(E)dE - F_1(r)\int_{1\,ev}^{\infty} \Sigma_T(E)X_1(E)dE$$

$$+ F_1(r)\int_{1\,ev}^{\infty}\left[\int_{1\,ev}^{\infty} \Sigma_s(E' \rightarrow E)X_1(E')dE'\right]dE = 0 \qquad (2)$$

Next, we divide each of the above terms by $\int_{1\,ev}^{\infty} X_1(E)dE$ and define the following average quantities:

$$\bar{D}_1 = \frac{\int_{1\,ev}^{\infty} D_1(E)X_1(E)dE}{\int_{1\,ev}^{\infty} X_1(E)dE}$$

$$\bar{\Sigma}_T = \frac{\int_{1\,ev}^{\infty} \Sigma_T(E)X_1(E)dE}{\int_{1\,ev}^{\infty} X_1(E)dE}$$

$$\bar{\Sigma}_s = \frac{\int_{1\,ev}^{\infty}\left[\int_{1\,ev}^{\infty} \Sigma_s(E' \rightarrow E)X_1(E)dE'\right]dE}{\int_{1\,ev}^{\infty} X_1(E)dE}$$

$$\bar{\Sigma}_1 = \bar{\Sigma}_T - \bar{\Sigma}_s$$

Substitution of the aforementioned relationship into equation (2) results in the following differential equation:

$$\bar{D}_1\nabla^2 F_1(r) - \bar{\Sigma}_1 F_1(r) = 0$$

or

$$\nabla^2 F_1(r) - k_1^2 F_1(r) = 0$$

with $$k_1^2 = \frac{\bar{\Sigma}_1}{D_1} = \frac{1}{\tau_T} \quad ,$$

τ_T being the age of fast neutrons to thermal energy. We now return to the more conventional symbol for the spatial neutron flux and write the above equation as:

$$\nabla^2 \phi_1(r) - k_1^2 \phi_1(r) = 0 \tag{3}$$

The general solution to equation (3) in spherical coordinates is as follows:

$$\phi_1(r) = \frac{C_1 e^{-k_1 r}}{r} + \frac{C_2 e^{k_1 r}}{r} \tag{4}$$

The constants can be evaluated with the following boundary conditions:

1. $\phi_1(r)$ must be finite as r tends to ∞; therefore, $C_2 = 0$.
2. The $\lim_{r \to 0} 4\pi r^2 J_1(r) = S$, where $J = -D$ grad ϕ_1 and S = source strength

$$\phi_1(r) = \frac{S}{4\pi D_1 r} e^{-r/\sqrt{\tau_T}} \tag{5}$$

In that the thermal flux is dependent upon the fast flux, a solution for the thermal flux $\phi_2(r)$ was assumed and then verified.

$$\nabla^2 \phi_2(r) - k_2^2 \phi_2(r) + \frac{\Sigma_1}{D_2} \phi_1(r) = 0 \tag{6}$$

$$\phi_2(r) = S_3 \phi_1(r) + GZ_2(r) \tag{7}$$

Substitution of equation (7) into equation (6) and collecting similar terms results in the following expression:

$$G[\nabla^2 Z_2 - k_2^2 Z_2] + S_3[\nabla^2 \phi_1(r) - (k_2^2 - \frac{\Sigma_1}{D_2 S_3})\phi_1(r)] = 0 \qquad (8)$$

By comparison of the coefficients of the fast flux of equations (3) and (8), the coupling coefficient (S_3) must satisfy the following relation ship:

$$k_2^2 - \frac{\Sigma_1}{D_2 S_3} = k_1^2 \quad \text{or} \quad S_3 = \frac{D_1/\Sigma_2}{\tau_T - L^2}$$

in that $k_2^2 = \Sigma^2/D^2 = \frac{1}{L^2}$

$$\nabla^2 Z_2(r) - k_2^2 Z_2(r) = 0$$

The solution of the latter equation in spherical coordinates is

$$Z_2(r) = \frac{C_3 e^{-k_2 r}}{r} + \frac{C_4 e^{k_2 r}}{r}$$

so that $\phi_2(r) = S_3\phi_1(r) + GZ_2$

$$\text{or } \phi_2(r) = \frac{D_1/\Sigma_2}{\tau_T - L^2}\phi_1(r) + \frac{C_5 e^{-k_2 r}}{r} + \frac{C_6 e^{k_2 r}}{r}$$

The boundary conditions for thermal flux for evaluation of the constants are as follows:

1. $\phi_2(r)$ must be finite except at origin; therefore, $C_6 = 0$.

2. $\phi_2(r)$ for a point source is zero at the point source

   i.e., $\lim_{r \to 0} 4\pi r^2 J_2(r)$, where $J_2(r) = -D_2 \text{ grad } \phi_2(r)$

The final solution is:

$$\phi_2(r) = \frac{SL^2}{4\pi D_2(L^2-\tau_T)r}\left[e^{-r/L} - e^{-r/\sqrt{\tau_T}}\right] \qquad (9)$$

The physical parameters τ, L, and D are now investigated for their temperature dependence.

B. TEMPERATURE DEPENDENCE OF NEUTRON AGE

Neutron age does not represent an elapsed time, but is proportional to the mean squared distance that a neutron travels between formation at birth with high energy (at the source) until thermal energy is obtained (approximately 0.025 ev) as a result of being moderated by the medium surrounding the source. A small value of age indicates that the neutrons have suffered little slowing down and have not diffused far from the source. The magnitude for age in a water moderator for Pu-Be source is given as 52.8 cm^2 [5] at ambient temperature. The temperature dependence of age is developed using the following basic relationships:

$$\tau \approx \frac{D}{\Sigma_s}$$

$$D = \frac{1}{\Sigma_{tr}} \qquad \tau = \frac{1}{\Sigma_s \Sigma_{tr}}$$

Taking the natural log and differentiating with respect to temperature, it is obtained

$$\frac{1}{\tau}\frac{d\tau}{dT} = \Sigma_s \Sigma_{tr} \frac{d\left(\frac{1}{\Sigma_s \Sigma_{tr}}\right)}{dT}$$

$$\Sigma_s = N\sigma_s$$

$$\Sigma_{tr} = N\sigma_{tr}$$

where N is the number of moderator nuclei per unit volume and σ_s and σ_{tr} are the microscopic scattering and transport cross sections respectively. Assuming that σ_s and σ_{tr} are only slightly temperature dependent in the range of interest the following approximation is made:

$$\frac{1}{\tau}\frac{d\tau}{dT} \approx 2Nd\frac{(\frac{1}{N})}{dT} \qquad (10)$$

Since the number of Nuclei (N) is inversely proportional to the volume, it follows that

$$N \approx \frac{1}{V} \qquad \frac{1}{\tau}\frac{d\tau}{dT} = \frac{2}{V}\frac{dv}{dT}$$

or , letting α_m be the temperature coefficient of volume expansion,

$$\frac{1}{\tau}\frac{d\tau}{dT} = 2\alpha_m$$

Over the region of temperature range investigated (25° C to about 75° C) the temperature coefficient of expansion (α_m) is nearly linear [4] and is approximated by the following expression:

$$\alpha_m \approx 9.0 \times 10^{-5} + 1.04 \times 10^{-5}T \quad (T \text{ in } ^\circ C) \qquad (11)$$

Substituting the expression for the temperature coefficient into equation (10) and integrating yields the following:

$$\tau(T) = C \text{ EXP } [1.8 \times 10^{-4}\ T + 1.04 \times 10^{-5}T^2]$$

Using the experimental value of age to indium resonance for a Pu-Be source (at T = 25° C) the constant was evaluated and the final expression for age with temperature dependence was determined:

$$\tau(25^\circ\ C) = 52.8 \pm 2.5\ cm^2$$

$$\tau(T) = 52.2\ EXP\ [1.8 \times 10^{-4}T + 1.04 \times 10^{-5}T^2] \qquad (12)$$

C. TEMPERATURE DEPENDENCE OF SCATTERING CROSS SECTION

Prior to the investigation of the temperature dependence, the energy dependence of the macroscopic scattering cross section (Σ_s) was considered. The microscopic scattering cross section of water decreases with increasing energy. The elastic scattering cross section is not usually measured directly because of experimental difficulties and is usually obtained by subtracting the cross section of all other processes (capture, inelastic, etc.) from the total cross section. The total cross section of water is essentially all scattering. The following empirical relation has been proposed [4] to express the scattering cross section as a function of energy in a water moderator.

$$\Sigma_s(E) = \Sigma_s(E_o)\left(\frac{E_o}{E}\right)^m \quad cm^{-1}$$

$$\sigma_s(E) = \sigma_s(E_o)\left(\frac{E_o}{E}\right)^m \quad barns$$

$$E_o = 0.025\ ev$$

$$m = 0.47$$

$$\Sigma_s(E_o) = 3.443\ cm^{-1}$$

$$\sigma_s(E_o) \cong 103\ barns$$

An analysis with a Taylor series expansion along with an iteration technique using the computer was conducted to check the non-integer m. Experimental data for microscopic scattering cross section[1] were fitted

---

[1] Approximate values for microscopic scattering cross section as a function of energy were obtained from a curve contained in BNL-325 [7] by taking the difference of the total cross section (σ_T) and the absorption cross section (σ_a)

by assuming an expression of similar form to the given empirical relation. A relationship was obtained by this procedure as shown in Appendix A. In order to attain greater accuracy the energy dependent scattering cross section data from the computer program Gasket-Flange II [6] was used and similar results were obtained. Two triple curve plots (Figs. 1 and 2) were plotted by the computer. One curve was based upon the FLANGE II data which represents the microscopic scattering cross section as a function of energy based upon the best available information. The second curve is dependent upon empirical relation (m = 0.281) obtained by fitting measured scattering data (0 to .5 ev range) for water. Figure 1 shows that the value of m = 0.281 yields results very close to the Gasket-Flange II data. The validity of the empirical non-integer (m) of Ref. 1 was not confirmed. Further investigation was conducted by using extended energy ranges (Fig. 2) up to 1.5 ev and a revised m (.255); however, similar results were obtained. All functions that are dependent upon the non-integer (m) were evaluated, using both values of m. The temperature dependence of the scattering cross section was analyzed in a similar manner to that used for age:

$$\Sigma_s = N\sigma_s \quad -$$

$$\frac{1}{\Sigma_s}\frac{d\Sigma_s}{dT} = \frac{1}{N}\frac{dN}{dT}$$

$$N \sim \frac{1}{v} \quad \frac{dN}{dT} \simeq \frac{1}{v^2}\frac{dv}{dT}$$

$$\frac{1}{\Sigma_s}\frac{d\Sigma_s}{dT} = -\frac{1}{v}\frac{dv}{dT} = -\alpha_m \qquad (13)$$

where α_m was established in Section B to be

$$\alpha_m \simeq 9.0 \times 10^{-5} + 1.04 \times 10^{-5}\, T$$

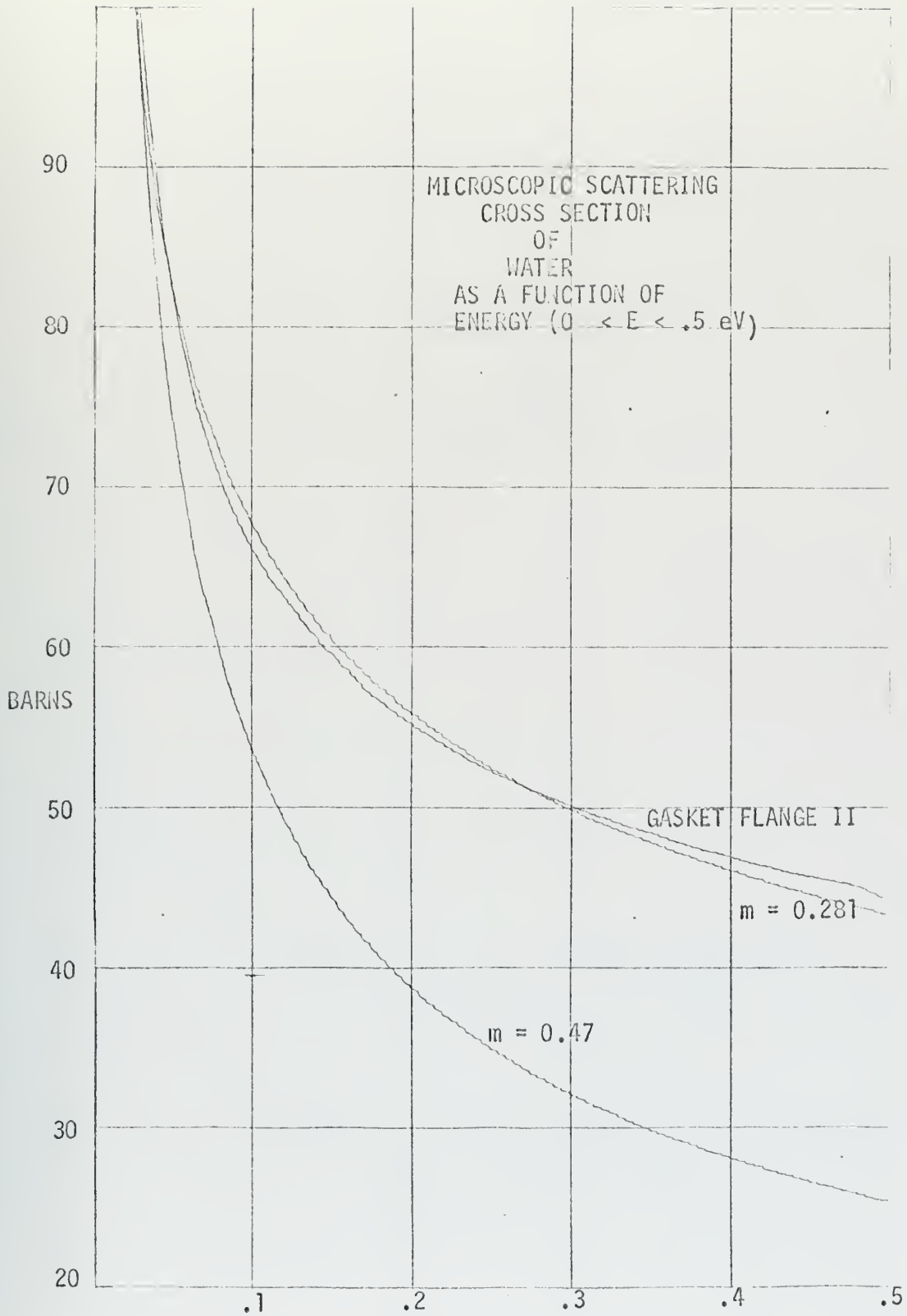
MICROSCOPIC SCATTERING
CROSS SECTION
OF
WATER
AS A FUNCTION OF
ENERGY (0 < E < .5 eV)
90
80
70
60
BARNS
50
40
30
20
GASKET FLANGE II
m = 0.281
m = 0.47
.1
.2
.3
.4
.5
NEUTRON ENERGY (eV)

FIGURE 1

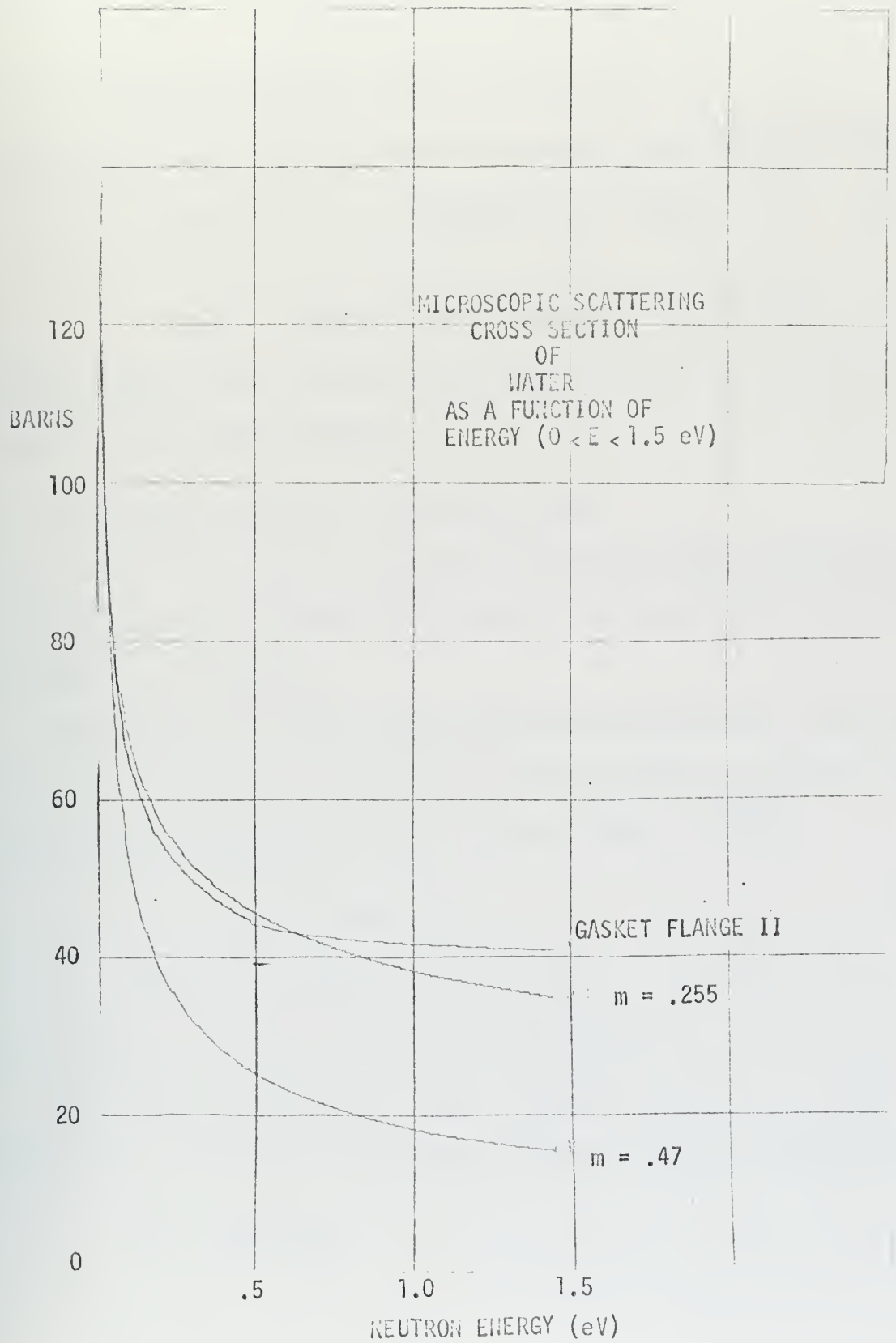
MICROSCOPIC SCATTERING
CROSS SECTION
OF
WATER
AS A FUNCTION OF
ENERGY (0 < E < 1.5 eV)
BARNS
120
100
80
60
40
20
0
.5
1.0
1.5
NEUTRON ENERGY (eV)
GASKET FLANGE II
m = .255
m = .47

FIGURE 2

Substituting the temperature coefficient into equation (13) and integrating,

$$\Sigma_s(T) = C \text{ EXP } [-9.0 \times 10^{-5} T - 5.2 \times 10^{-6} T^2]$$

The constant is evaluated at thermal energy with the following values:

$$\Sigma_s = 3.443 \text{ cm}^{-1} \quad : \quad E = 0.025 \text{ ev} \quad , T = 20^\circ \text{ C}$$

$$\Sigma_s(T) = 3.456 \text{ EXP } [-9.0 \times 10^{-5} T - 5.2 \times 10^{-6} T^2] \qquad (14)$$

The macroscopic cross section is illustrated in Fig. 3 as a function of temperature for thermal energy.

D. TEMPERATURE DEPENDENCE OF DIFFUSION LENGTH

The diffusion length is one-sixth of the mean square distance that a neutron travels from the point at which it becomes thermal to the point at which it is captured.

An empirical relationship based upon prior experimental observations [5] with a Pu-Be source in a container of similar geometry was used to express the temperature dependence of the diffusion length as follows:

$$L(T) = 2.64 + 0.0061 \, T \text{ cm} \qquad (15)$$

where T is in degrees centigrade.

E. TEMPERATURE DEPENDENCE OF DIFFUSION COEFFICIENT

The temperature dependence of the diffusion coefficient for the thermal flux was studied by using the following empirical relation [4]:

$$D(E) \simeq D(E_o)\left(\frac{E}{E_o}\right)^m$$

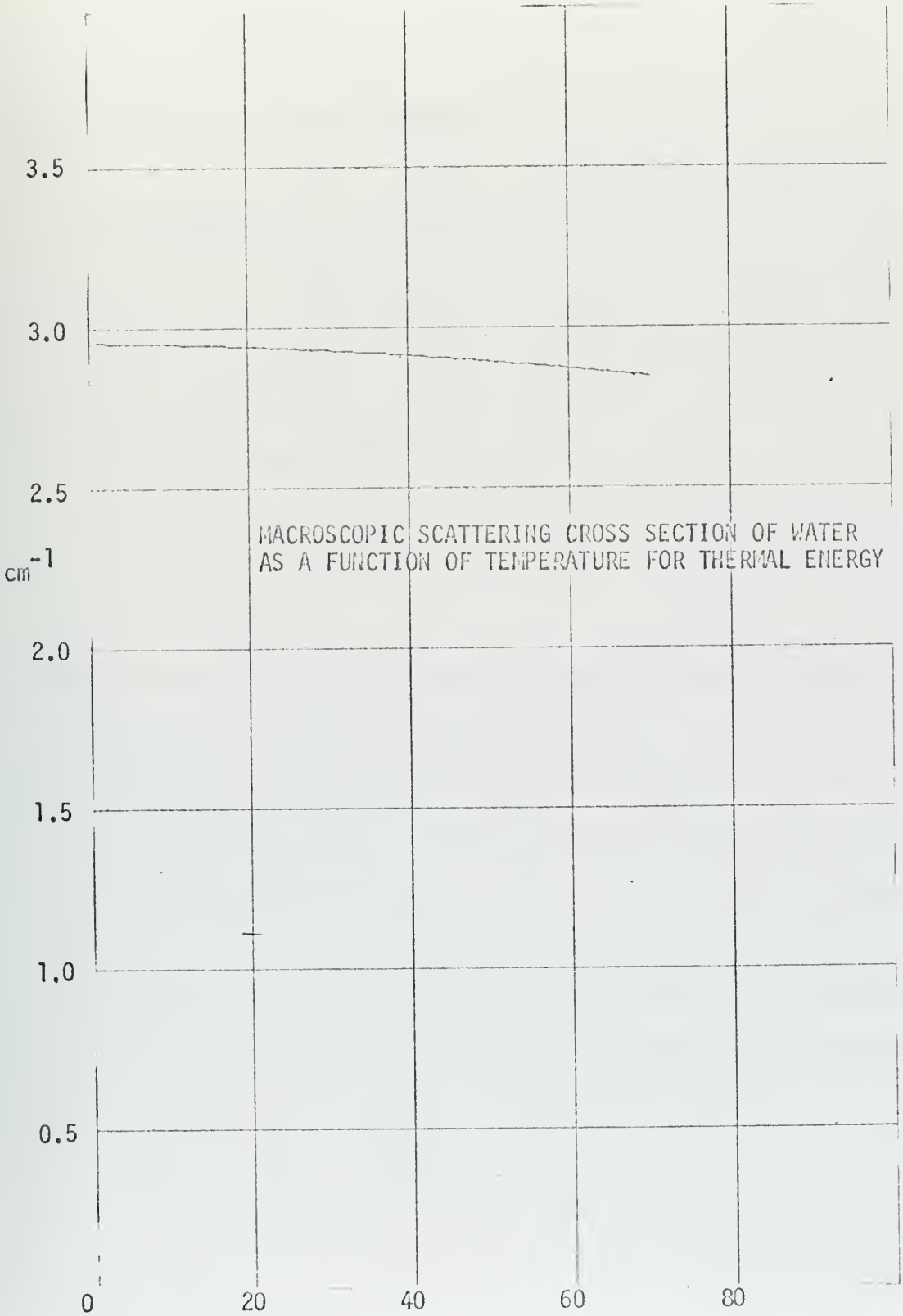
MACROSCOPIC SCATTERING CROSS SECTION OF WATER
AS A FUNCTION OF TEMPERATURE FOR THERMAL ENERGY
cm-1
3.5
3.0
2.5
2.0
1.5
1.0
0.5
0
20
40
60
80
TEMPERATURE (°C)

FIGURE 3

By definition

$$\bar{D} = \frac{D(E)\phi(E)dE}{\phi(E)de}$$

Assuming a Maxwellian energy spectrum:

$$\bar{D} = D(Eo)Eo^{-m} \frac{\int_0^\infty E^{m+1} e^{-E/KT} dE}{\int_0^\infty Ee^{-E/KT} de}$$

$$\bar{D} = \Gamma(m + 2)D(Eo)\left(\frac{kT}{Eo}\right)^m$$

$$\bar{D} = \Gamma(m + 2)D(Eo)\left(\frac{T}{To}\right)^m$$

$$To = 293.61^\circ \text{ K}$$

For material having essentially constant scattering cross section, $m = 0$ and the average thermal diffusion coefficient is temperature independent; however, for a water medium the non-integer (m) is not equal to zero and the diffusion coefficient is temperature dependent. As outlined in Section C, the empirical value for m was 0.47 and the value determined by fitting data from FLANGE II was determined to be 0.281. By normalizing the diffusion coefficient to the value at the reference temperature $To = 25^\circ$ C, a temperature dependent expression is obtained as follows:

$$\bar{D}(To) = .16 \text{ cm} \qquad [4]$$

$$D(Eo) = \frac{.16}{\Gamma(m + 2)}$$

$$D(Eo) = 0.1229 \text{ cm} \qquad m = .47$$

$$D(Eo) = 0.1387 \text{ cm} \qquad m = .281$$

A graphical presentation of the diffusion length as a function of temperature is illustrated in Fig. 4.

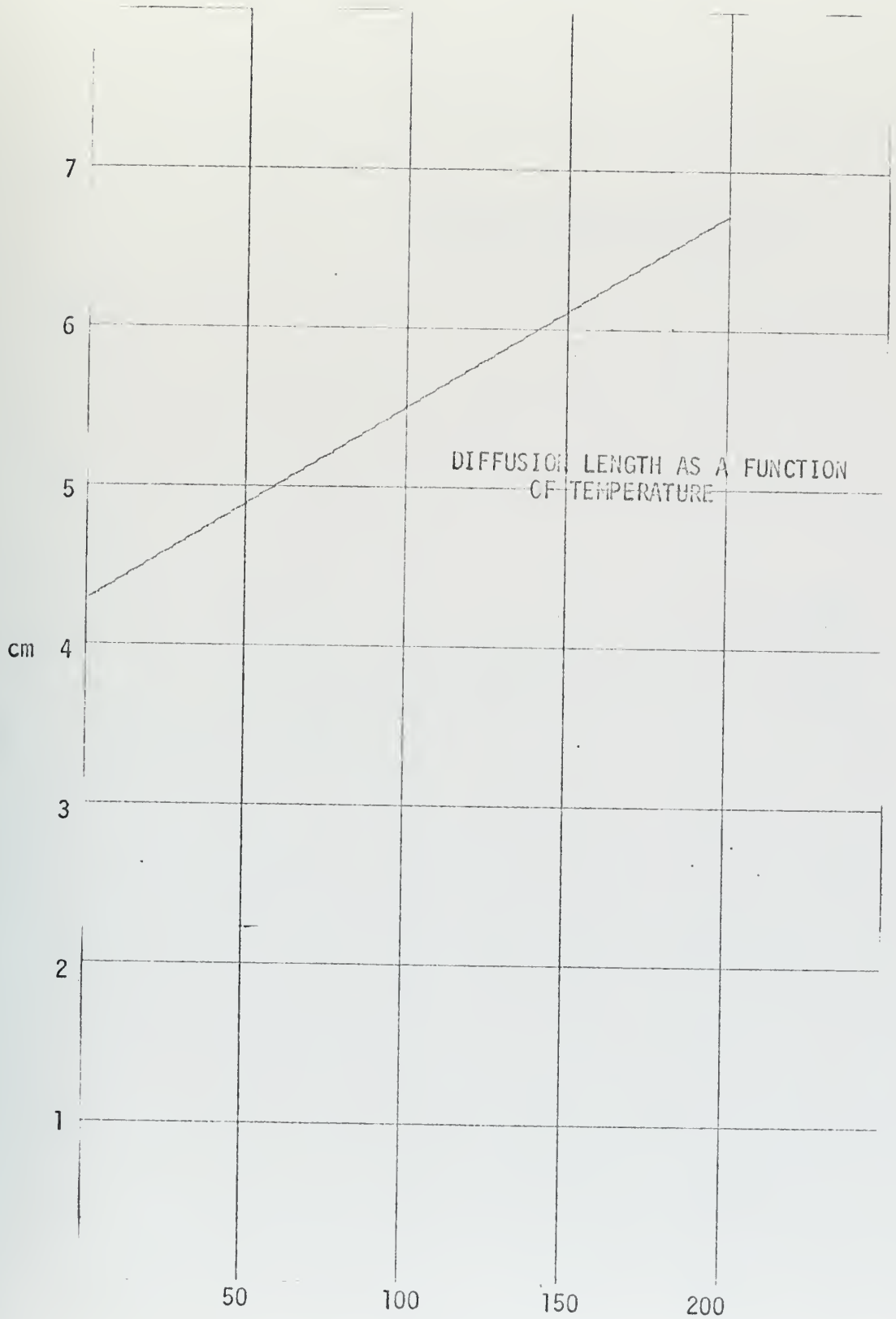
DIFFUSION LENGTH AS A FUNCTION
OF TEMPERATURE
cm
7
6
5
4
3
2
1
50
100
150
200
TEMPERATURE (°C)

FIGURE 4

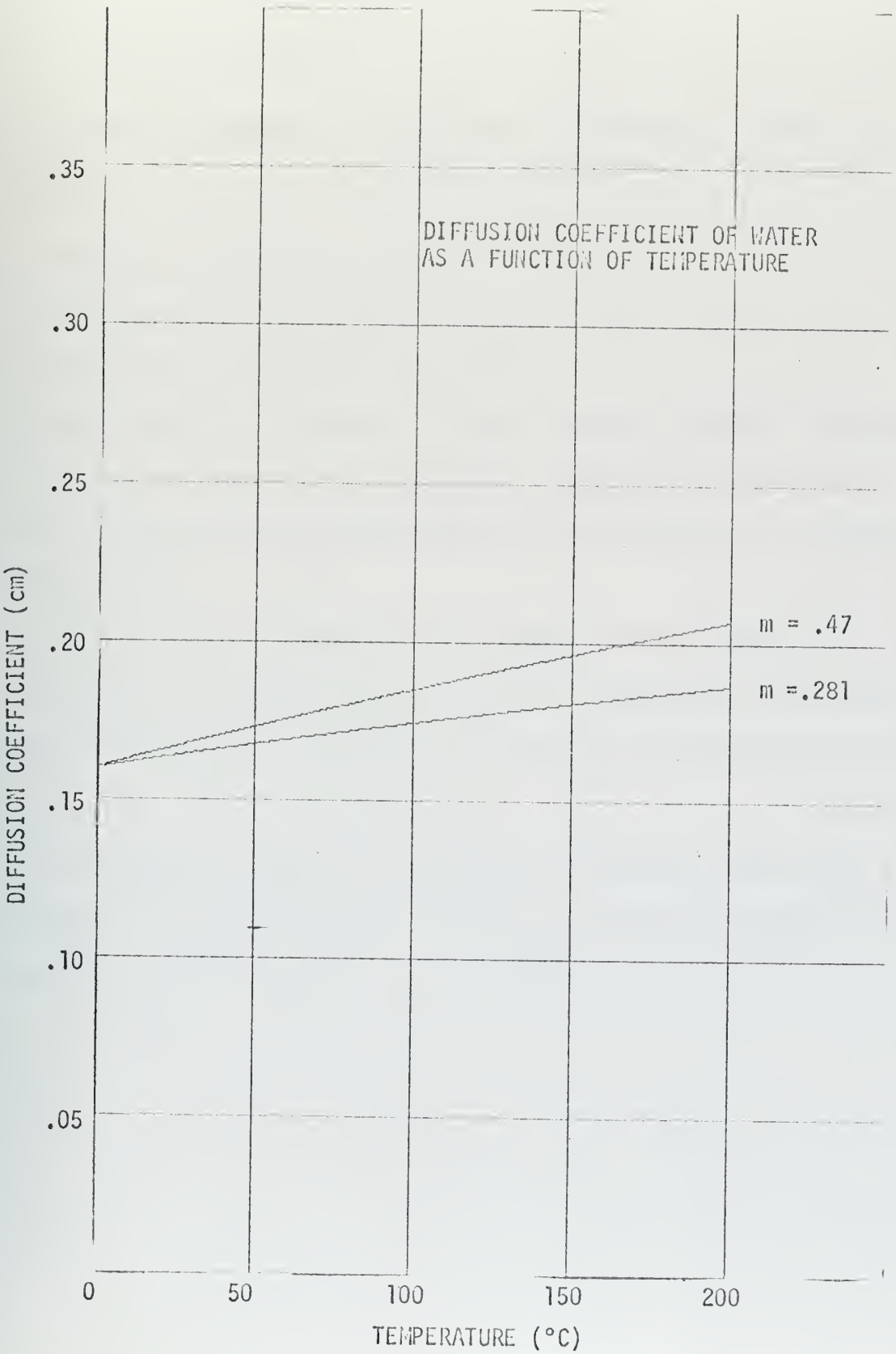
DIFFUSION COEFFICIENT OF WATER
AS A FUNCTION OF TEMPERATURE
.35
.30
.25
.20
.15
.10
.05
DIFFUSION COEFFICIENT (cm)
m = .47
m =.281
0
50
100
150
200
TEMPERATURE (°C)

FIGURE 5

$$\bar{D}(T) = 0.16 \left(\frac{T}{To}\right)^{.47} \tag{16}$$

$$\bar{D}(T) = 0.16 \left(\frac{T}{To}\right)^{.281} \tag{17}$$

The temperature dependence of the diffusion coefficient is illustrated in Fig. 5.

F. SUMMARY OF THEORETICAL ANALYSIS

The two-group diffusion theory was used to obtain an expression for the thermal flux. The parameters of this solution were investigated for their temperature dependence. Several computer programs (Appendices A, B, and C) were used for compilation and tabulation of data along with providing graphical presentations of all parameters as a function of temperature.

The graphical presentation of the computer plotted thermal flux as a function of distance from the source and temperature illustrates only a slight increase in flux with an increase in temperature (Figs. 6 and 7).

An additional illustration relating the theoretical temperature dependence of related parameters; namely, age, diffusion length and migration area (M^2), where $M^2 = \tau_T + L^2$ cm^2, is contained within Fig. 8.

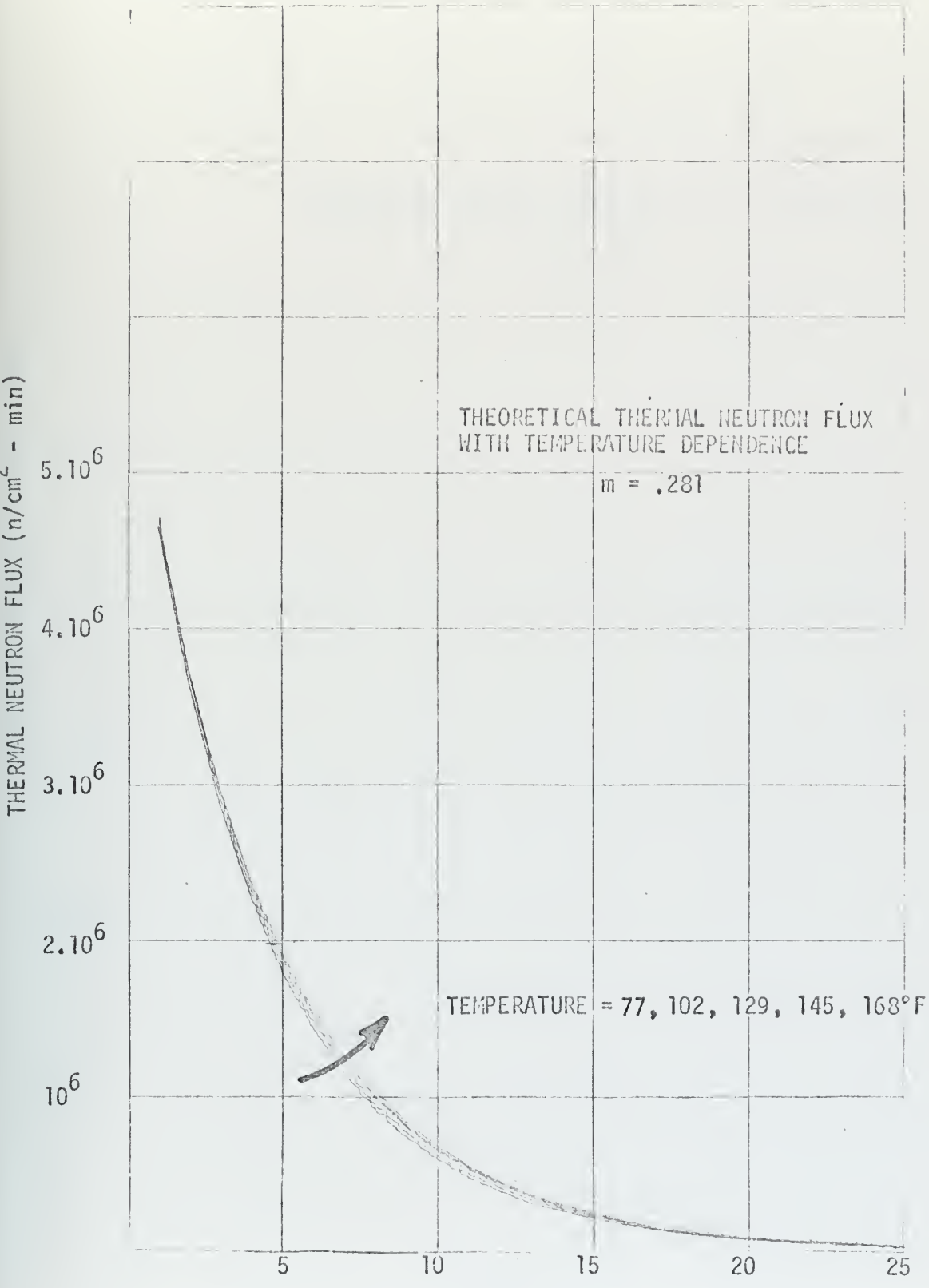
THEORETICAL THERMAL NEUTRON FLUX
WITH TEMPERATURE DEPENDENCE
m = .281
TEMPERATURE = 77, 102, 129, 145, 168°F
THERMAL NEUTRON FLUX (n/cm² - min)
5.10⁶
4.10⁶
3.10⁶
2.10⁶
10⁶
5
10
15
20
25
DISTANCE (cm)

FIGURE 6

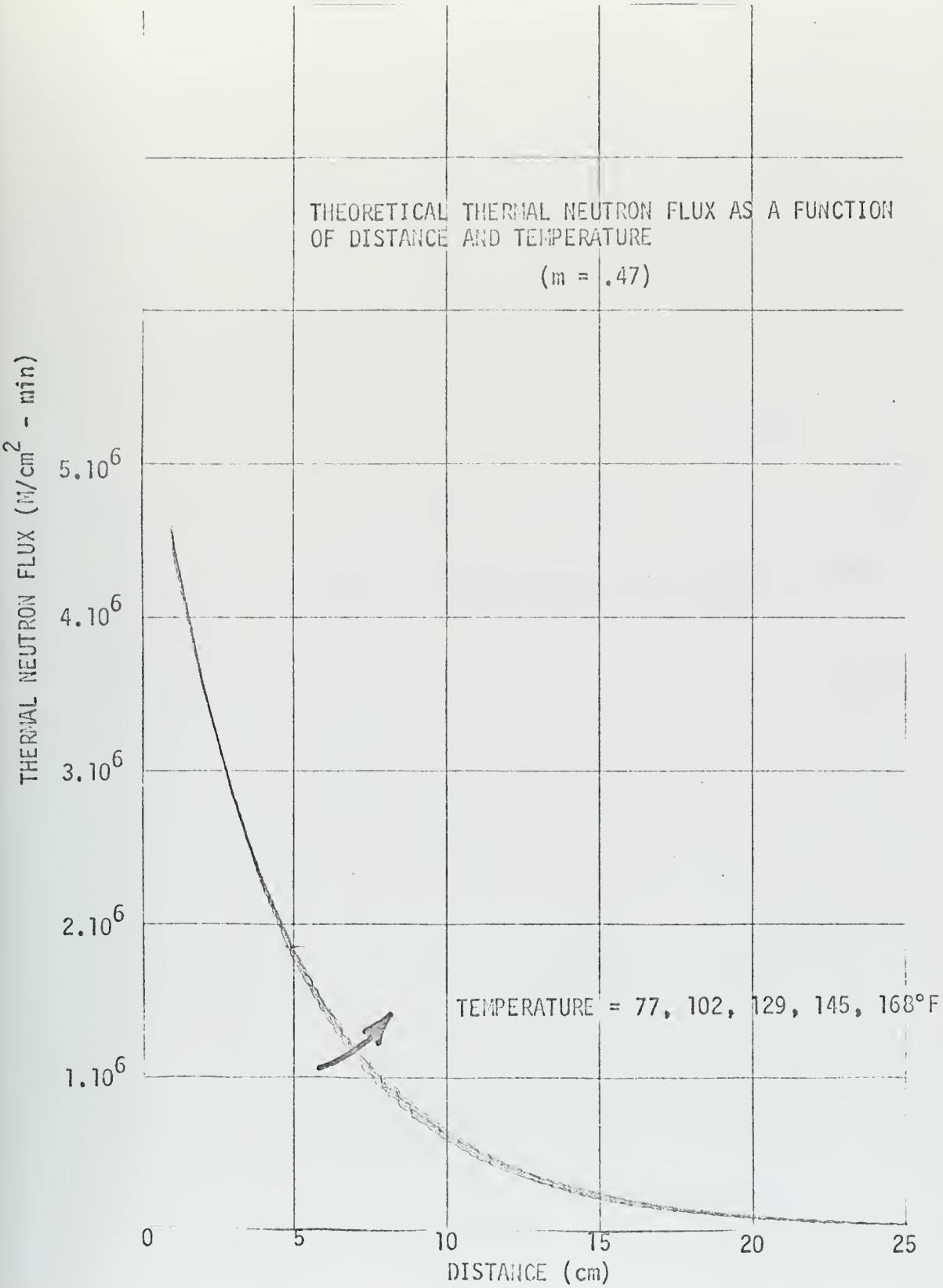
THEORETICAL THERMAL NEUTRON FLUX AS A FUNCTION OF DISTANCE AND TEMPERATURE
(m = .47)
THERMAL NEUTRON FLUX (N/cm^2 - min)
5.10^6
4.10^6
3.10^6
2.10^6
1.10^6
0
5
10
15
20
25
DISTANCE (cm)
TEMPERATURE = 77, 102, 129, 145, 168°F

FIGURE 7

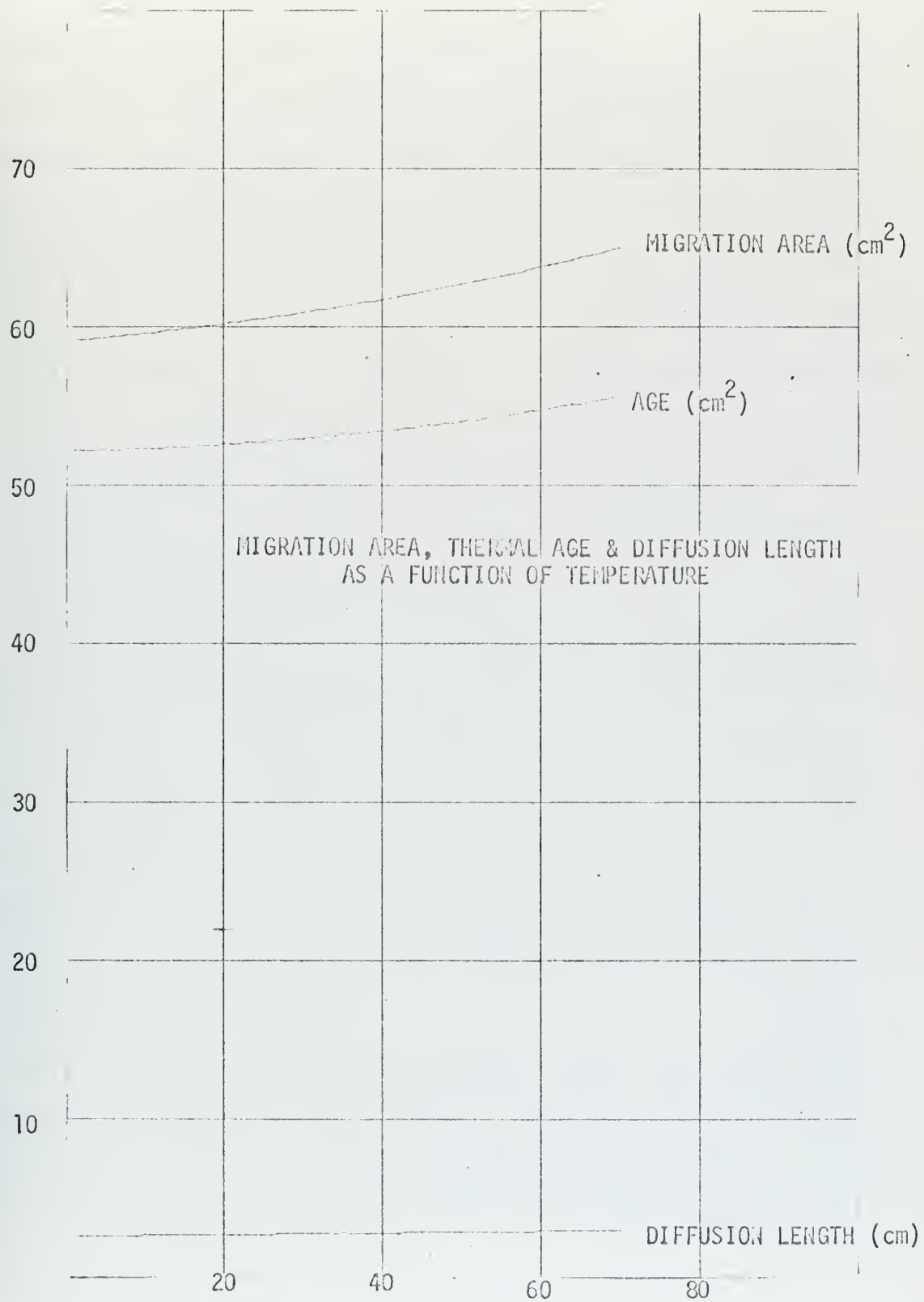
70
60
50
40
30
20
10
MIGRATION AREA (cm^2)
AGE (cm^2)
MIGRATION AREA, THERMAL AGE & DIFFUSION LENGTH
AS A FUNCTION OF TEMPERATURE
DIFFUSION LENGTH (cm)
20
40
60
80
TEMPERATURE (°C)

FIGURE 8

III. EXPERIMENTAL DATA WITH INDIUM FOILS

A. DESCRIPTION OF EXPERIMENT USING INDIUM FOILS

A VISIFLUX neutron howitzer was utilized to conduct the flux measurement using the Plutonium-Berylium (Pu-Be) source and Indium foils. The VISIFLUX howitzer is a plexiglass cylindrical tank having a 2 foot diameter and a 2 1/4 foot height and is specifically designed for nuclear experimentation. A water level of 45 gallons was maintained during the periods of foil irradiations. Electric immersion type heaters along with a control unit were used to obtain and stabilize the desired operating temperature. An agitation type mixer was used to insure uniform tank temperature. The VISIFLUX howitzer and associated equipment are illustrated in Fig. 9.

The Indium foils were 1.0 inch in diameter and 0.010 inch thick. A total of 20 foils were used with 10 foils enclosed within individual cadmium covers of 0.020 inches thickness. Plastic foil holders were used to place the bare foils on one side of the source and the cadmium-covered foils on the opposite side of the source in a horizontal plane perpendicular to the center of the source. The foil weights were used as criteria for positioning with the lightest foil being placed nearest the source.

Both sets of foils were irradiated at the same time at a stabilized, predetermined temperature for a minimum period of 3 hours. The activity was determined by using an end-window Geiger-Mueller tube in a vertical lead shielded housing with an electronic timer-scaler counting device. Specific equipment used for the Indium foil experiment is listed in Table 1 and illustrated in Fig. 10.

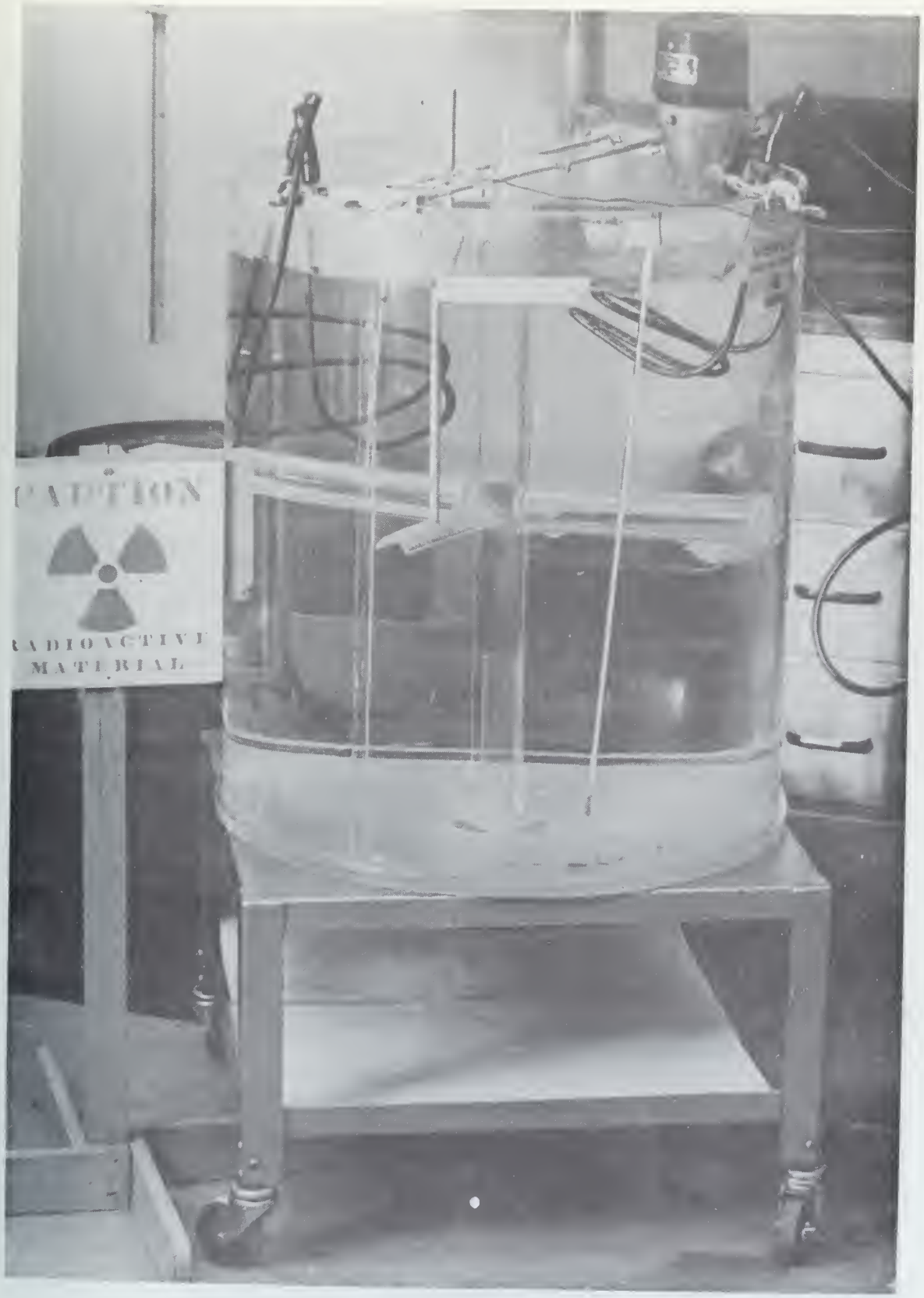

VISIFLUX NEUTRON HOWITZER

FIGURE 9

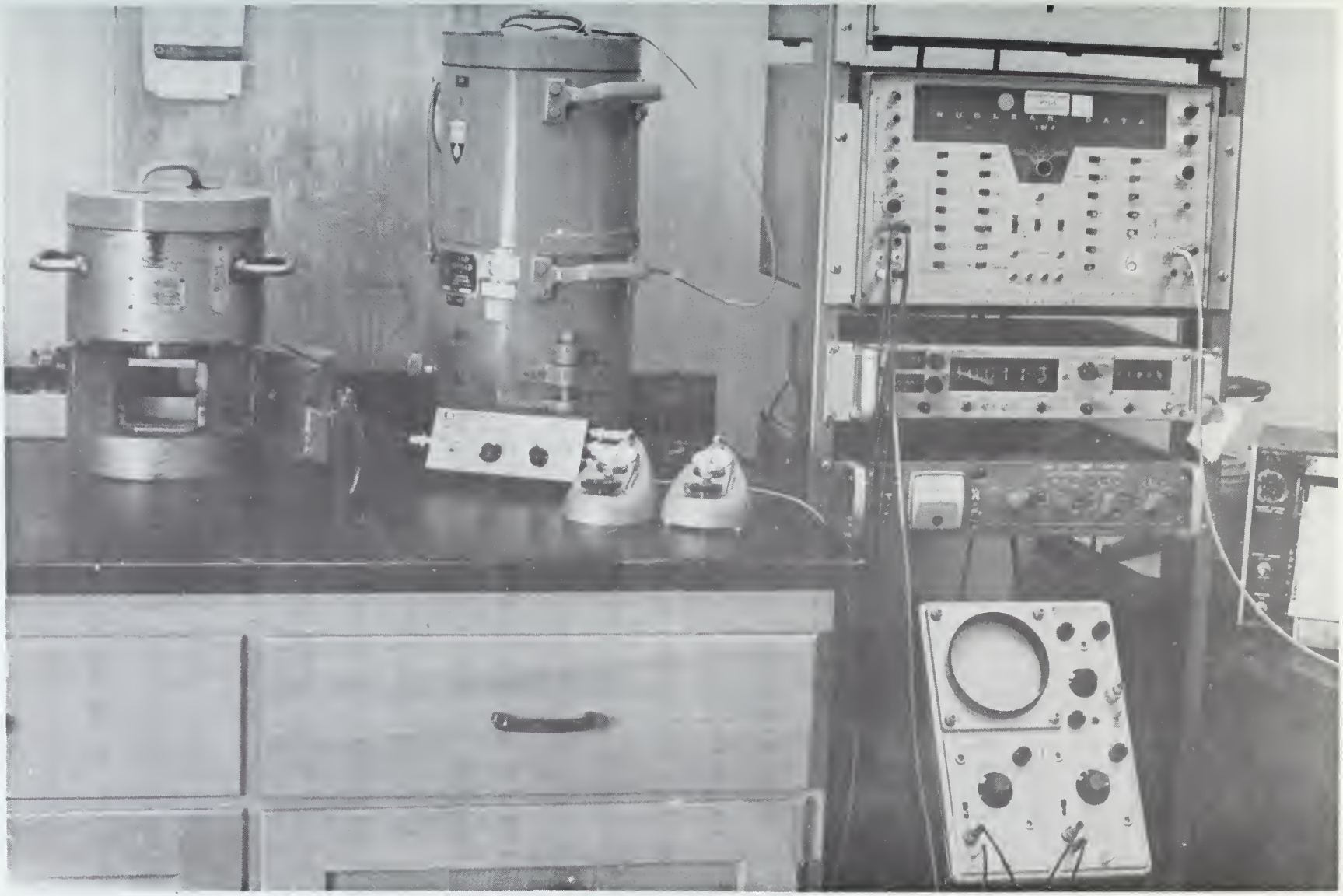

FIGURE 10

TABLE 1

EQUIPMENT

ITEM	MANUFACTURER	MODEL
Timer-Scaler	Hewlett-Packard	5201L
Preamplifier	Hewlett-Packard	55544
GM tube	Amperex	200HB
Vertical Lead Shield	Designers for Industry	AL-12A
High Voltage Power Supply	Power Designs Pacific, Inc.	2K-10

The same procedure was adhered to for each of the measurements at different temperatures. Background readings were obtained randomly before and during periods of irradiation. Background counts were found to vary considerably during the day time while in general, background counts were lower during the evening hours. The procedure was to count the bare foils first, starting with the foil located closest to the source. Each foil was allowed to decay for three minutes to insure the desired count rate from the 54 minute activity was not influenced by the 13 second half life of In^{116}. To attain maximum consistency in the counting procedure all foils were counted for five minutes with the surface of the foil closest to the source being placed facing the G-M tube. Prior to conducting the experiment a preliminary investigation was conducted on the counting equipment to determine the G-M tube plateau for proper operating voltage, and dead time correction factor for the counting equipment and also a statistical analysis to establish the presence of other than statistical variations.

The operating voltage for the G-M tube was determined by plotting observed count-rate versus increasing high-voltage [2]. The G-M plateau voltage was determined to be 1200 volts.

A dead-time correction factor is required in that the period immediately following a G-M tube discharge the electric field is reduced because of presence of positive ions. Any particle entering the tube during the period of reduced electric field will not trigger a discharge and subsequently the observed counting rate will be less than the actual count rate. A split-source of radium was used to determine the dead-time correction factor [2] with a period of 38 micro-seconds. To verify that the counting equipment was operating normally, the following technique was applied [2].

The standard deviation is defined by the expressions:

$$\sigma = \left(\frac{r_1}{t_1} + \frac{r_2}{t_2}\right)1/2 = \left(\frac{85190}{10} + \frac{84474}{10}\right)^{1/2} = 130.2$$

$$|r_1 - r_2| \geq K\sigma \quad \text{or} \quad K = \frac{71.6}{130.2} = .55$$

r_1 and r_2 are observed count rates using a Co^{60} (0.97 micro-curie) source.

t_1 and t_2 are length of time of observation .

The method consists of calculating the standard error of the difference between two counting rates which are obtained from the same source under identical circumstances. The standard error is then compared with the observed difference between the two counting rates. A probability table (Table 2) is used to determine if the deviations are due to causes other than the statistical nature of the disintegration process.

TABLE 2

PROBABILITY P OF OBTAINING $/r_1 - r_2/ \geq k\sigma$

k	1.0	1.2	1.4	1.6	2.0	2.5	3.0
P	0.159	0.115	0.081	0.055	0.023	0.006	0.001

The results of the analysis indicate that the counting equipment was not subject to receiving erratic counts and implies the error incurred will only be of a statistical nature. This technique was applied several times during the course of experimentation with similar results obtained.

B. DETERMINATION OF SATURATED ACTIVITIES AT DIFFERENT TEMPERATURES

The purpose of Indium foil activation was to determine the neutron distribution as a function of both temperature and position. The production rate of the Indium isotope (In^{116}) is proportional to the neutron flux density and the activation cross section, i.e.,

$$P = \Sigma_{ac}\phi V$$

where P = production rate

Σ_{ac} = macroscopic activation cross section of Indium

Φ = total neutron flux density

V = volume of Indium foil

In that the isotope (In^{116}) has a 54 minute half-life and is subject to decay while being irradiated the following expression represents the production process

$$\frac{dN}{dT} = \Sigma_{ac}\phi V - \lambda N \qquad (18)$$

where

$\frac{dN}{dT}$ = production rate

λN = rate of decay

λ = decay constant (1.28×10^{-2} min^{-1})

Integration of equation (18) yields the following:

$$N_1 = \frac{\Sigma_{ac}\phi V(1 - e^{-\lambda t_1})}{\lambda}$$

where

N_1 = the no. of atoms of In^{116} existing at time t_1

λN_1 = the absolute activity at time t_1

such that

$$A_1 = k\Sigma N_1 = k\Sigma_{ac}V(1-e^{-t_1})$$

where k is a proportionality constant between the absolute activity (N_1) and the counting activity (A_1).

For a large irradiation time t_1 the saturated activity would be obtained, i.e., $As = k\Sigma_{ac}\phi V$ such that the activity at time t_1 can be represented by $A_1 = As(1 - e^{-\lambda t_1})$. In that the saturated activity is the quantity being sought and A_1 is the actual extent of activation we express the saturated activity in terms of the actual activity:

$$As = A_1/(1 - e^{-\lambda t_1})$$

As mentioned previously, a waiting period of about three minutes was applied because of a Beta emission with a 14 second half-life. At the time the counting begins (t_2) the activity of the foil has been reduced and is represented by

$$A_2 = A_s(1 - e^{-\lambda t_1})e^{-\lambda(t_2 - t_1)}$$

such that

$$A_s = \frac{A_2}{(1 - e^{-\lambda t_1})(e^{-\lambda(t_2 - t_1)})}$$

Noting that A_2 is the activity at the time t_2 and that the actual count rate as observed by the detector is for the period $(t_3 - t_2)$, the total count (C) can be calculated as follows:

$$C = \int_0^{t_3 - t_2} A(t)dt$$

where $t_3 - t_2$ = counting time

C = observed activation count

A(t) = activity

$$\text{or } C = A_s(1 - e^{-\lambda t_1})e^{-\lambda(t_2 - t_1)} \int_0^{t_3 - t_2} e^{-\lambda t} dt$$

such that

$$A_s = \frac{\lambda C}{(1 - e^{-\lambda t_1})(e^{-\lambda(t_2 - t_1)} - e^{-\lambda(t_3 - t_1)})} \qquad (19)$$

where

t_1 = irradiation time

$t_2 - t_1$ = decay time

$t_3 - t_1$ = decay time + counting time

The same expression was used for the cadmium-covered foils. A correction factor for the absorption of fast neutrons by the cadmium cover based on foil thickness was obtained from the interpolation of a graph by Tittle as presented by Price [2].

The observed count rates (corrected for background) as a fundtion of distance were used as input data for a computer program listed in Appendix D. This computer program provided the following data for both the bare and cadmium covered foils as a function of distance:

1) saturated activity
2) saturated activity times distance squared
3) saturated activity times distande to the fourth power
4) the standard deviation of the saturated activity which is designated as sigma (σ)

Four graphical presentations were obtained: a semi-logarithmic plot of both the bare and cadmium-covered activities times distance squared and linear plots of the same curves for ultimate area integration.

C. DETERMINATION OF RELAXATION LENGTH WITH TEMPERATURE DEPENDENCE

In contrast to charged particles which have a defined range, neutrons and gamma rays are stopped approximately in an exponential manner. The relaxation length is the thickness of a material that causes a drop in intensity by a factor of e owing to slowing down or absorption [8]. The relaxation length is energy dependent and will have a specific length for a specific known neutron energy; namely, the relaxation length of thermal neutrons (E = 0.025 eV) is equal to the thermal diffusion length and for Pu-Be neutrons (E = 4MeV) the relaxation length is of the order of 10 cm.

In view of the nearly linear temperature-dependent behavior of the theoretical relationship established for the macroscopic scattering cross section (Ref. II-C) and the inverse relationship of the relaxation

length, $b \approx 1/\Sigma s(E)$, it was assumed that the relaxation length would be essentially linear with temperature over the range of temperatures investigated.

At large distances from the source the activity curve is exponential in nature. The spatial dependence of the slowing down density (q) resulting from a point source (at large distance from the source) is given by $q \approx \frac{e^{-\Sigma s r}}{r^2}$. In that the thermal flux is proportional to the slowing down density the following relationship was obtained.

$$As(r) \approx (e^{-\Sigma s r})/r^2$$

or $$\ell n As(r) r^2 \approx -\Sigma s r$$

and $$\ell n As(r) r^2 \approx -r/b$$

where b is the relaxation length, and As(r) is the activation activity. The problem that remained to be resolved was the determination of the value r beyond which equation (2) became valid.

D. DETERMINATION OF MIGRATION AREA, AGE AND DIFFUSION LENGTH

The Fermi Age ($\tau(E_o,E)$) is defined as being equal to one-sixth of the average crow flight distance from the point source where a neutron is born (E_o) to the point where the neutron acquires the energy E [4]. A similar relation holds true for the Migration Area except the distance extends to the point of capture. The difference between Migration Area and Age is the diffusion length squared. Relationships between area, lengths and mean square distances are listed as follows:

$\tau = 1/6\ \bar{r}_s^2$ τ = age $\sqrt{\tau}$ = slowing-down length

$M^2 = 1/6\ \bar{r}_t^2$ M^2 = Migration area, M = Migration length

$L^2 = 1/6\ \bar{r}_{th}^2$ L = Diffusion length

$M^2 = \tau + L^2$

$\bar{r}_t^2 = \bar{r}_s^2 + \bar{r}_{th}^2$

The mean square distances $\bar{r}_t^2$ can be expressed as a function of activity by the following relationship:

$$\bar{r}_t^2 = \frac{\int_0^\infty Asr^4 dr}{\int_0^\infty Asr^2 dr} = 6M^2$$

A similar relationship holds true for the age using the cadmium activity data such that

$$\bar{r}_s^2 = \frac{\int_0^\infty As(cd)r^4 dr}{\int_0^\infty As(cd)r^2 dr} = 6\tau$$

To account for the energy difference (1.45 to 0.025 eV) and neutron travel between the Indium resonance and thermal energy a value of 1.8 cm^2 is added to the computed value of age as recommended by Valente [9] such that

$$L = \sqrt{M^2 - (\tau + 1.8)}$$

The computation of M^2, τ, and L were conducted by the computer (Appendix E). To evaluate the moments of activities (Asr^2, Asr^4, $As(cd)r^2$, and $As(cd)r^4$) the area under the curves was determined by a Simpson's approximation.

Two segments of the curve were considered in evaluating the area; namely, the experimental data with a smooth curve drawn through the data points and the exponential portion which is proportional to $e^{-r/b}$. An intercept and slope were determined from a computer semi-logarithmic plot of activity times distance squared versus distance and used to construct an expression of the form $Ce^{-r/b}$ to represent the exponential portion of the curve in the integration process. The constant C was actually expressed as an exponential in view of the magnitudes incurred (Appendices D and E are germane).

E. DISCUSSION OF EXPERIMENTAL RESULTS

Five sets of experimental observations at different temperatures (77, 102, 129, 145, 168°F) were obtained and analyzed. Three graphical presentations for each run observed (Figs. 11 through 25) in addition to tabulated data (Appendix D) are presented. All the graphical plots and analyzed data were obtained by computer programming (Appendices D, E). Figures 11 through 25, in addition to the experimental data points, also have a smooth curve. The smooth curve is actually comprised of two curves, one light and one heavy. The light curve was determined by the relaxation length parameter (b) and was superimposed by the computer on the experimental data points as an aid in resolving the exponential curve fit. The heavier curve was drawn through the data points to obtain magnitude versus distance such that an area integration using Simpson's approximation with the computer could be accomplished. The results of the evaluation of the area moments for ultimate determination of the migration area, age and diffusion lengths are listed in Table 3 and reflect an increasing trend with temperature. The relaxation lengths are also included within the same table.

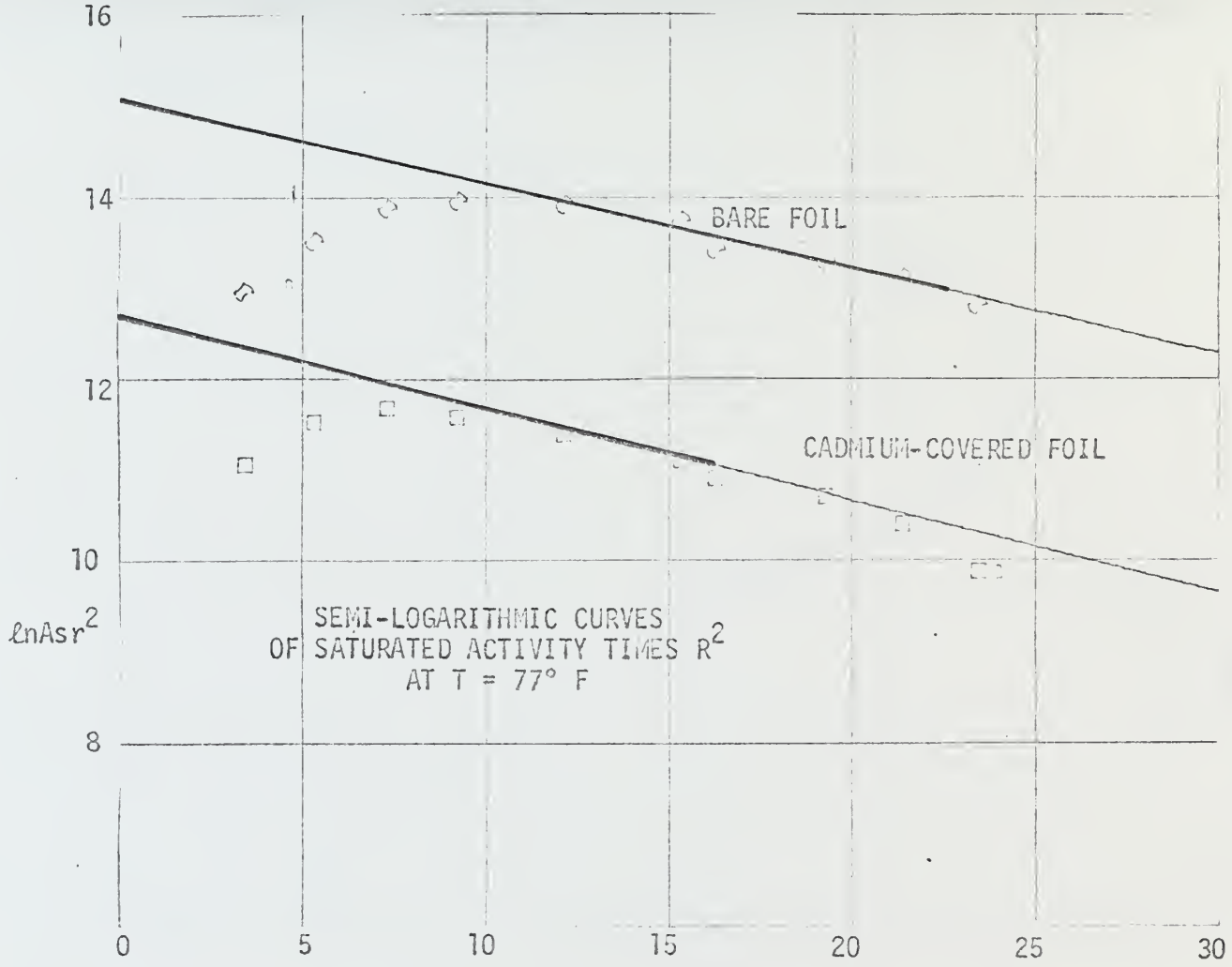
16
14
12
10
8
BARE FOIL
CADMIUM-COVERED FOIL
SEMI-LOGARITHMIC CURVES
OF SATURATED ACTIVITY TIMES R2
AT T = 77° F
lnAsr2
0
5
10
15
20
25
30
DISTANCE (cm)

FIGURE 11

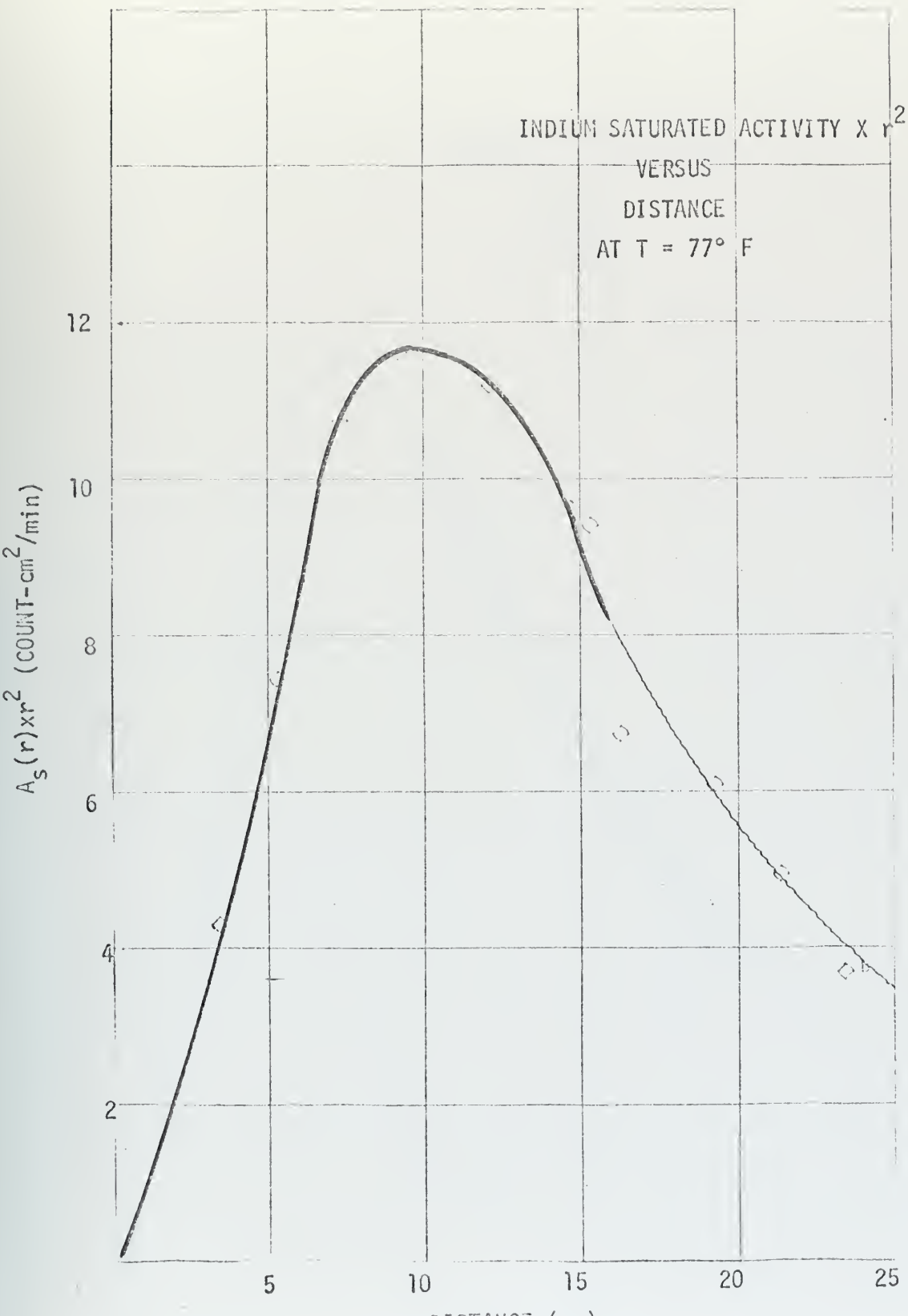
INDIUM SATURATED ACTIVITY X r2
VERSUS
DISTANCE
AT T = 77° F
12
10
8
6
4
2
5
10
15
20
25
As(r)xr2 (COUNT-cm2/min)
DISTANCE (cm)

FIGURE 12

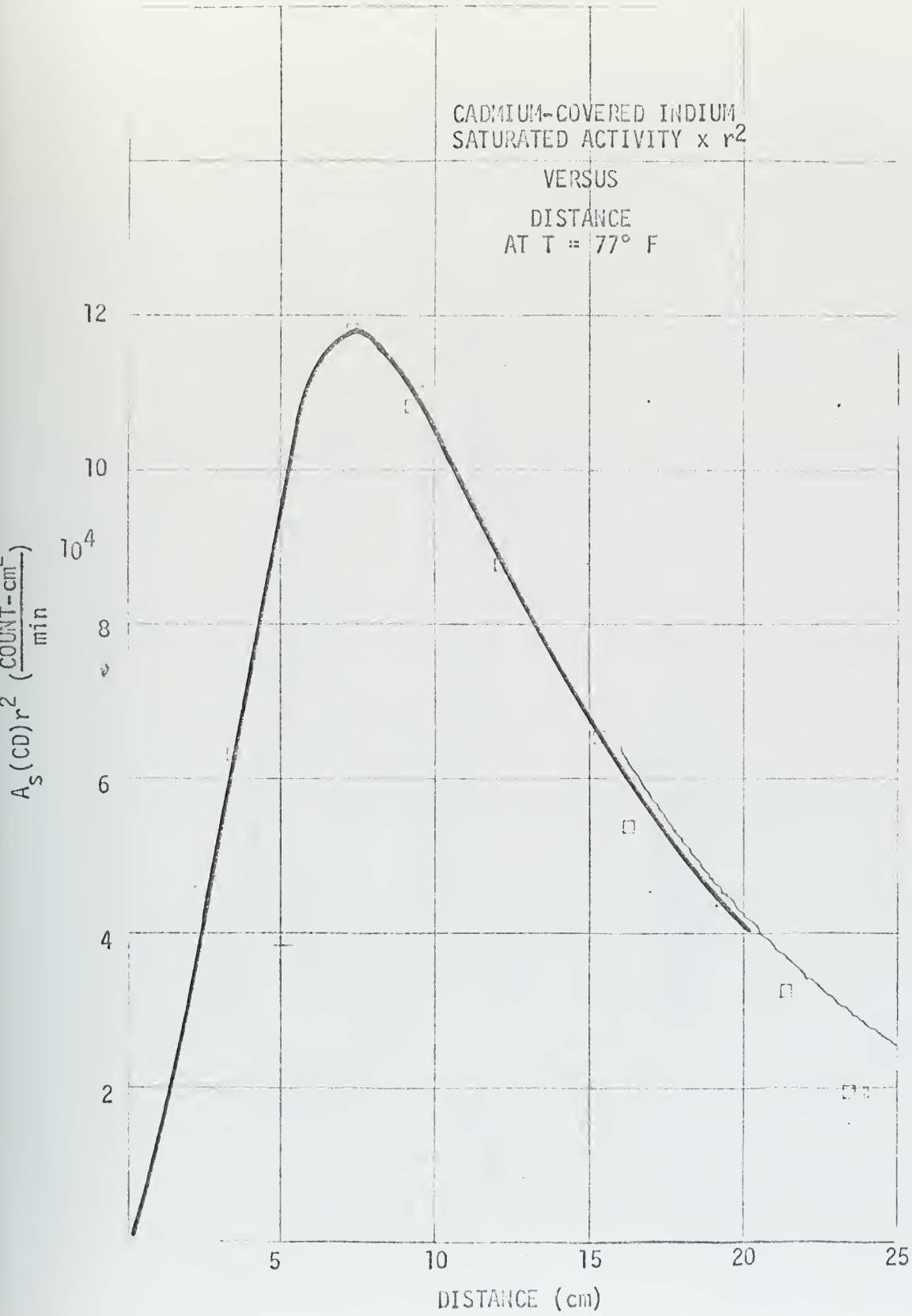
CADMIUM-COVERED INDIUM
SATURATED ACTIVITY x r2
VERSUS
DISTANCE
AT T = 77° F
12
10
10^4
8
6
4
2
As(CD)r2 (COUNT-cm2/min)
5
10
15
20
25
DISTANCE (cm)

FIGURE 13

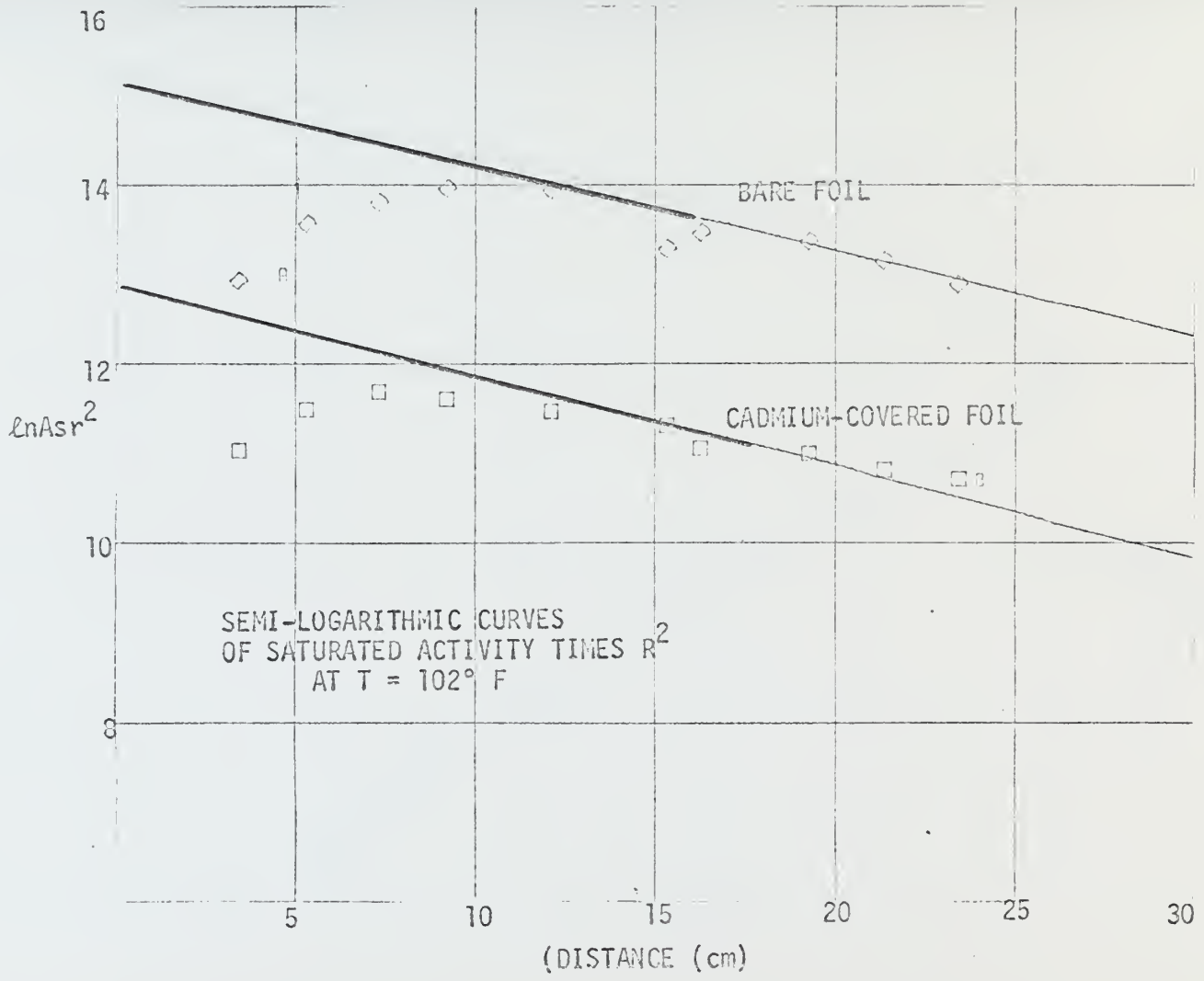
16
14
12
10
8
ℓnAsr²
BARE FOIL
CADMIUM-COVERED FOIL
SEMI-LOGARITHMIC CURVES
OF SATURATED ACTIVITY TIMES R²
AT T = 102° F
5
10
15
20
25
30
(DISTANCE (cm)

FIGURE 14

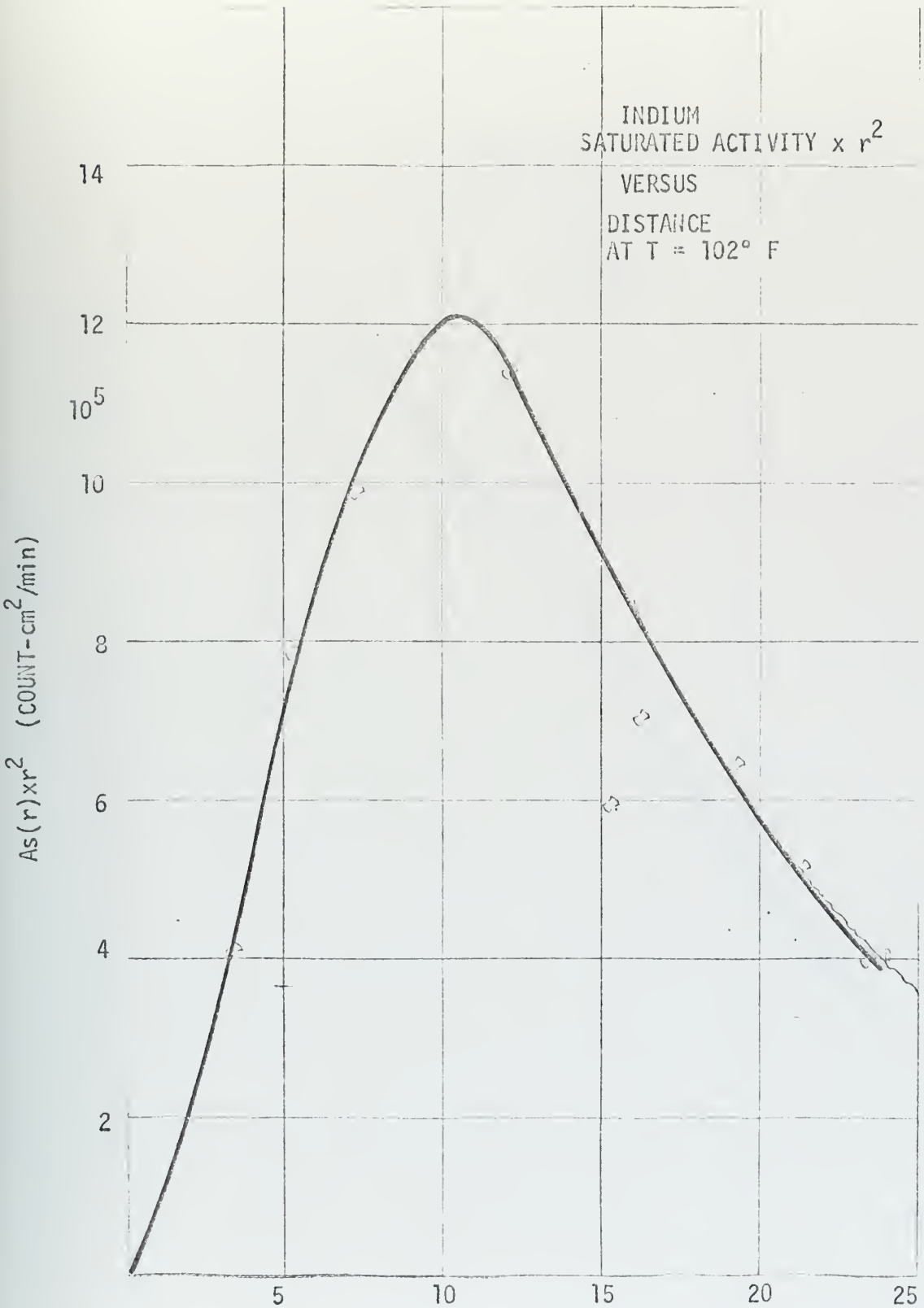
INDIUM
SATURATED ACTIVITY x r^2
VERSUS
DISTANCE
AT T = 102° F
14
12
10^5
10
8
6
4
2
$As(r)xr^2$ (COUNT-cm^2/min)
5
10
15
20
25
DISTANCE (cm)

FIGURE 15

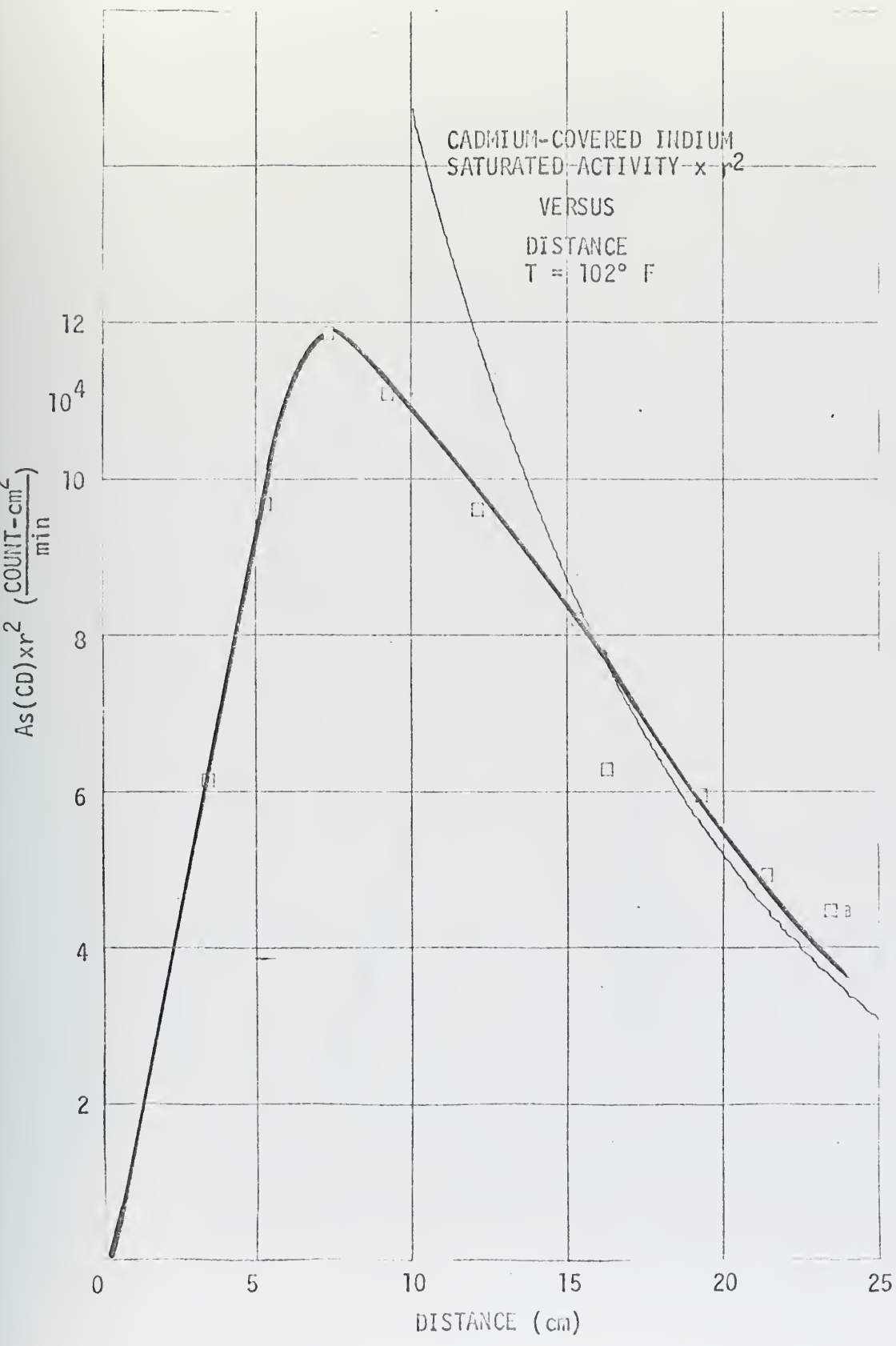
CADMIUM-COVERED INDIUM
SATURATED ACTIVITY x r²
VERSUS
DISTANCE
T = 102° F
12
10⁴
10
8
6
4
2
As(CD)xr² (COUNT-cm²/min)
0
5
10
15
20
25
DISTANCE (cm)

FIGURE 16

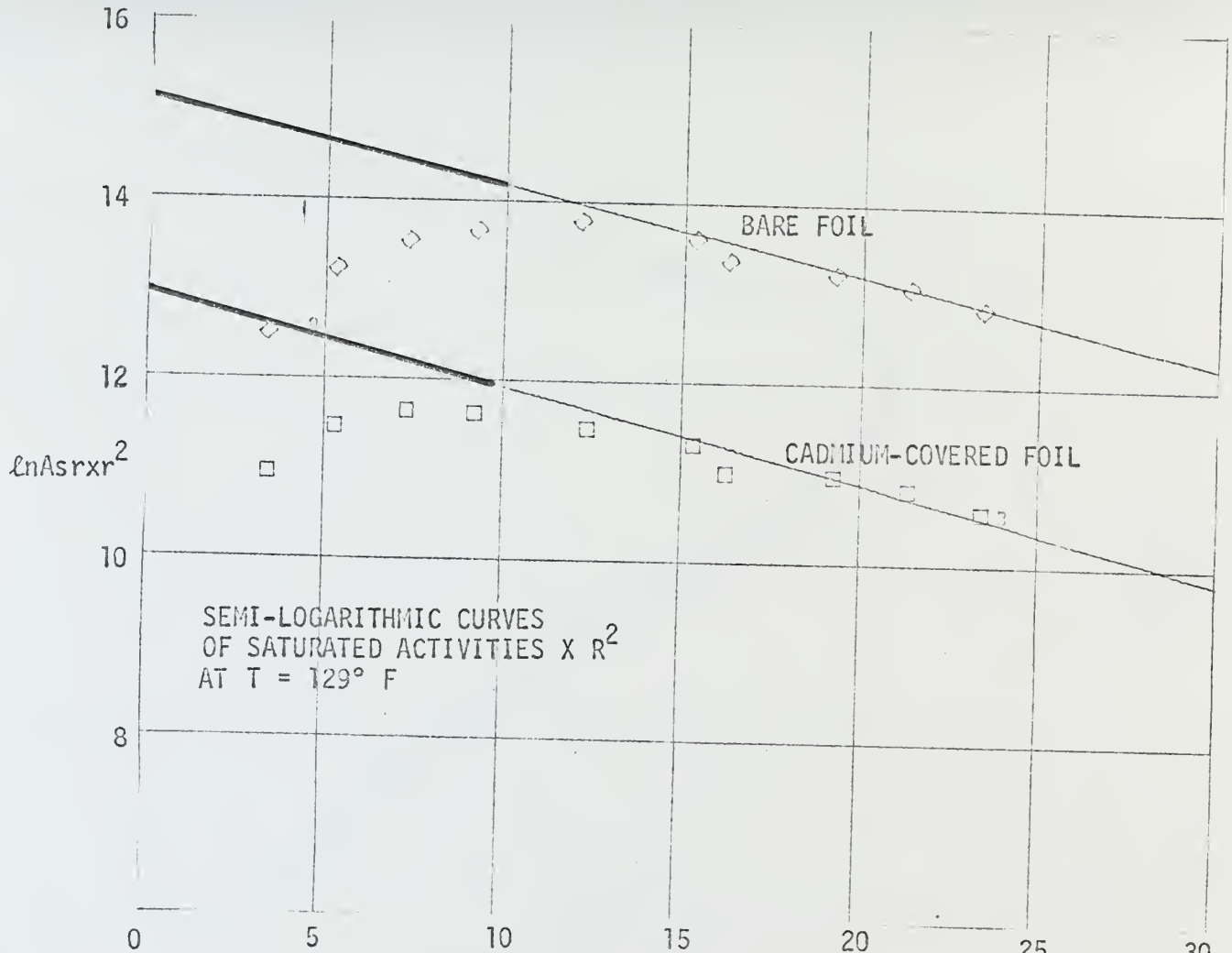
16
14
12
10
8
ℓnAsrxr^2
BARE FOIL
CADMIUM-COVERED FOIL
SEMI-LOGARITHMIC CURVES
OF SATURATED ACTIVITIES X R^2
AT T = 129° F
0
5
10
15
20
25
30
DISTANCE (cm)

FIGURE 17

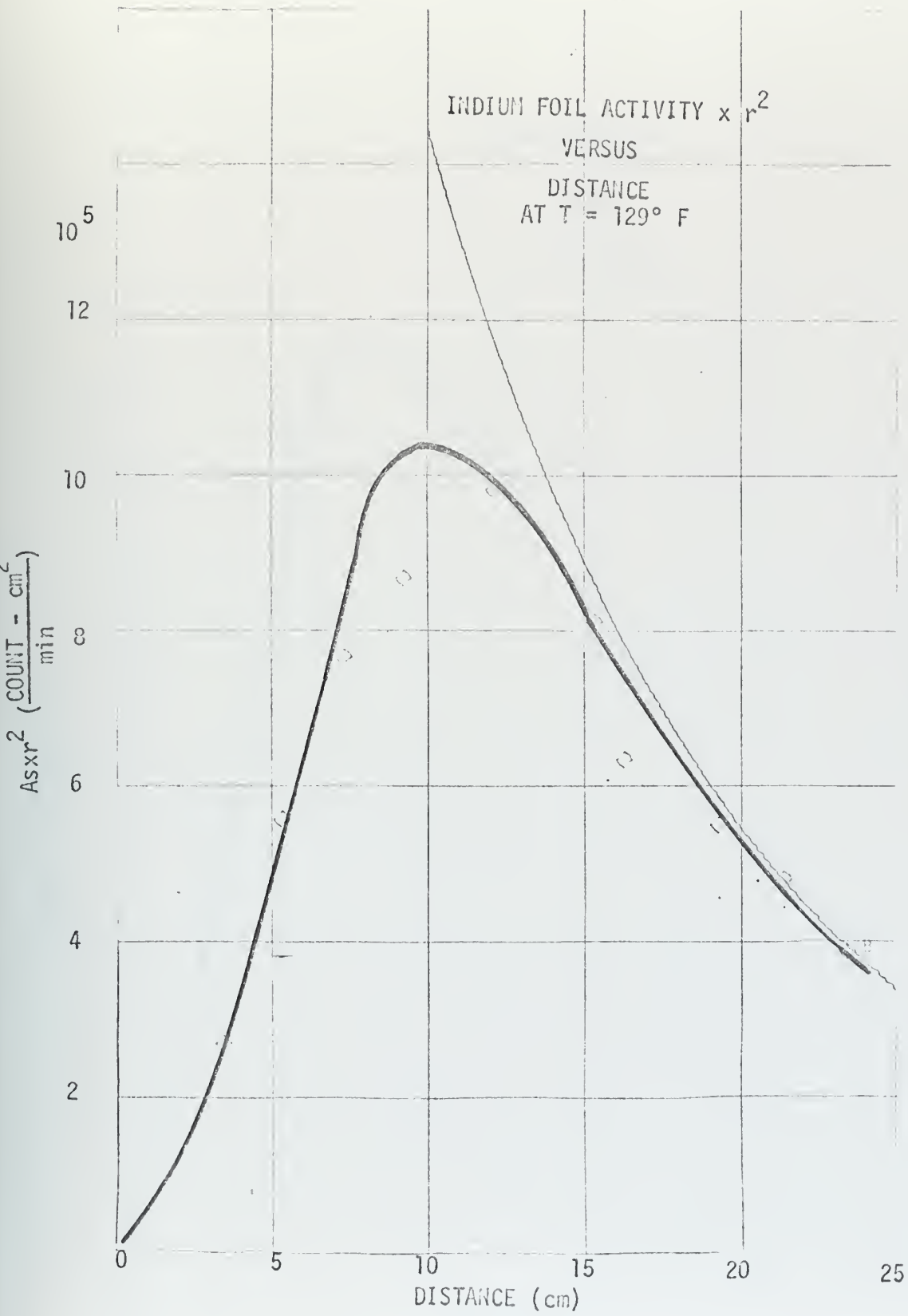
INDIUM FOIL ACTIVITY x r2
VERSUS
DISTANCE
AT T = 129° F
10 5
12
10
8
6
4
2
Asxr2 (COUNT - cm2 / min)
0
5
10
15
20
25
DISTANCE (cm)

FIGURE 18

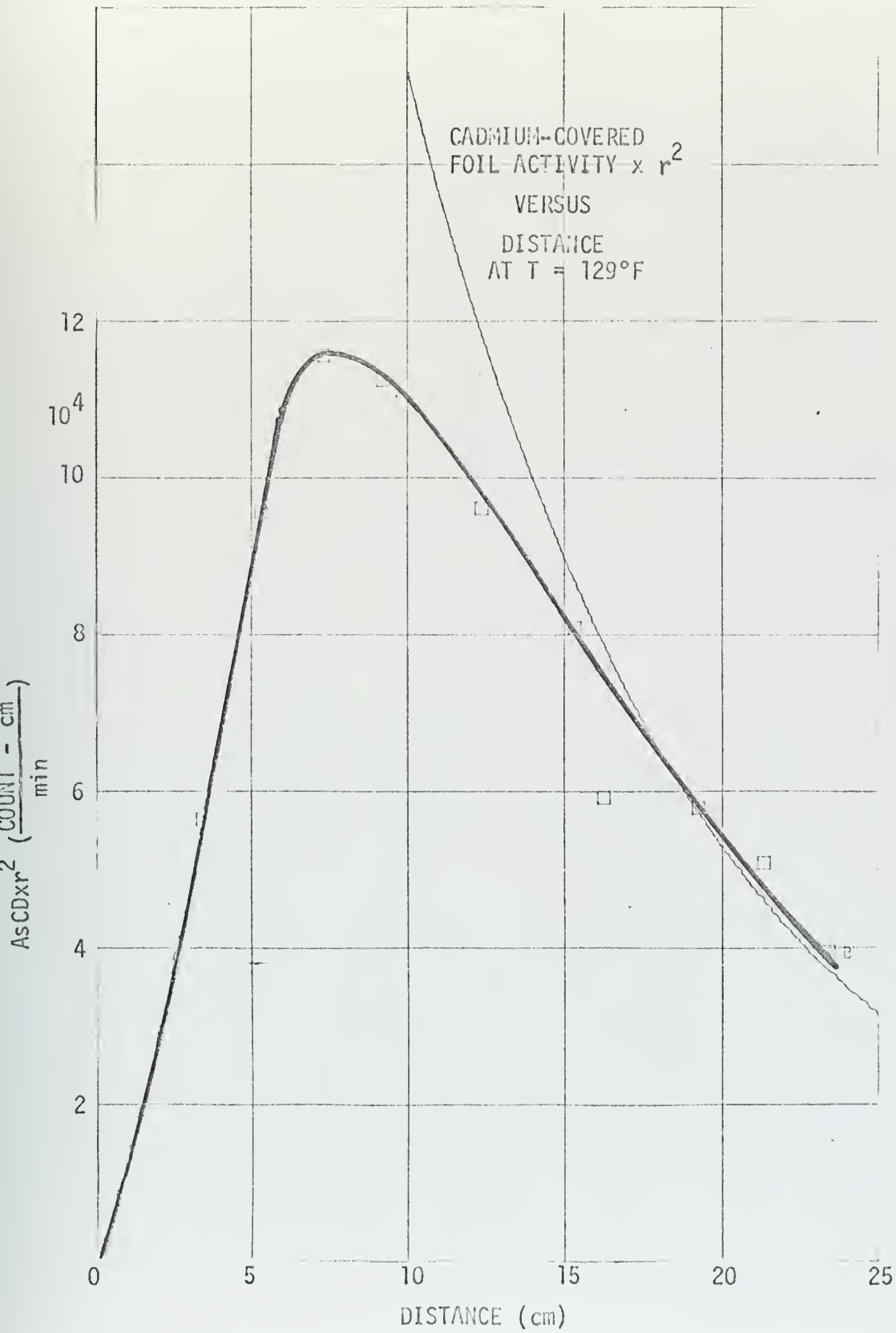
CADMIUM-COVERED
FOIL ACTIVITY x r^2
VERSUS
DISTANCE
AT T = 129°F
12
10^4
10
8
6
4
2
0
5
10
15
20
25
$A_s C_D x r^2$ ($\frac{COUNT - cm^2}{min}$)
DISTANCE (cm)

FIGURE 19

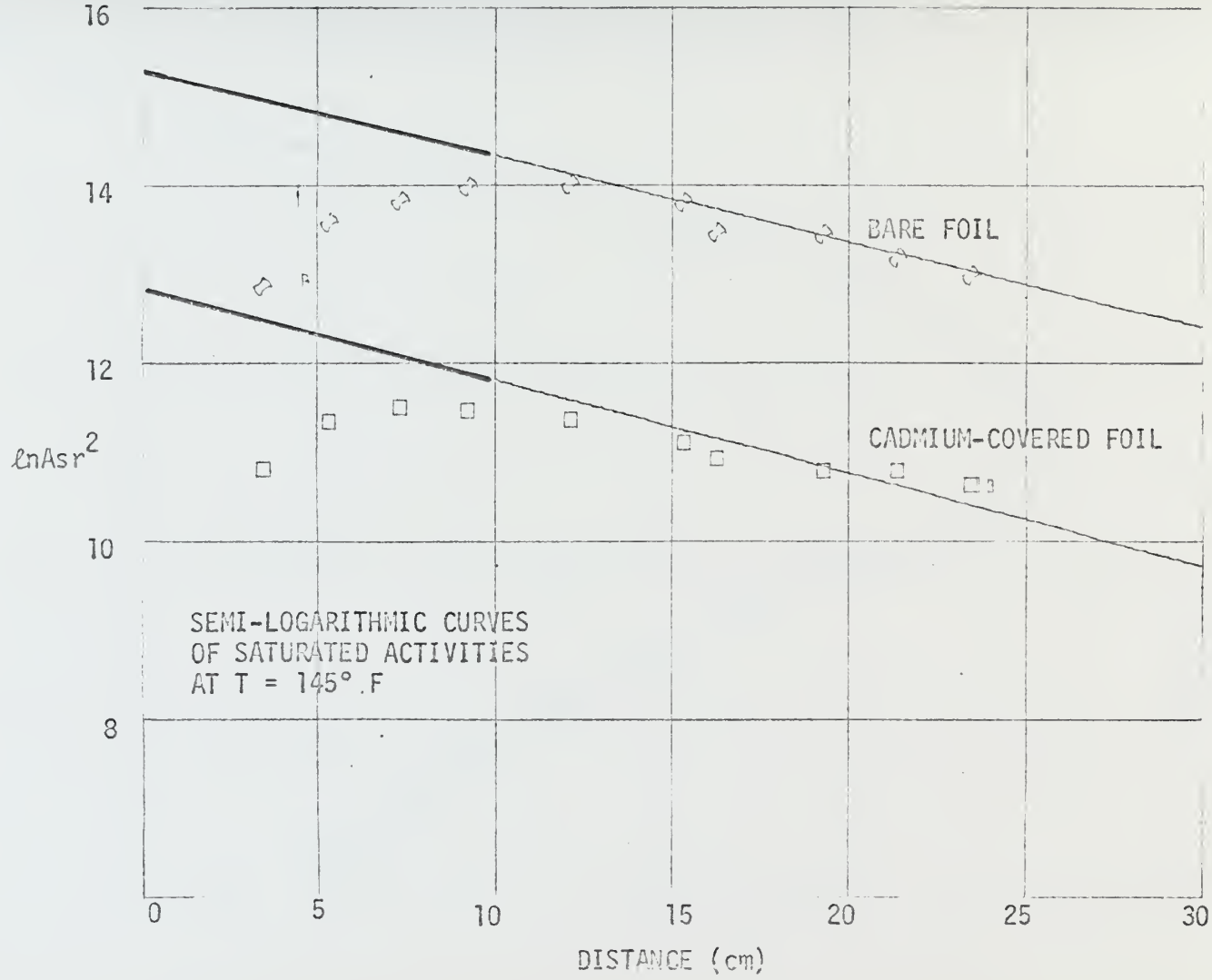
16
14
12
10
8
ℓnAsr²
BARE FOIL
CADMIUM-COVERED FOIL
SEMI-LOGARITHMIC CURVES
OF SATURATED ACTIVITIES
AT T = 145°.F
0
5
10
15
20
25
30
DISTANCE (cm)

FIGURE 20

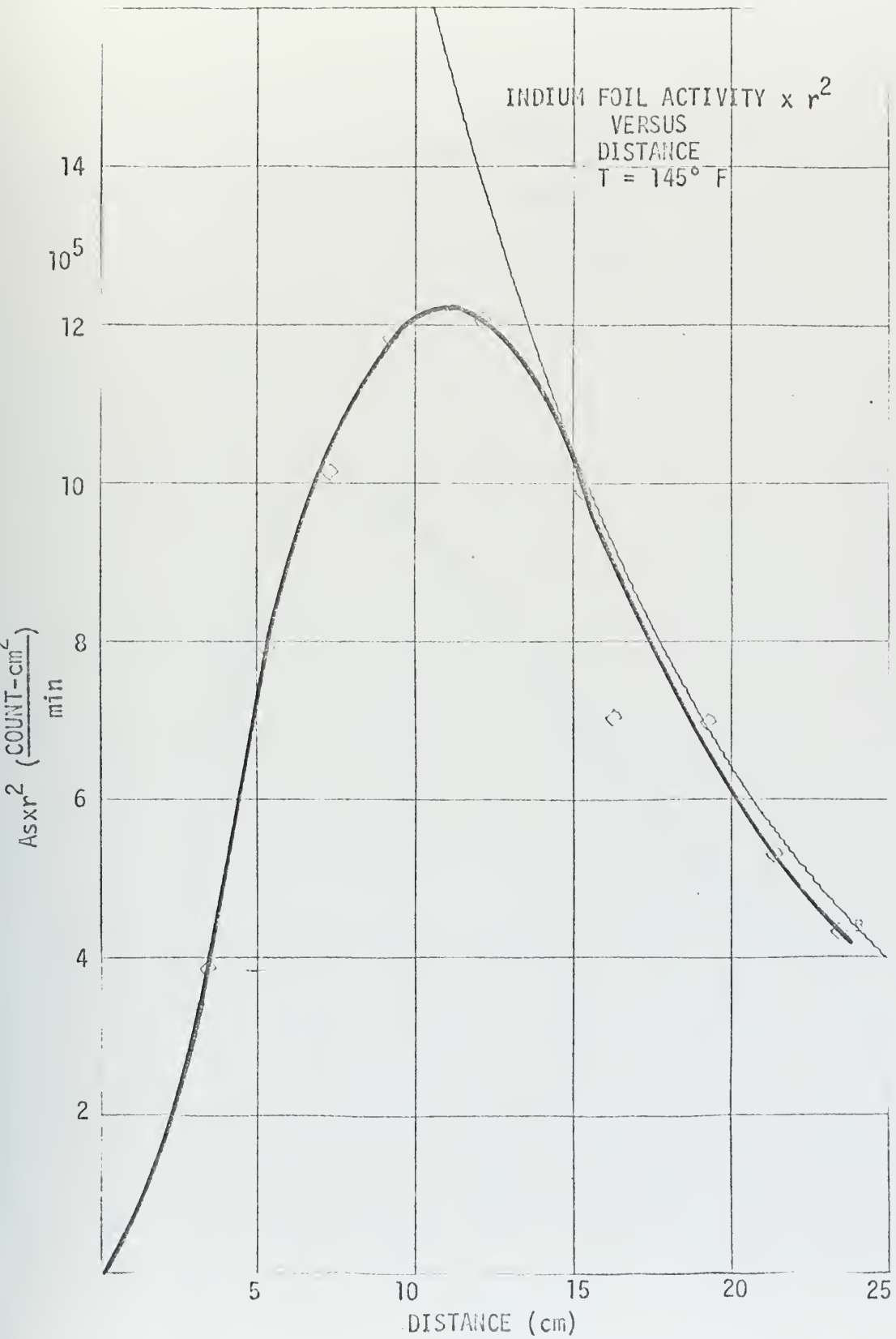
INDIUM FOIL ACTIVITY x r^2
VERSUS
DISTANCE
T = 145° F
14
10^5
12
10
8
6
4
2
$Asxr^2$ ($\frac{COUNT-cm^2}{min}$)
5
10
15
20
25
DISTANCE (cm)

FIGURE 21

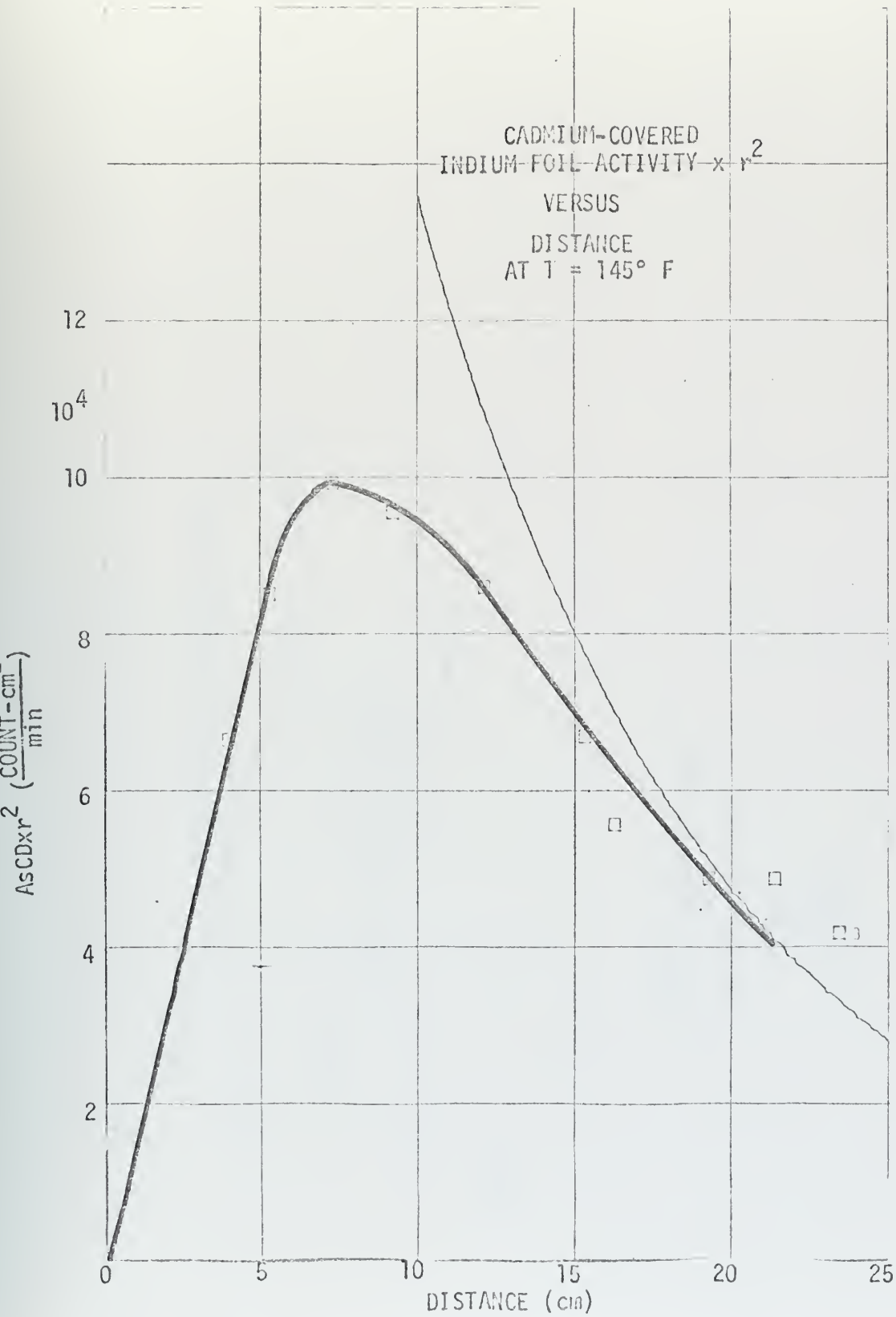
CADMIUM-COVERED
INDIUM-FOIL-ACTIVITY x r²
VERSUS
DISTANCE
AT T = 145° F
12
10⁴
10
8
6
4
2
0
5
10
15
20
25
DISTANCE (cm)
AsCDxr² (COUNT-cm²/min)

FIGURE 22

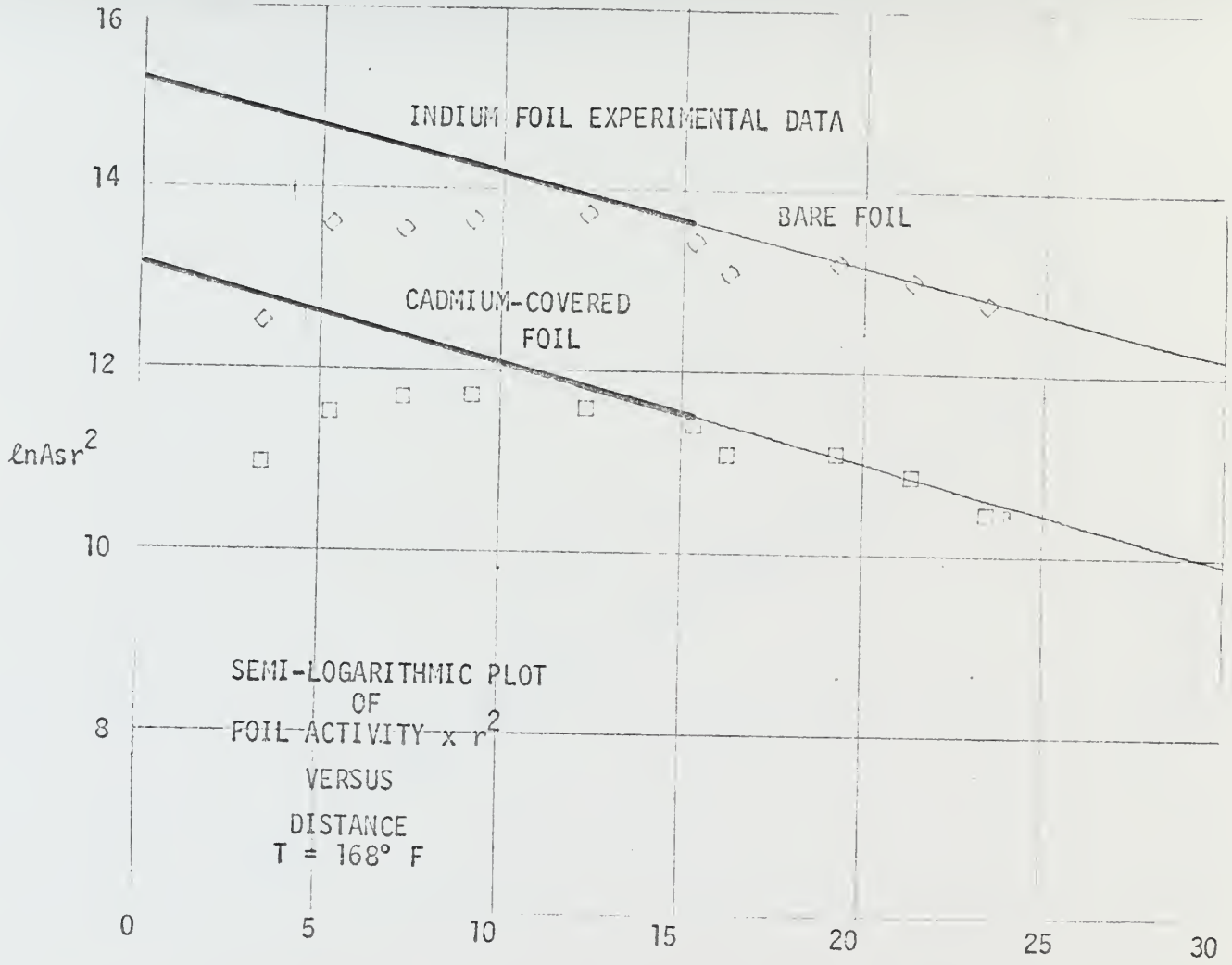
16
14
12
10
8
0
5
10
15
20
25
30
INDIUM FOIL EXPERIMENTAL DATA
BARE FOIL
CADMIUM-COVERED FOIL
ℓnAsr²
SEMI-LOGARITHMIC PLOT
OF
FOIL ACTIVITY x r²
VERSUS
DISTANCE
T = 168° F
DISTANCE (cm)

FIGURE 23

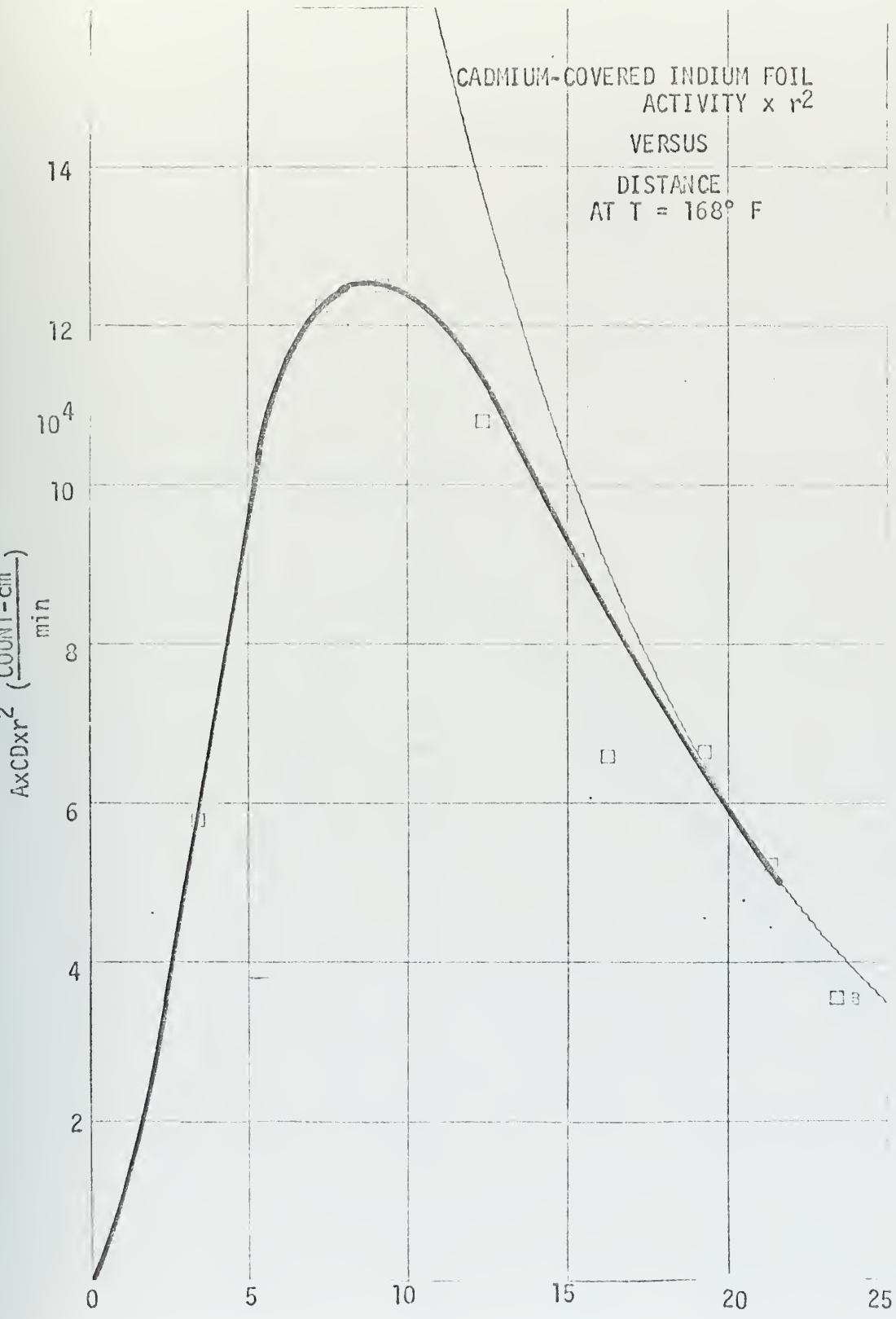
CADMIUM-COVERED INDIUM FOIL
ACTIVITY x r2
VERSUS
DISTANCE
AT T = 168° F
14
12
10^4
10
8
6
4
2
0
5
10
15
20
25
AxCDxr2 (COUNT-cm2/min)
DISTANCE (cm)

FIGURE 24

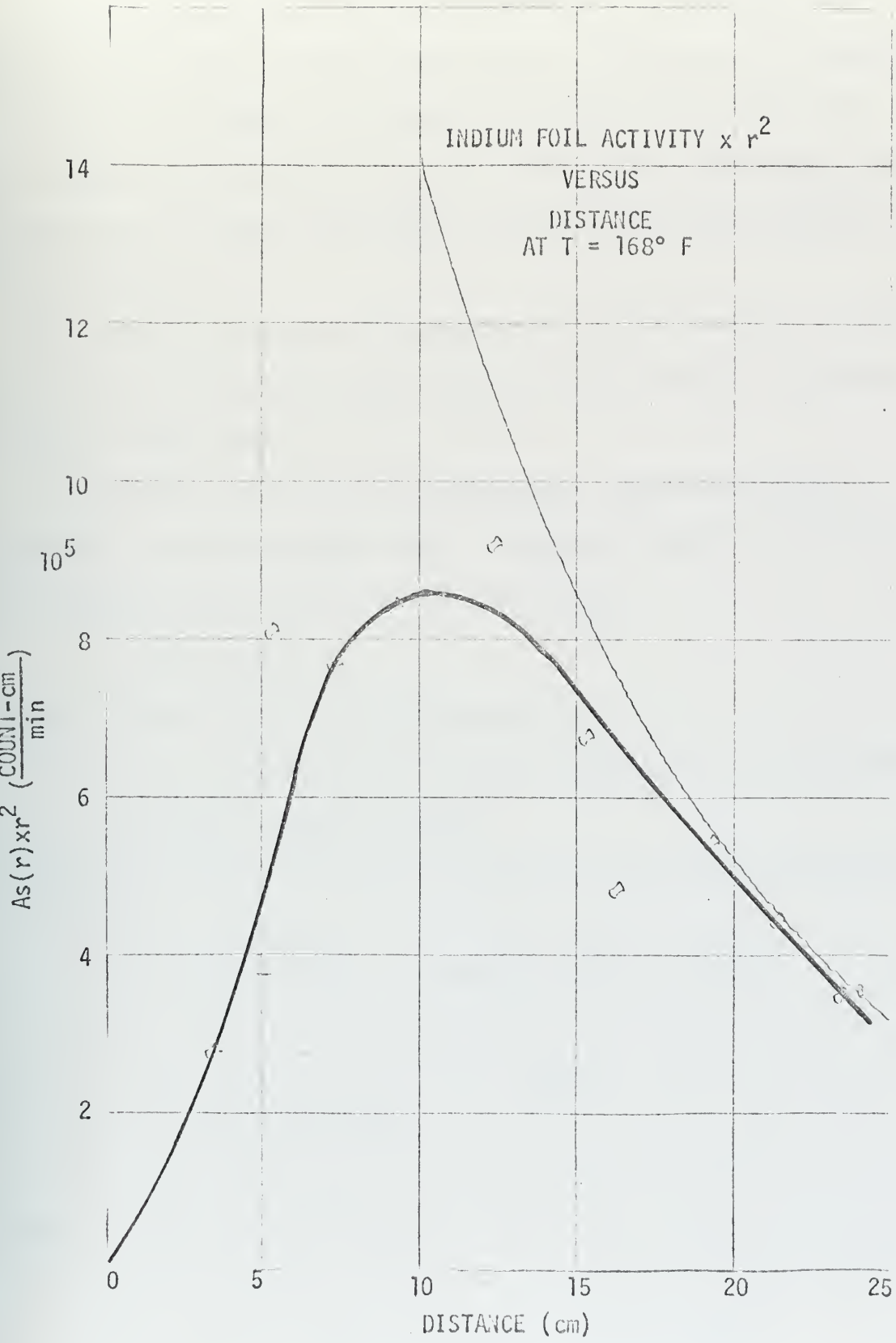
INDIUM FOIL ACTIVITY x r2
VERSUS
DISTANCE
AT T = 168° F
14
12
10
10^5
8
6
4
2
0
5
10
15
20
25
As(r)xr2 (COUNT-cm2/min)
DISTANCE (cm)

FIGURE 25

An error analysis based upon the statistical error (sigma) was conducted for one set of experimental data (T = 102°F) and is illustrated in Fig. 26. Two points of the experimental data do not fall within the region where the smooth curves have been drawn. These points were assumed to reflect poor experimental results and were not considered in the area analysis.

The additional errors considered were inaccuracies of foil positioning (±0.1 inch), foil removal/decay timing (±5 sec), temperature variations (±1°F) and human error.

An additional analysis of the Indium foil data was conducted to determine the thermal neutron flux. The neutron flux was obtained from the saturated activities in the following manner:

$$\phi(r) = CAs(r)$$

where $\phi(r)$ reflects the total neutron flux

C is a proportionality constant dependent on the Indium foils

As is the saturated activity

The proportionality constant was evaluated by the following expression:

$$Q = 4\pi\Sigma a \int_0^\infty \phi(r) r^2 dr = 4\pi\Sigma a C \int_0^\infty As(r) r^2 dr \quad [n/min]$$

or

$$C = \frac{Q}{4\pi\Sigma a \int_0^\infty As(r) r^2 dr} \quad [cm^{-2}]$$

where $\Sigma a = 2.22 \times 10^{-2} \ cm^{-1}$

Σa = macroscopic absorption cross section for water $[cm^{-1}]$

Q = neutron emission from source [neutrons/min]

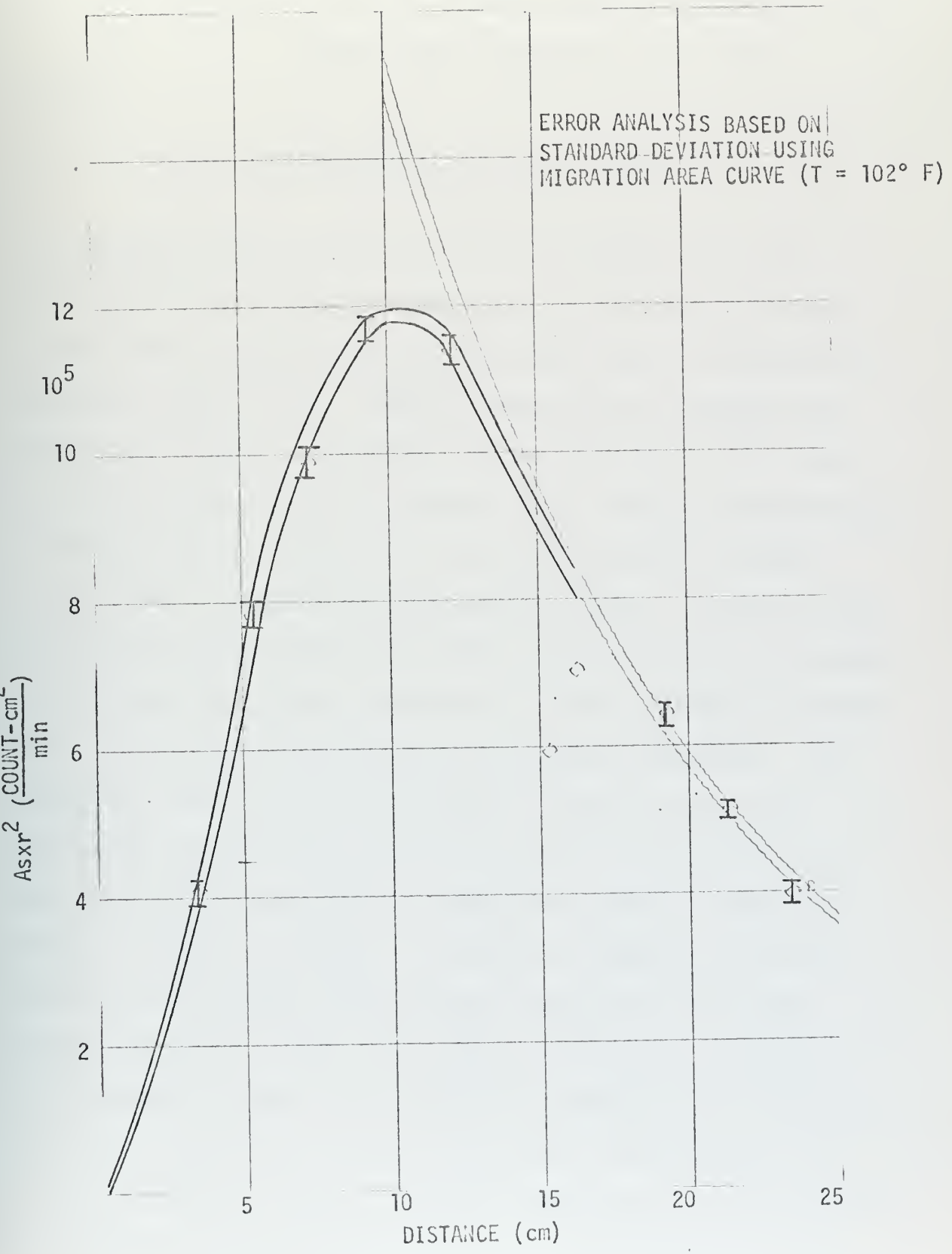
ERROR ANALYSIS BASED ON
STANDARD DEVIATION USING
MIGRATION AREA CURVE (T = 102° F)
12
10^5
10
8
6
4
2
Asxr^2 (COUNT-cm^2 / min)
5
10
15
20
25
DISTANCE (cm)

FIGURE 26

$$\int_0^\infty As(r)r^2dr = 2.172 \times 10^7 \text{ [count-cm}^3\text{/min] as determined from computer data (Appendix E) for T = 102°F}$$

such that

$$C = \frac{3.24 \times 10^8}{4\pi \times 2.22 \times 10^{-2} \times 2.172 \times 10^7} = 53.8 \text{ cm}^{-2}$$

A computer program (Appendix F) was used to evaluate the total and fast fluxes from their respective activities as a function of distance and temperature and also provide tabulated data (Table 4) and graphical presentation (Figs. 27-29). Computer computations also included the thermal flux by taking the difference of the total and the fast fluxes. The graphical plots of the fluxes do not clearly show the increasing trend of flux magnitude with temperature because the temperature increase is small (range of temperature investigated is small). In order to draw conclusions about the measured foil data, the tabulated data as presented in Table 4 must be analyzed. A review of this data reflects the general trend of increasing flux magnitude as a function of temperature. The experimental values of relaxation length as listed in Table 3 were investigated for temperature dependence. Figure 30 illustrates the linear relationship with temperature dependence which was found to be prevalent for relaxation length. Two curves are contained within the illustration and represent the relaxation lengths of the bare foils and the cadmium-covered foils. The slopes of both curves were found to be approximately the same. The difference in magnitudes was attributed to the smaller neutron population as seen by the cadmium-covered foil in that the relaxation length is inversely proportional to the scattering cross section of the surrounding medium. The assumption was made that

TABLE 3

Temperature	Migration Area	Age	Diffusion Length	Relaxation Length	
				Bare Foil	Cad Cov'd
°F	cm^2	cm^2	cm	cm	cm
77±1	63.47±2.5	52.7±2.5	$2.99^{+3.88}_{-2.99}$	10.51±.20	9.8±.20
102±1	64.83±2.5	54.7±2.5	$2.88^{+3.65}_{-2.88}$	10.44±.20	9.62±.20
129±1	66.4±2.5	55.9±2.5	$2.95^{+3.83}_{-2.95}$	10.31±.20	9.51±.20
145±1	66.31±2.5	55.85±2.5	$2.95^{+3.70}_{-2.95}$	10.32±.20	9.51±.20
168±1	67.4±2.5	55.8±2.5	$3.12^{+3.85}_{-3.12}$	10.01±.20	9.25±.20

TABLE 4

THERMAL FLUX AS DETERMINED FROM INDIUM ACTIVITY

AS A FUNCTION OF DISTANCE AND TEMPERATURE

Distance	Temperature (°F)				
cm	77	102	129	145	168
3.40	1705260	1602060	984089	1555272	1012910
5.31	1214872	1298770	874258	1338927	1340424
7.29	963343	873243	652245	918427	649144
9.20	664918	667324	477019	687269	452583
12.13	369541	378685	323021	406223	283719
15.32	197416	116835	166670	210250	133464
16.26	128919	129614	116461	132876	84164
19.28	81971	84217	70903	93521	68497
21.34	55770	54647	50530	56519	46092
23.41	35558	34542	33847	38232	30639

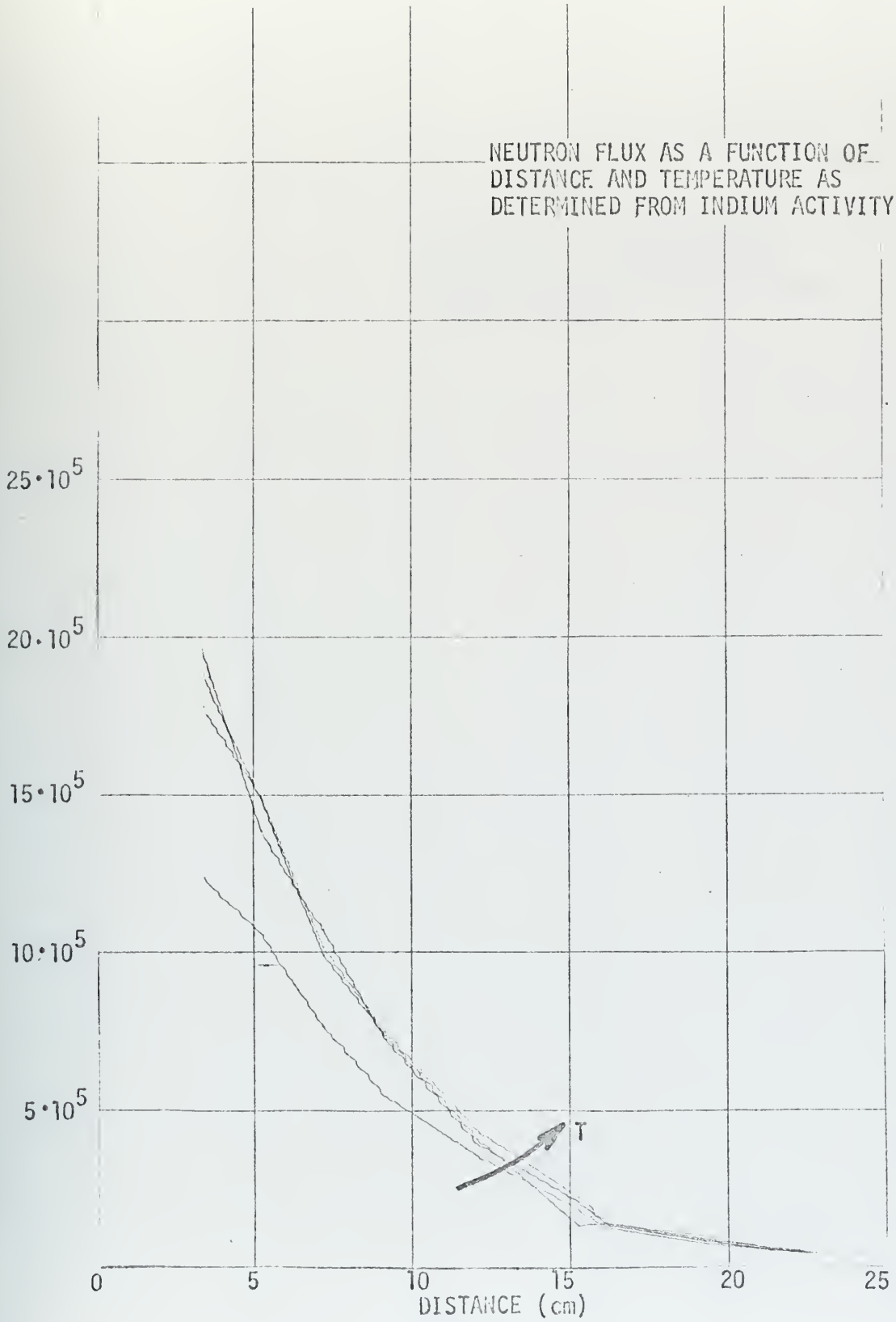
NEUTRON FLUX AS A FUNCTION OF
DISTANCE AND TEMPERATURE AS
DETERMINED FROM INDIUM ACTIVITY
25·10^5
20·10^5
15·10^5
10·10^5
5·10^5
T
0
5
10
15
20
25
DISTANCE (cm)

FIGURE 27

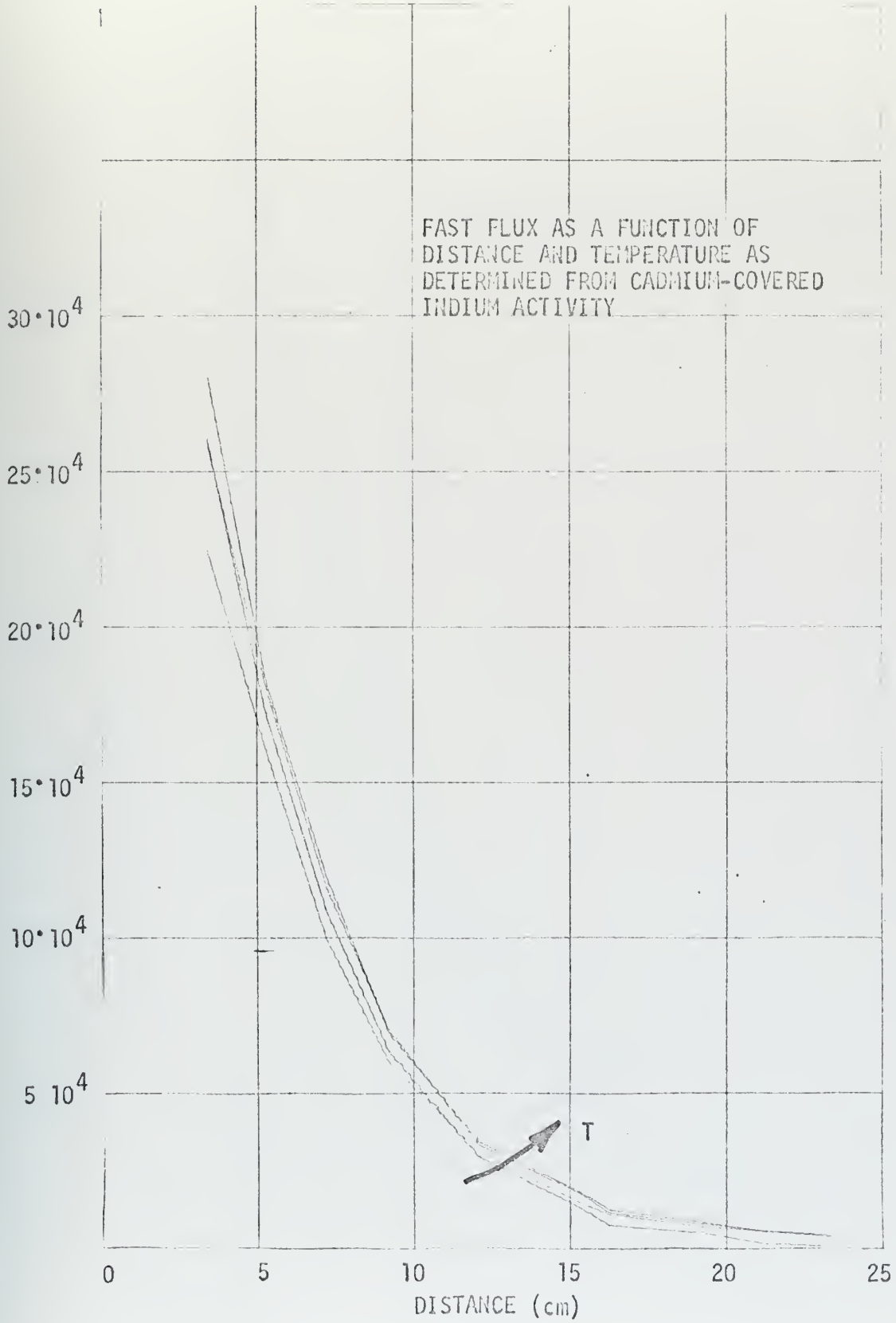
FAST FLUX AS A FUNCTION OF
DISTANCE AND TEMPERATURE AS
DETERMINED FROM CADMIUM-COVERED
INDIUM ACTIVITY
30·10^4
25·10^4
20·10^4
15·10^4
10·10^4
5 10^4
T
0
5
10
15
20
25
DISTANCE (cm)

FIGURE 28

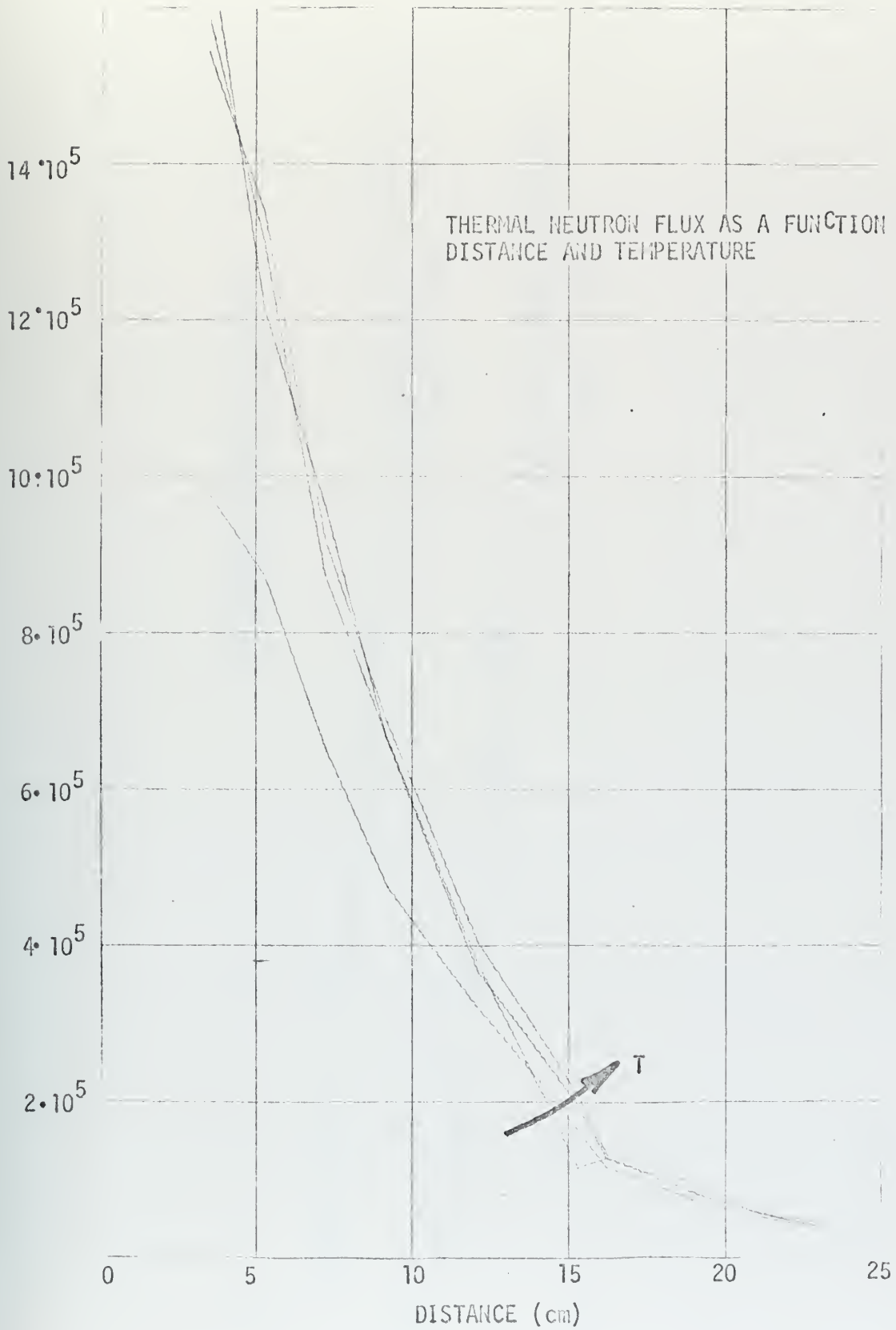
THERMAL NEUTRON FLUX AS A FUNCTION OF DISTANCE AND TEMPERATURE
14·10^5
12·10^5
10·10^5
8·10^5
6·10^5
4·10^5
2·10^5
T
0
5
10
15
20
25
DISTANCE (cm)

FIGURE 29

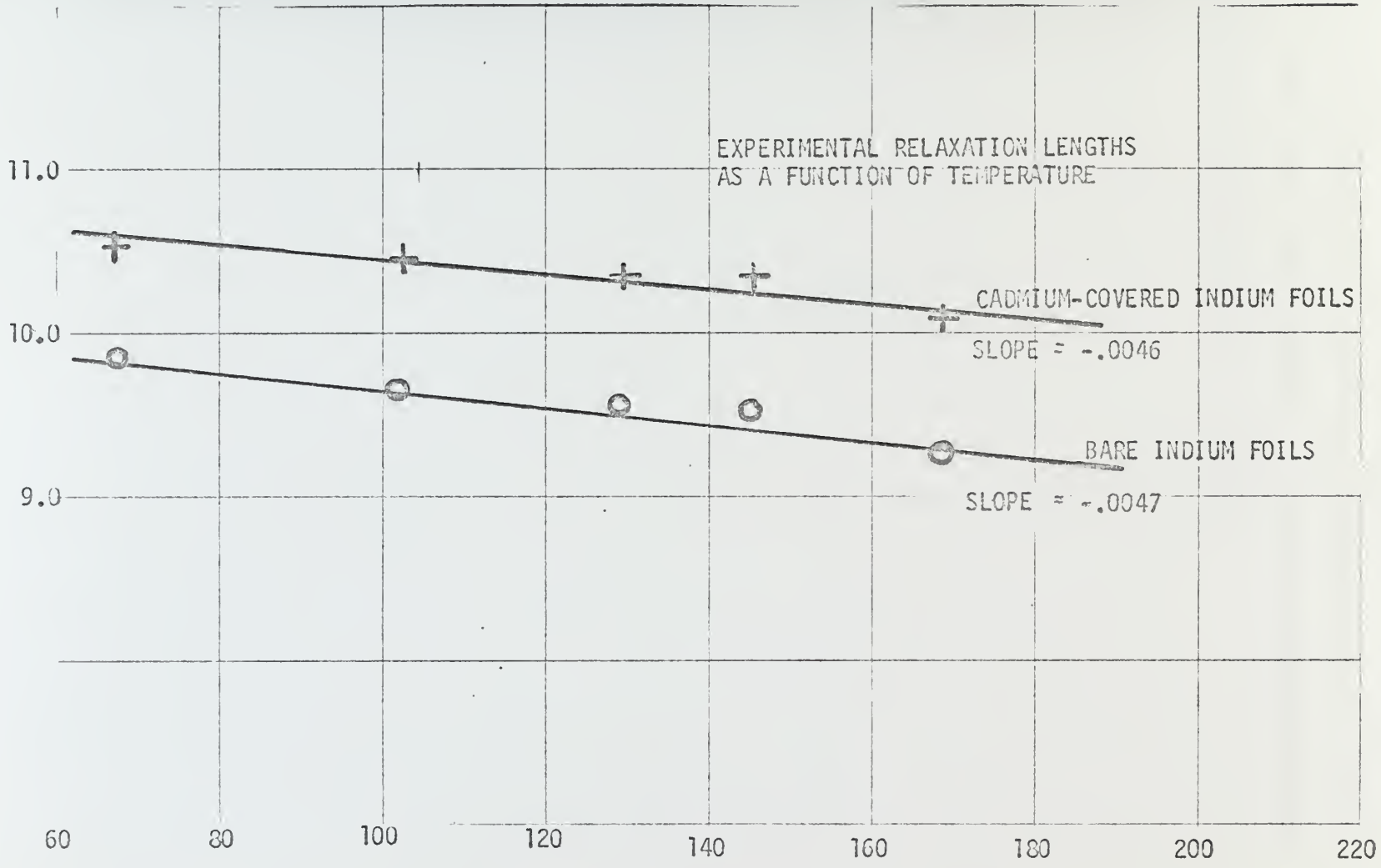
EXPERIMENTAL RELAXATION LENGTHS
AS A FUNCTION OF TEMPERATURE
CADMIUM-COVERED INDIUM FOILS
SLOPE = -.0046
BARE INDIUM FOILS
SLOPE = -.0047
11.0
10.0
9.0
60
80
100
120
140
160
180
200
220
TEMPERATURE (°F)

FIGURE 30

the relaxation length would be essentially linear in the temperature range investigated and this assumption is confirmed by the experimental results. Correlation of the theoretical versus the experimental data will be discussed in the comparison of results.

IV. EXPERIMENTAL DATA WITH CRYSTAL

A. DISCUSSION OF CRYSTAL DETECTOR

The basis of a scintillation counting system is the inherant characteristic of a phosphor to convert into light some fraction of the energy lost by ionization of a charged particle, while the particle passes through the phosphor material. The light that is emitted is detected by a photomultiplier tube (PM) and conmerted into an electrical pulse which is proportional to the magnitude and duration of the light source. The phosphor (crystal) used for the experiment was Lithium-Iodide with Europium enrichment (LiI(Eu)).

The interaction of the phosphor with the neutrons is as follows [1]:

$$ {}_{3}Li^{6} + {}_{0}n^{1} \rightarrow {}_{2}He^{4} + {}_{1}H^{3} + Q $$

To attain a greater freedom of manipulation in the source of experimentation a 5-1/2 foot section of flexible 1/4 inch light pipe was used to transmit the light signal from the crystal to the photomultiplier tube. An aluminum holder was used to provide a means of securing the light pipe to the photomultiplier tube. A light film of silicon grease was placed between the light pipe and the PM tube to insure maximum surface contact. The PM tube was then sealed by wrapping the tube with black rubber sheeting to insure no light leakage aside from the signal source received via the light pipe. The light pipe was in turn connected directly to the crystal by means of a hollow cylinder. The light pipe was secured to the aluminum cylinder by set screws. The crystal was placed inside the cylinder flush-up against the light pipe and was held secure by a washer, spring

and screw arrangement. Silicon grease was placed between adjoining surfaces of the light pipe and crystal. The arrangement described above provided easy access to the crystal which was required for insertion of a cadmium cover when measuring fast activities. The cadmium cylinder and washer were fabricated to fit around the crystal. The specific equipment used in this experiment is summarized in Table 5 and illustrated in Figs. 31 and 32.

TABLE 5

CRYSTAL DETECTOR EQUIPMENT

ITEM	DIMENSION	MANUFACTURER	MODEL
Crystal	4 mm	Harshaw Chemical	LiI(Eu)
Light Pipe	5-1/2' x 1/4"	American Optical Co.	---
Photomultiplier		Dumont	6292
Preamplifier		Hewlett-Packard	10615A
Voltage Supply		Hewlett-Packard	6516A
Timer-Scaler		Hewlett-Packard	5201L
Chart Recorder		Museley	7100B
Pu-Be Source (3 curie)		Baird-Atomic, Inc.	NUMEC-M

B. DETERMINATION OF CRYSTAL TEMPERATURE DEPENDENCE

The LiI(Eu) crystal's performance has been shown to be optimum at liquid nitrogen temperature [1]. The question that had to be resolved was to determine to what extent, if any, a variation in the temperature of the crystal affected the counting efficiency of the crystal.

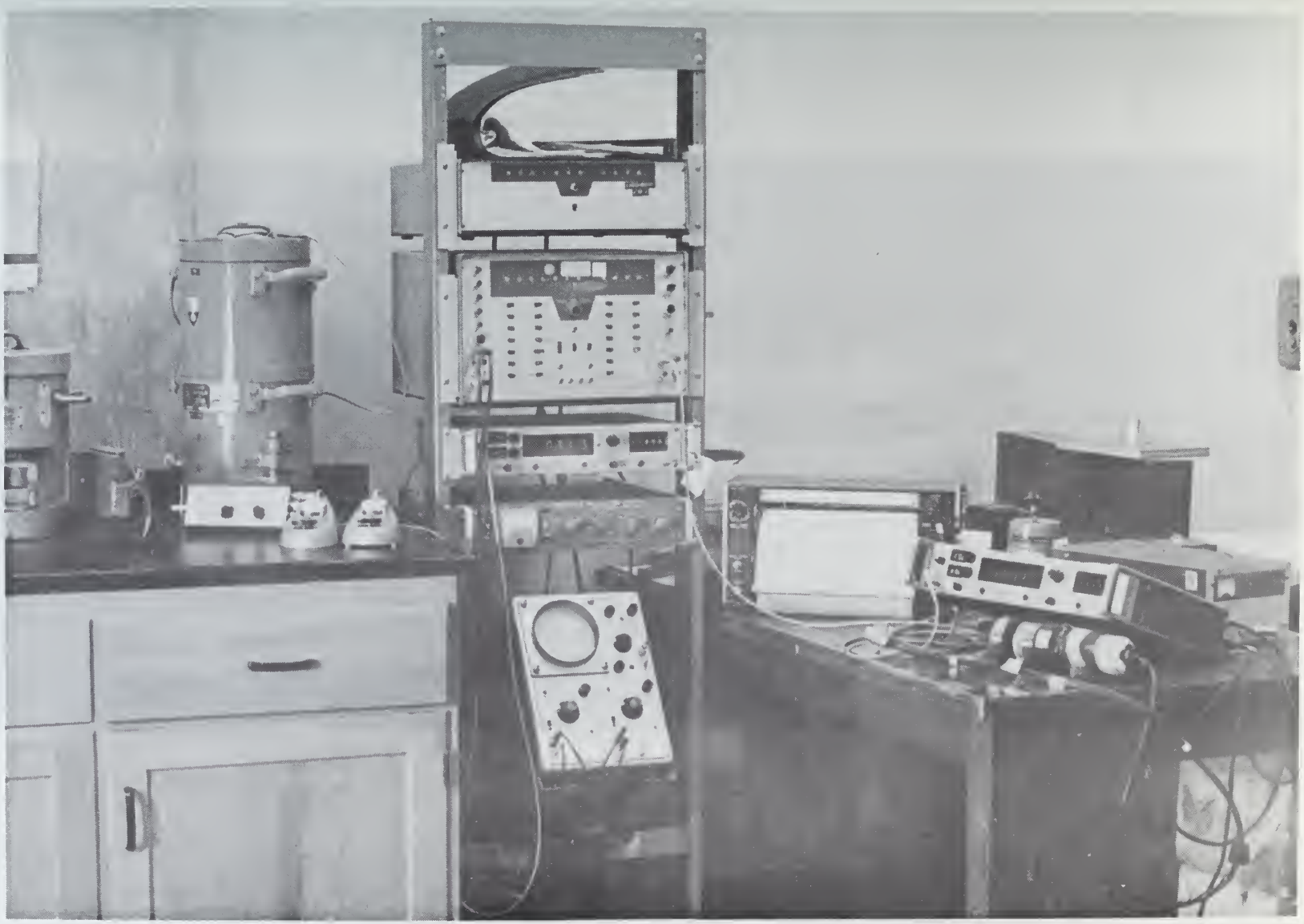

FIGURE 31

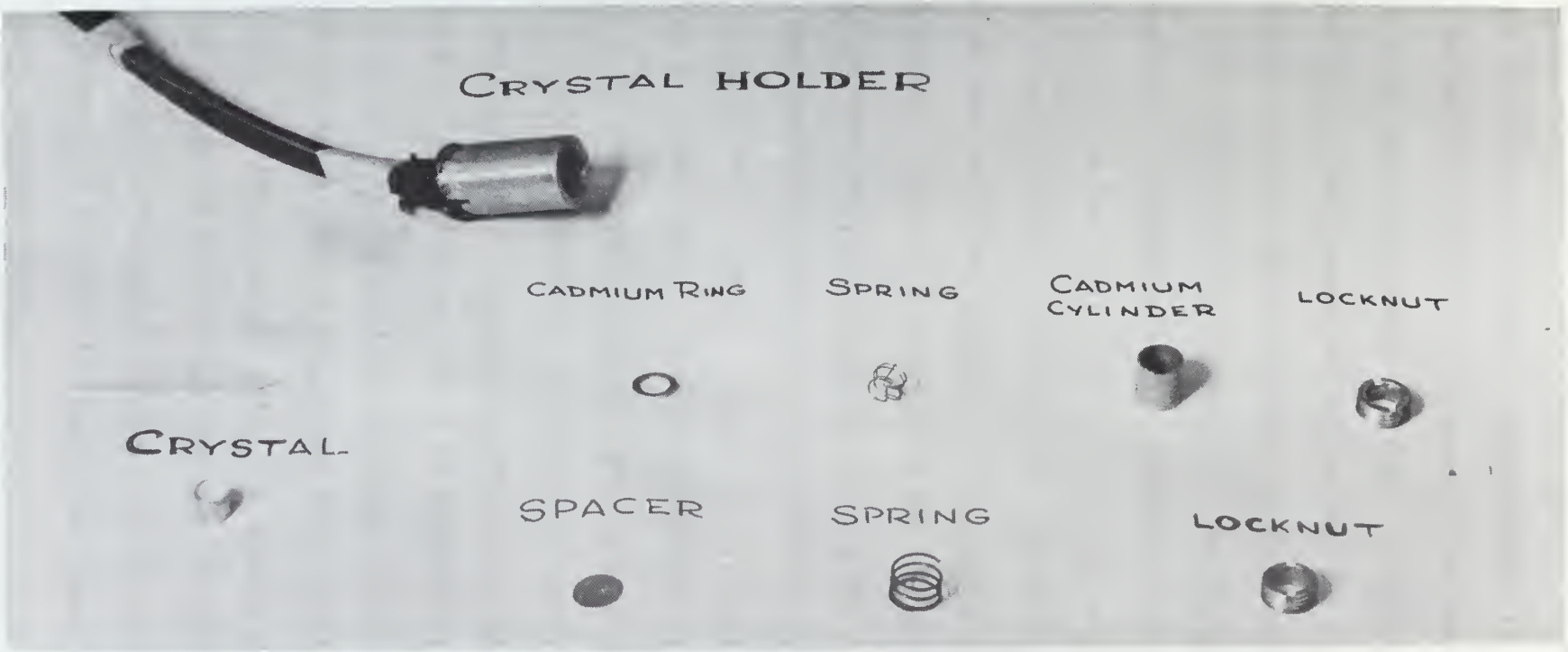
CRYSTAL HOLDER
CADMIUM RING
SPRING
CADMIUM CYLINDER
LOCKNUT
CRYSTAL
SPACER
SPRING
LOCKNUT

FIGURE 32

To establish the nature of temperature dependence on the crystal the following system was fabricated. Approximately 10 feet of flexible plastic (TYGON) tubing (1-1/4 inch OD) was bent in the shape of a U and partially inserted into the neutron howitzer. A rubber stopper was placed on the light pipe between the crystal and the PM tube. A thermocouple was inserted within the cylindrical aluminum holder containing the crystal such that the crystal temperature could readily be observed on a pen recorder. The aluminum holder containing the crystal and thermocouple and attached to the light pipe was inserted into the TYGON tubing and placed in close proximity to the source. The stopper was inserted into the end of the tubing and sealed. A Tee connection mating a smaller section of flexible tubing (1/2 inch OD) to the larger tubing was installed just below the rubber stopper sealing the light pipe.

The 1/2 inch section of tubing was connected to a water faucet. The remaining end of the 1 1/4 inch section was returned to the sink to function as a return line. By using hot and cold water the temperature in the vicinity of the crystal could be varied over a moderate range (63° F to 131° F) corresponding to the region of temperature interest. Figure 33 illustrates the arrangement of the crystal and the flexible tubing utilized to determine the effect of temperature on the crystal counting efficiency. The VISIFLUX howitzer was filled with 45 gallons of water which was maintained at a constant temperature. A Pu-Be source was placed within the source holder after the crystal was positioned adjacent midway between the source and the edge of the tank.

The aforementioned arrangement allowed a series of observations to be made at a constant neutron flux while the actual crystal temperature was varied over a moderate range.

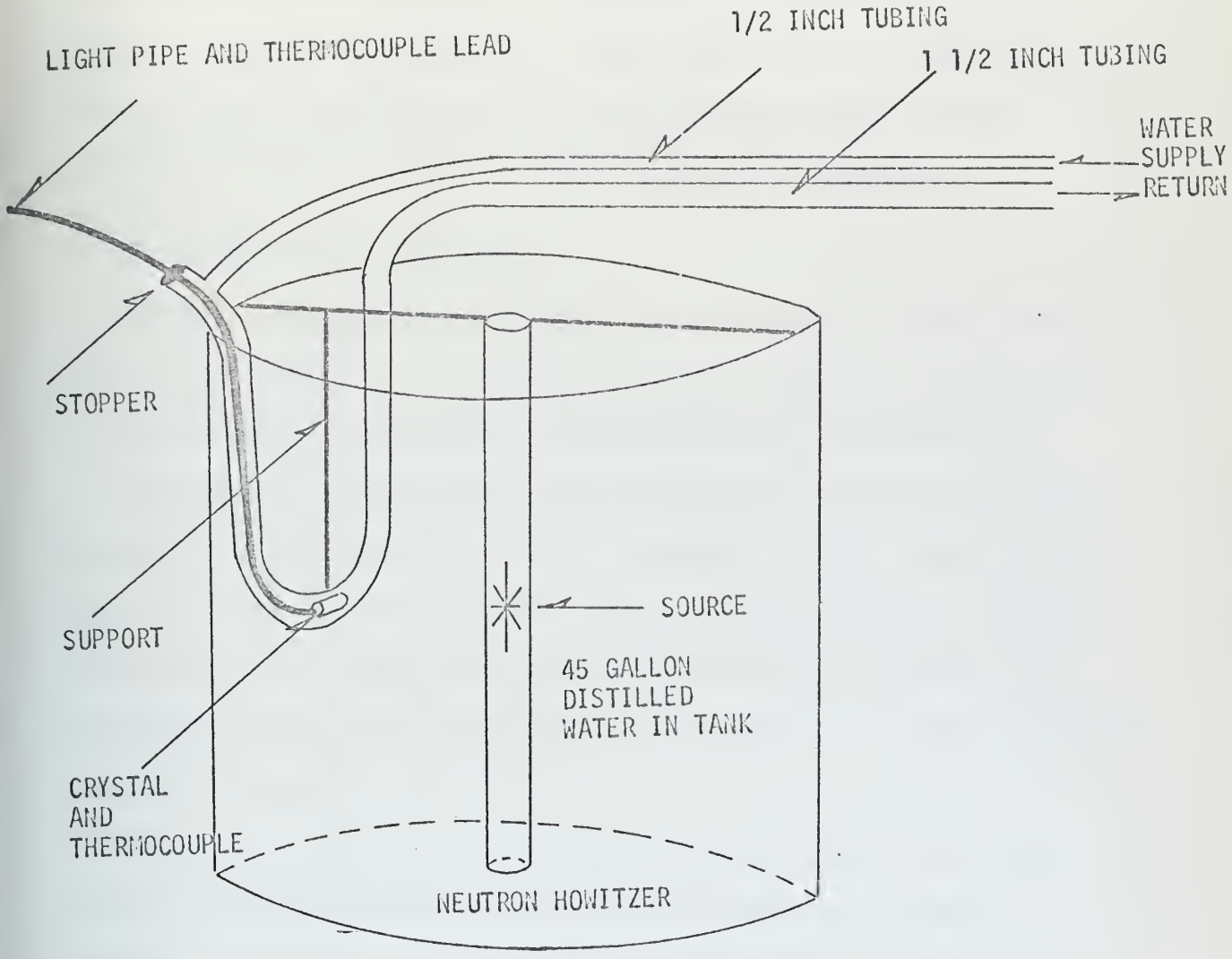

FLEXIBLE TUBING ARRANGEMENT USED IN DETERMINATION OF CRYSTAL TEMPERATURE DEPENDENCE

FIGURE 33

The observations indicated only random minor differences which in view of the large count rate are attributed to statistical error only. The conclusion drawn from this phase of the investigation was that the crystal counting characteristic is independent of temperature for the range of temperatures investigated. Experimental data as presented by Murray [3] partly substantiates the aforementioned; however, most of Murray's research pertains to temperatures well below zero.

C. DESCRIPTION OF THE EXPERIMENT

The major advantage of the phosphor detector and light pipe arrangement was the capability of obtaining considerable data in a short period of time as compared to the foil activation method of experimentation.

Measurement of neutron fluxes was obtained with the crystal detector by positioning the detector at varying distances from the source. The detector was shifted in a horizontal plane perpendicular to the center of the source. For comparison purposes the conditions at which foil measurements were carried out (position, water level, etc.) were duplicated as closely as possible.

The detection equipment was carefully tested for proper operating condition in the same manner as used for the Indium foil detection equipment; the results indicated that only statistical variations were in evidence. Two separate sets of readings of count rate versus distance were obtained for each temperature investigated. One set of readings reflected the total neutron population as seen by the crystal; whereas, the second set of readings represented only the fast neutron population as seen by the cadmium covered crystal. Background readings were taken at random before, during and after count rate observations. The recorded

data was corrected for background and the thermal flux was determined by taking the difference between corrected total and fast observed experimental values as listed in Tables 6 and 7. Table 8 lists the thermal flux with distance from the source in centimeters for comparison purposes with thermal fluxes obtained by alternate methods.

D. DISCUSSION OF RESULTS OF CRYSTAL EXPERIMENTAL DATA

A computer program was written for evaluating and plotting of the total, fast and thermal flux magnitudes versus distance at different temperatures. The computer program and experimental observations are listed in Appendix C and shown in Figs. 34, 35 and 36. The experimental data indicates a general increase in magnitude with an increase in temperature. The observed data as listed in Tables 6 and 7 reflect some inconsistencies in indicated counting rates; namely, some activities were found to be smaller in magnitude for the next higher temperature investigated. The aforementioned inconsistencies are attributed to a combination of statistical errors and positioning errors (location of detector from source); however, the overall trend of increased count rate as a function of temperature is apparent and consistent with the Two-Group solution as discussed in Section II-F.

The experimental data is only relative in magnitude in that an absolute monoenergetic neutron source was not available for calibration purposes. Collimated neutrons when incident normal to the crystal surface are absorbed at a rate proportional to the number of absorbing atoms present. The following expression relates the incident neutrons (Io) to the number of neutrons transmitted (I)

$$I = Io\, e^{-\Sigma i X} \qquad (18)$$

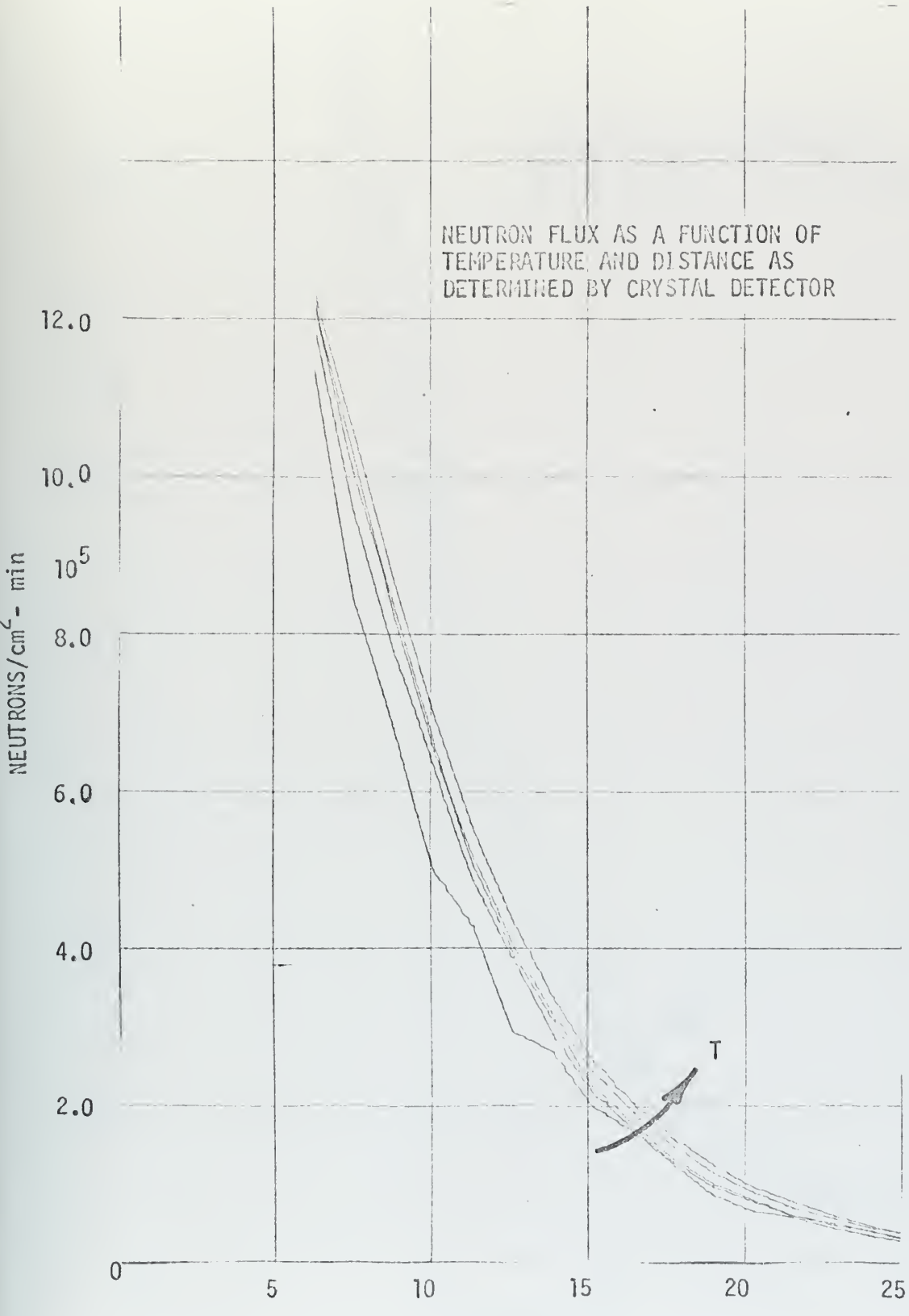
NEUTRON FLUX AS A FUNCTION OF
TEMPERATURE AND DISTANCE AS
DETERMINED BY CRYSTAL DETECTOR
12.0
10.0
10^5
8.0
6.0
4.0
2.0
0
NEUTRONS/cm^2- min
T
5
10
15
20
25
DISTANCE (cm)

FIGURE 34

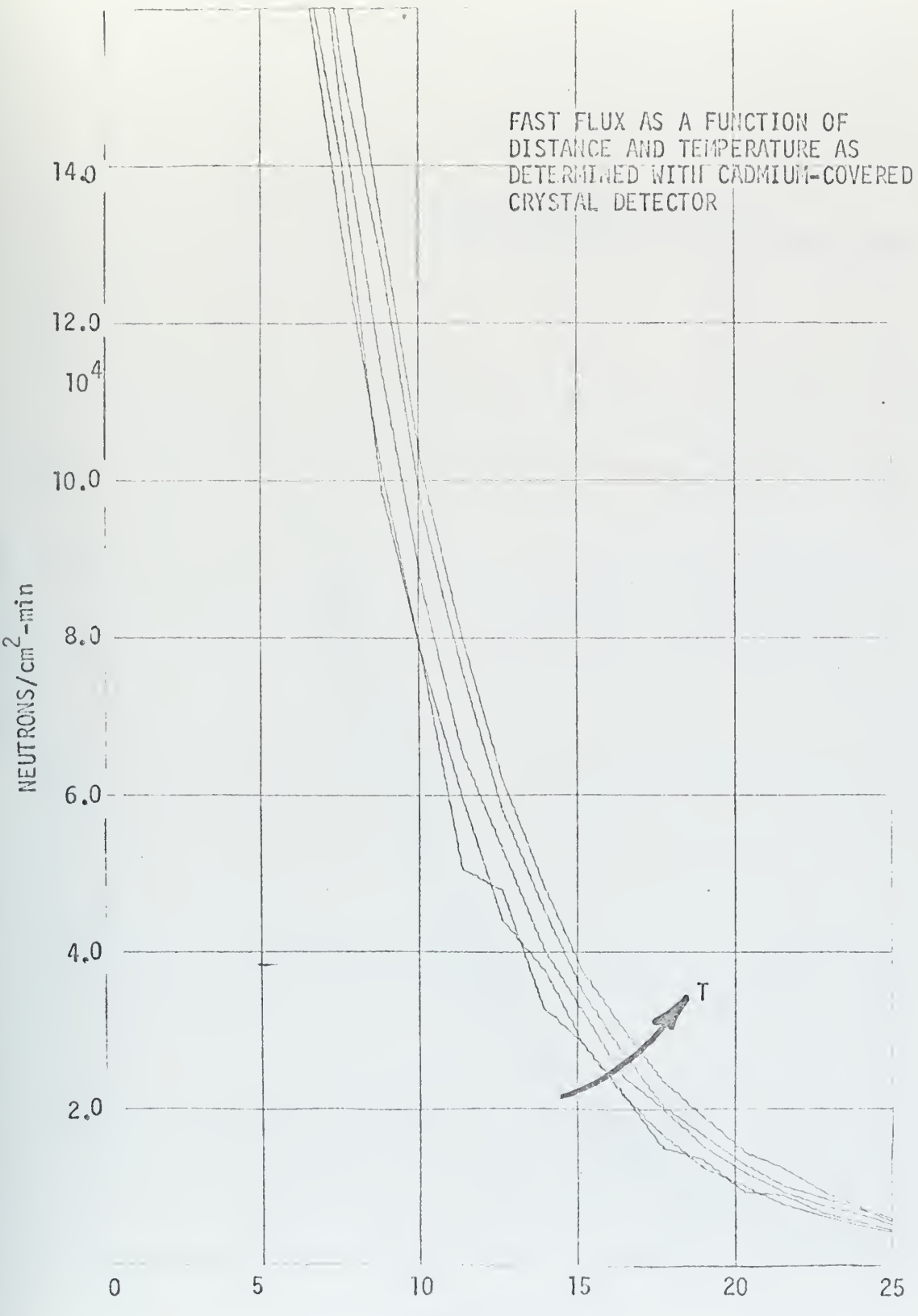
FAST FLUX AS A FUNCTION OF DISTANCE AND TEMPERATURE AS DETERMINED WITH CADMIUM-COVERED CRYSTAL DETECTOR
14.0
12.0
10^4
10.0
8.0
6.0
4.0
2.0
NEUTRONS/cm^2-min
T
0
5
10
15
20
25
DISTANCE (cm)

FIGURE 35

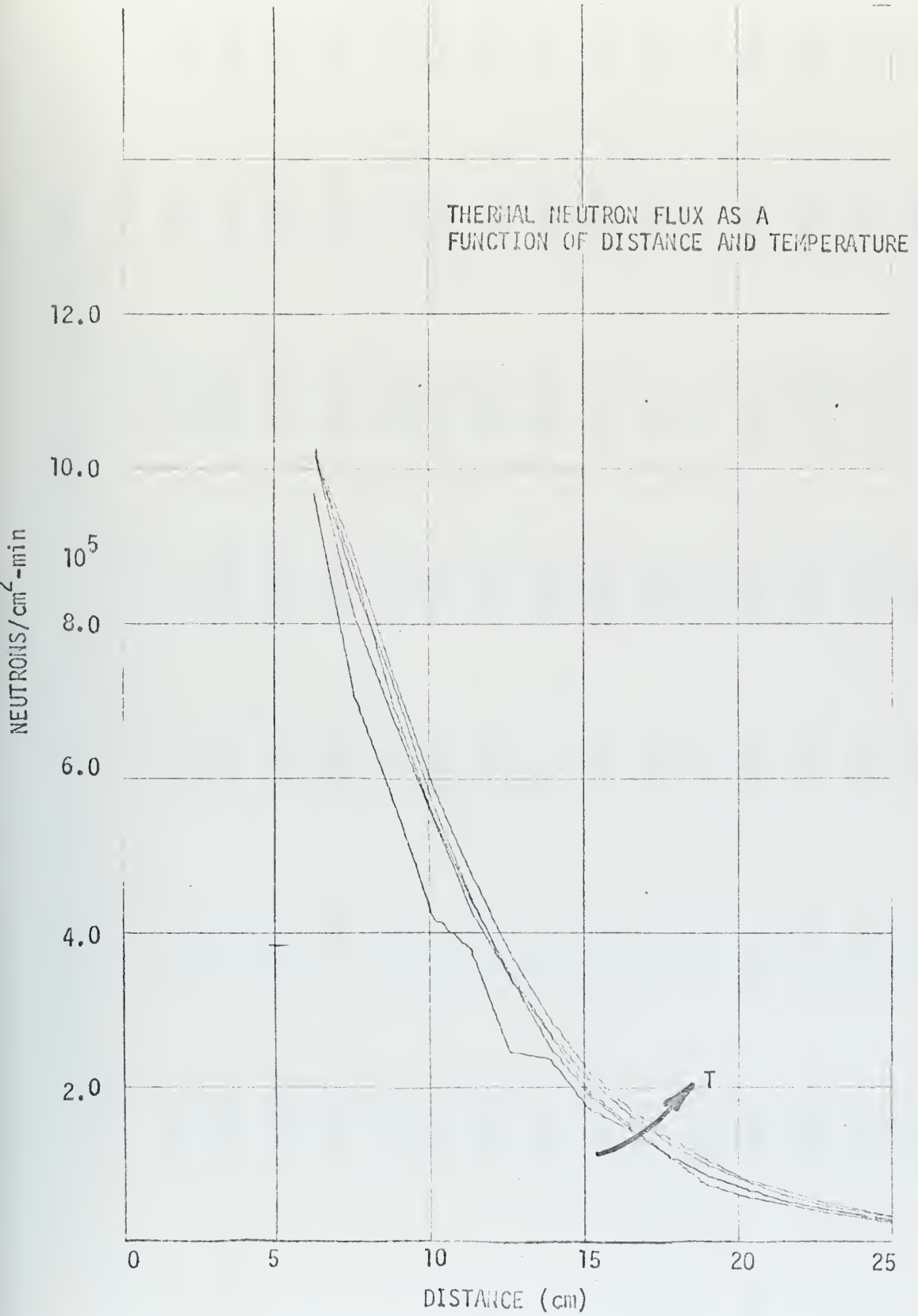
THERMAL NEUTRON FLUX AS A
FUNCTION OF DISTANCE AND TEMPERATURE
12.0
10.0
10^5
8.0
6.0
4.0
2.0
NEUTRONS/cm^2-min
T
0
5
10
15
20
25
DISTANCE (cm)

FIGURE 36

TABLE 6

EXPERIMENTAL CRYSTAL DATA AT DIFFERENT TEMPERATURES VERSUS DISTANCE

DISTANCE (Inches)	T = 84 F	T = 102 F	T = 123 F	T = 129 F	T = 134 F	T = 145 F	T = 168 F
2.5	286000	298446	292799	304331	302686	304526	308636
3.0	211020	238571	247936	250689	275102	257125	264682
3.5	170437	194947	202954	210380	204537	206885	218133
4.0	125252	157924	155945	165014	163311	163323	174308
4.5	107430	121938	122240	127491	125830	130007	139286
5.0	73602	97301	96021	99014	98310	101831	109333
5.5	67413	72725	73011	77283	76006	79350	84545
6.0	50353	54764	55792	56832	57974	61414	64731
6.5	42305	42625	42309	44264	45789	48344	51227
7.0	31785	32223	32369	33433	35257	37399	39509
7.5	22070	24868	25937	25664	26593	29334	31651
8.0	16985	19805	20837	20489	21410	22987	24080
8.5	14543	15123	16153	15482	17410	17900	19660
9.0	11477	12139	12337	12787	13301	14122	15045
9.5	8890	10051	10303	10082	10598	11385	11891
10.0	6962	7770	7700	7382	8085	9009	9266

TABLE 7

EXPERIMENTAL CADMIUM COVERED CRYSTAL DATA AT DIFFERENT TEMPERATURES VERSUS DISTANCE

DISTANCE (Inches)	T = 84 F	T = 102 F	T = 123 F	T = 129 F	T = 134 F	T = 145 F	T = 168F
2.5	42120	42500	47994	48047	48439	49418	51678
3.0	32922	35100	37768	36670	38106	39975	41314
3.5	25465	24760	29652	28599	29069	32006	33215
4.0	19332	19393	22496	21626	22181	24080	25314
4.5	12662	14962	17673	16400	17154	19019	20101
5.0	11976	11038	13502	13258	13554	14521	15515
5.5	8207	9473	10210	10125	10308	11399	12106
6.0	7127	7141	7749	8101	7981	8724	9375
6.5	5507	5500	5907	6086	6070	6811	7582
7.0	3765	4200	4781	5008	4799	5144	5908
7.5	3424	3193	3778	3821	3916	4185	4769
8.0	2395	2567	2918	3013	3073	3288	3687
8.5	2265	1968	2463	2388	2318	2566	3125
9.0	1671	1559	1968	1910	2037	2167	2364
9.5	1373	1290	1513	1625	1645	1765	1841
10.0	1074	1020	1300	1204	1223	1313	1427

TABLE 8

CRYSTAL THERMAL FLUX MAGNITUDES

AS A FUNCTION OF DISTANCE AND TEMPERATURE

Distance	Temperature (°F)				
cm	84	102	129	145	168
6.349	975520	1023784	1025136	1020432	1027832
7.619	712392	813884	856076	876076	893432
8.889	579838	680748	727124	699516	739672
10.16	423680	554124	573552	557172	595976
11.42	379072	428048	444364	443952	476740
12.70	246504	345052	343024	349240	375272
13.96	236824	253008	268632	271804	289756
15.24	172904	190492	194924	210760	221424
16.50	147192	148500	152712	166132	174580
17.77	112080	112092	113700	129020	134404
19.04	74584	86700	87372	100596	107528
20.31	58360	68952	69904	78796	81572
21.58	49112	52620	52376	61336	66140
22.85	39224	42320	45408	47820	50724
24.12	30068	35044	33828	38460	40308
25.39	23552	27000	24712	30784	31356

Σi = linear absorption coefficient

X = thickness of crystal

The crystal used during this phase of the investigation was a hermetically sealed unit in that the LiI(Eu) phosphor is extremely hygroscopic (moisture sensitive). The crystal thickness (X) was on the order of 4 millimeters. The linear absorption coefficient is reported as 16.7 cm^{-1} [1]. The composition of the enriched LiI crystal along with relative properties [1] are listed in Table 9.

TABLE 9

Nucleus	Relative Concentration	Ni (n/cm^3)	σi (barns)	$Ni\sigma i$ (cm^{-1})
Li^7	4.4	$8x10^{20}$	0.033	--
Li^6	95.62	$1.74x10^{22}$	950	16.5
I	100.0	$1.82x10^{22}$	6.3	0.115
Eu	0.05	$1.09x10^{19}$	4300	0.048
				16.663

The efficiency for the LiI(Eu) crystal can be computed by the following expression [1]:

$$\eta = \frac{(Ni\sigma i)Li^6}{\Sigma i}\left[1 - e^{-\Sigma i X}\right]$$

$$\eta \simeq \frac{16.5}{16.7}\left[1 - e^{-16.7(.4)}\right] \simeq 92.6\%$$

The calculated value for the efficiency is impressive; however, the size of the crystal must be considered. The number of neutrons that are transmitted through the crystal (do not interact) can be determined by evaluating equation (18) as follows:

$$I = Io\ e^{-16.7(0.4)} = 0.00125\ Io$$

The number of neutrons that interact = (1 - 0.00125)Io, thus further emphasizing the calculation for high efficiency.

The efficiency equation applies rigorously to a crystal with a very large radius. Since the crystal used for this phase of the experiment had a very small radius (4mm) it is expected that many neutrons escape the crystal radially resulting in a reduced efficiency.

E. SOFT GAMMA INFLUENCE AND MULTICHANNEL ANALYZER ANALYSIS OF DATA

The Pu-Be source used for the experimental phase of the investigation was a 3 curie source with an approximate yield of 5.4×10^6 neutrons per second and a half-life of 24,400 years distributed by Baird-Atomic, Inc. (Model NUMEC-M). The neutrons are obtained from the Pu-Be source by the following reactions

$$_{94}Pu^{239} \rightarrow {}_{2}He^{4} + \gamma + X^{*} \rightarrow$$

$$_{4}Be^{9} + {}_{2}He^{4} \rightarrow {}_{6}C^{12} + {}_{0}n^{1}$$

Energetic Gamma rays can also react with beryllium to emit neutrons; however, the gamma rays of the plutonium do not have adequate energy for the reaction to occur and are distinguished as soft gamma rays. In an attempt to ascertain the effectiveness of the cadmium-covered crystal a multichannel analyzer was used to obtain the spectrum of the crystal. Figure 37 illustrates the results obtained on the multichannel analyzer and represents two separate input presentations; namely, the crystal without cadmium and the crystal with cadmium. The spectrum results indicate that the cadmium cover has removed virtually all the thermal neutrons and that the crystal is subjected to only fast neutrons when enclosed by the cadmium.

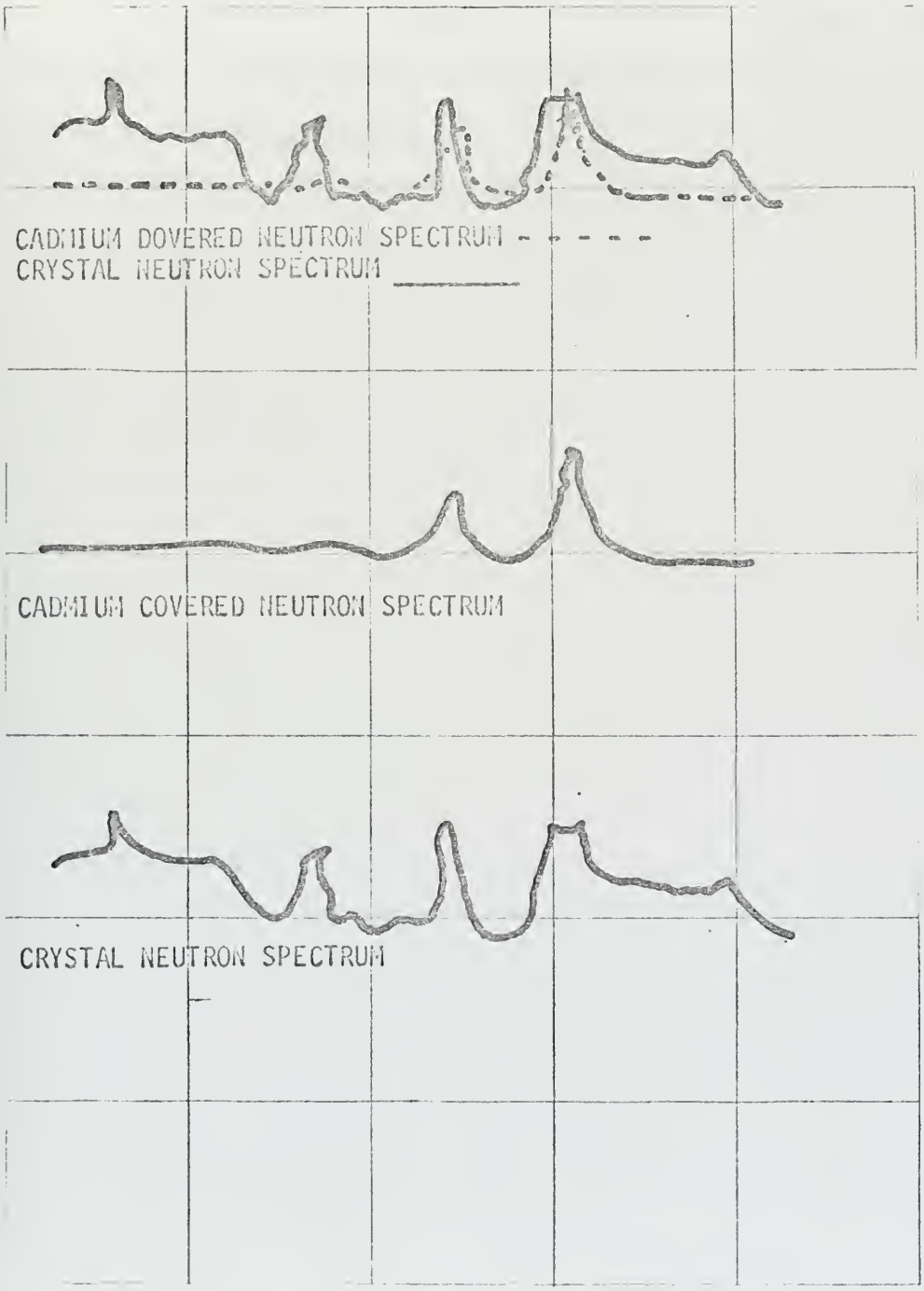
CADMIUM DOVERED NEUTRON SPECTRUM - - - - -
CRYSTAL NEUTRON SPECTRUM _____
CADMIUM COVERED NEUTRON SPECTRUM
CRYSTAL NEUTRON SPECTRUM

FIGURE 37

A discrimination technique whereby the gamma influence can be separated from the neutron population as proposed by Furuta, Kinbara, and Kaieda [10] was considered for a more sophisticated approach to the analysis. This technique was not applied and the data presented merely reflects the trend of the influence of the cadmium cover with the crystal as observed on the spectrum analyzer.

V. COMPARISON OF THEORETICAL AND EXPERIMENTAL RESULTS

A. THEORETICAL VERSUS INDIUM FOIL DATA

The theoretical and the Indium foil data show excellent correlation in comparison of flux magnitudes. A pair of curves (T=102° F) representing the thermal flux as determined from theory and by Indium experimental data are illustrated in Fig. 38. The curves were plotted from the computer data (Appendices C and F) as listed in Tables 4 and 10. This tabulated data has been rounded off for simplicity of presentation. The temperature trend of both the theoretical and the foil thermal fluxes indicate an increase in magnitude at higher temperatures.

The experimental values of migration area, thermal age and diffusion length have been superimposed upon the theoretical curves of these temperature dependent parameters as per Figs. 39 and 40. The experimental values with the exception of diffusion length were found to be slightly higher than the theoretical values. The discrepancies between the theoretical and experimental data are mostly attributed to one assumption used in the derivation of the theoretical expression. The theoretical equation for thermal flux was derived for an infinite medium; whereas, the experimental thermal flux was actually determined from a finite medium. The experimental phase was effected by neutron leakage, i.e., neutrons were lost at the extremities of the VISIFLUX howitzer. The infinite medium has no neutron leakage in that all are absorbed within the medium. The investigation into relaxation length established several theoretical relationships such as a small positive slope for relaxation length with temperature dependence and also that the magnitude was on the order of 10. With reference to Fig. 30, the relaxation

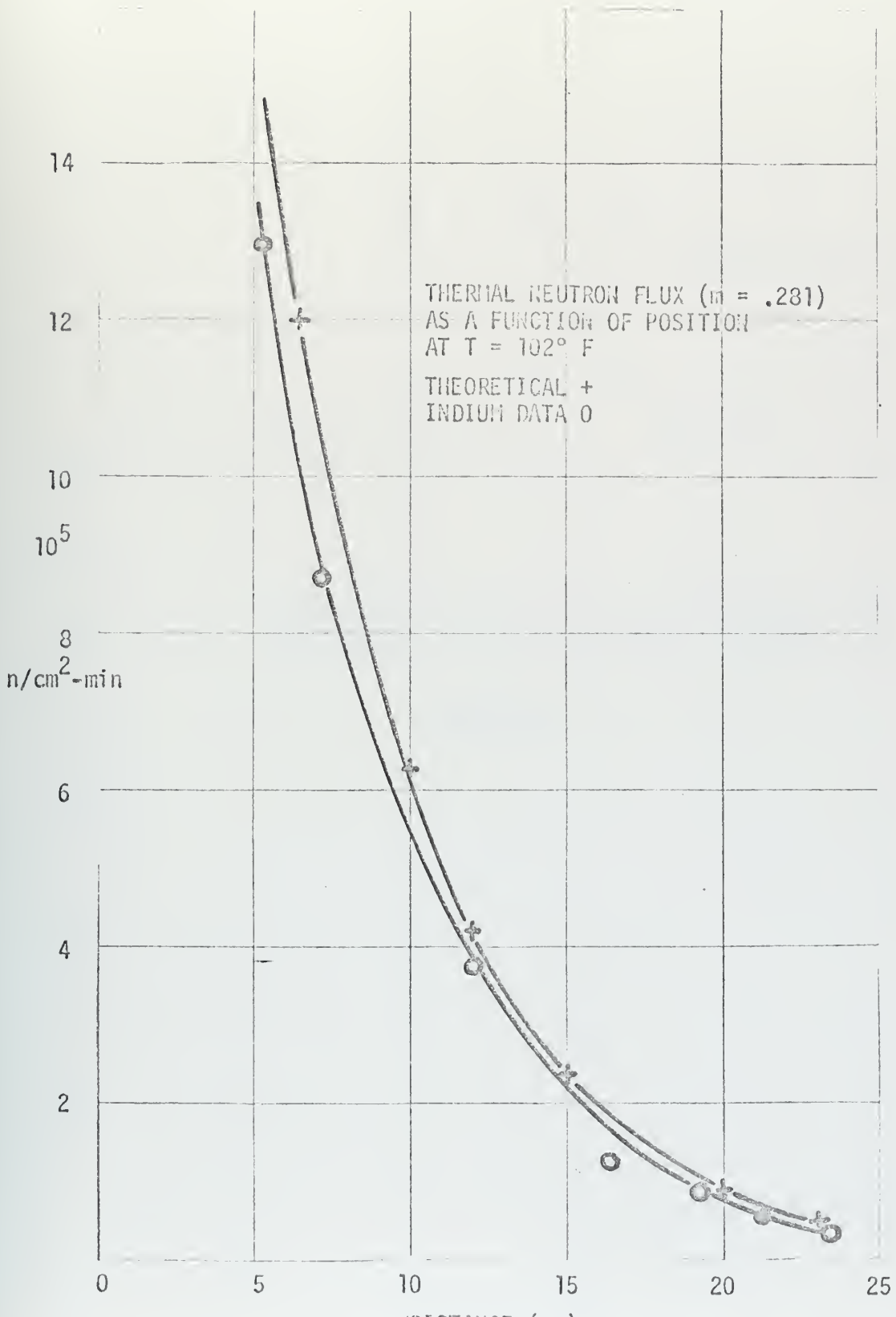
THERMAL NEUTRON FLUX (m = .281)
AS A FUNCTION OF POSITION
AT T = 102° F
THEORETICAL +
INDIUM DATA O
14
12
10
10^5
8
n/cm^2-min
6
4
2
0
5
10
15
20
25
DISTANCE (cm)

FIGURE 38

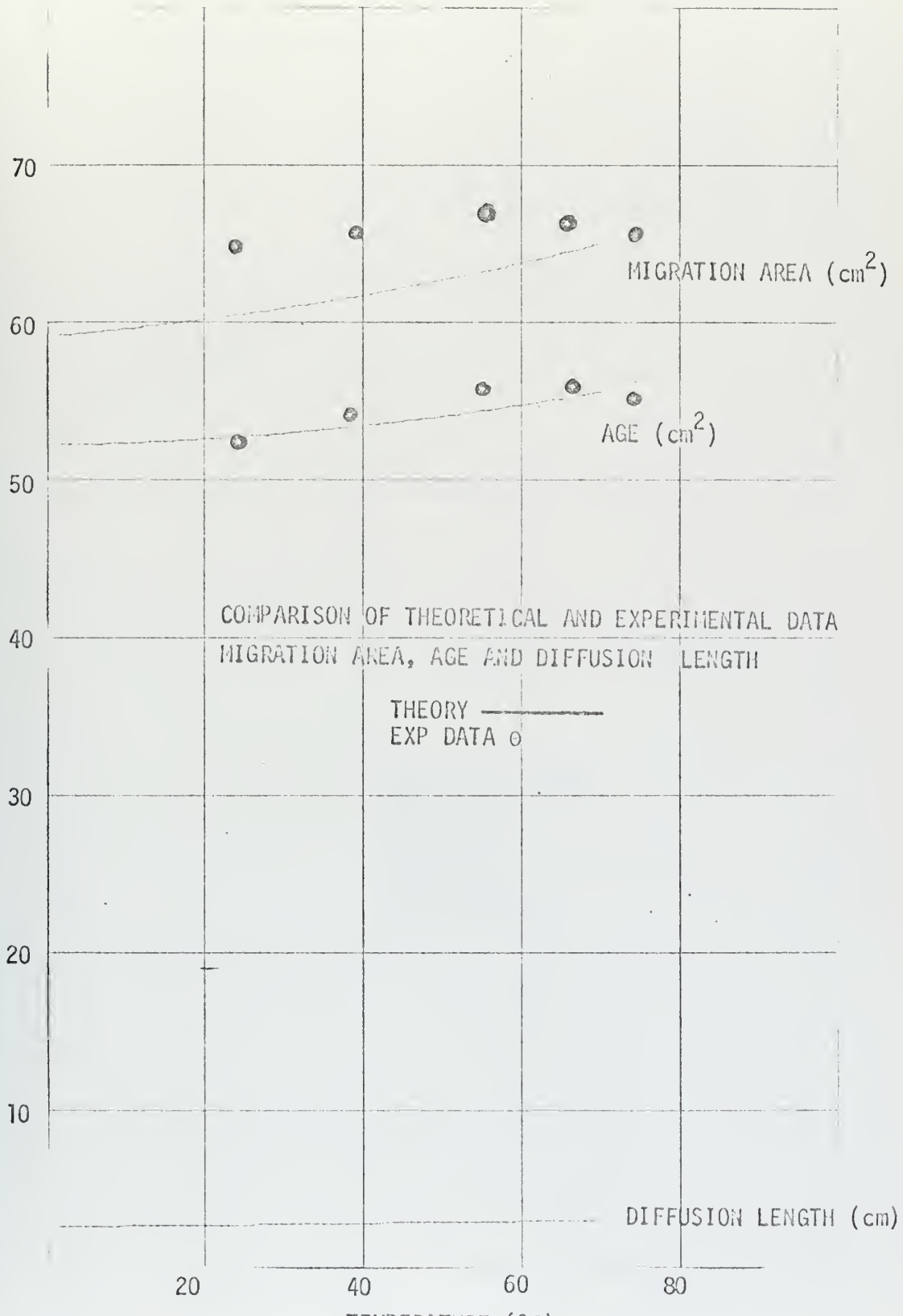
70
60
50
40
30
20
10
MIGRATION AREA (cm^2)
AGE (cm^2)
COMPARISON OF THEORETICAL AND EXPERIMENTAL DATA
MIGRATION AREA, AGE AND DIFFUSION LENGTH
THEORY
EXP DATA o
DIFFUSION LENGTH (cm)
20
40
60
80
TEMPERATURE (°C)

FIGURE 39

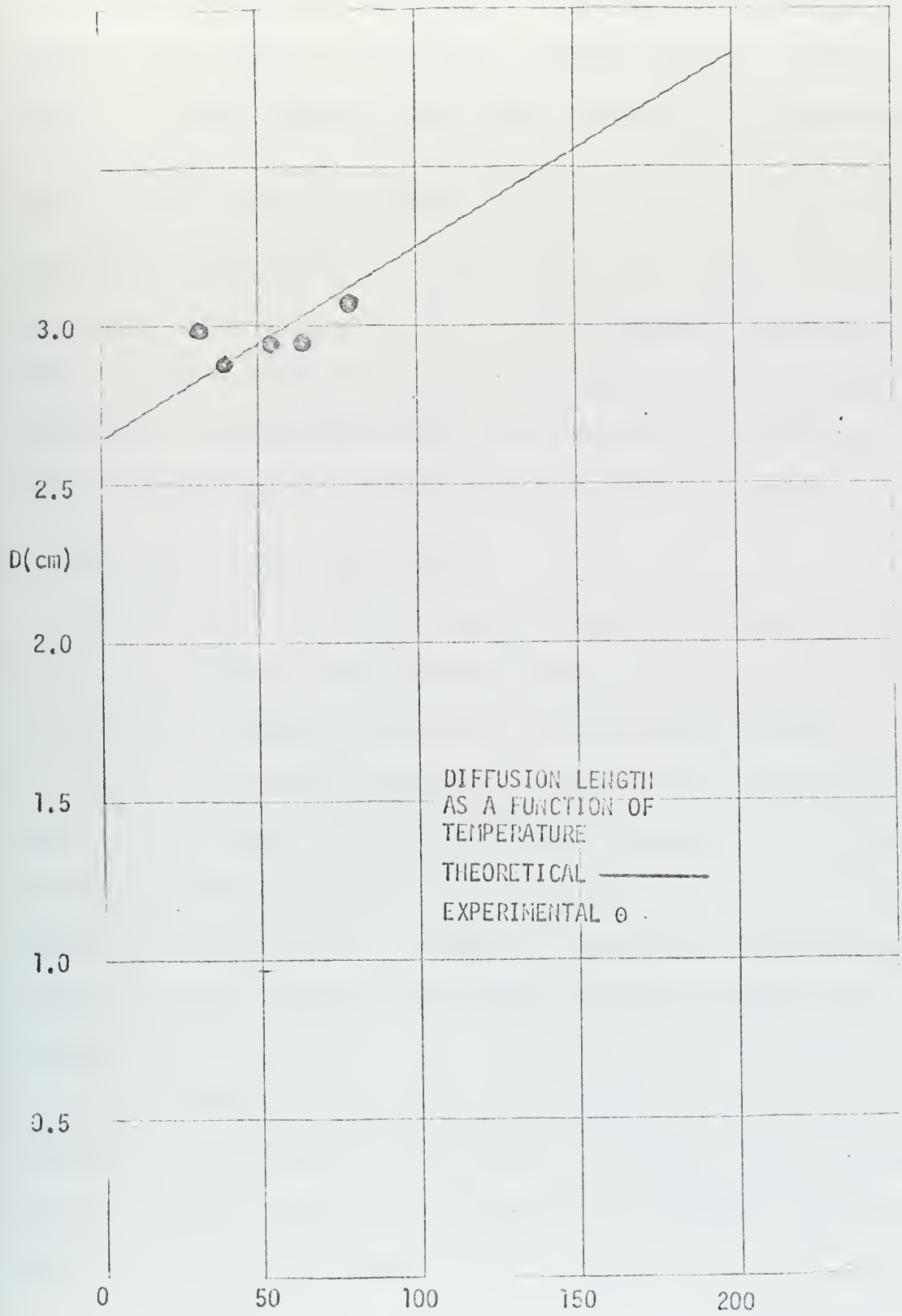
3.0
2.5
D(cm)
2.0
1.5
1.0
0.5
0
50
100
150
200
TEMPERATURE (°C)
DIFFUSION LENGTH
AS A FUNCTION OF
TEMPERATURE
THEORETICAL
EXPERIMENTAL o

FIGURE 40

lengths of both bare and cadmium-covered Indium have been plotted as a function of temperature. The slope of the experimental values in contrast to the theory was found to be slightly negative. Recall that the flux away from the source can be approximated by the expression

$\phi(r) \approx \frac{Ke^{-r/b}}{r^2}$ such that a smaller value of b implies a faster flux attenuation with distance or a larger leakage loss. Since raising the temperature of the medium has the effect of increasing the neutron kinetic energy it is expected that the leakage loss will increase with temperature. The decreasing trend of the experimental relaxation lengths with temperature confirms this observation.

B. THEORETICAL VERSUS CRYSTAL DATA

The theoretical and crystal thermal fluxes were plotted as per Fig. 41 for comparison with excellent agreement being obtained in the shape of the thermal flux curve at the temperature selected (T = 102° F). The general trend of the thermal flux as determined by the crystal also agrees with the theoretical analysis, i.e., an increase in flux magnitude was obtained for an increase in temperature. Crystal thermal flux magnitudes with distance and temperature dependence are tabulated in Table 8 as determined from the computer program listed in Appendix C.

A minor drawback in using the crystal was the nonavailability of a standard for calibration of the crystal. An overall system efficiency of 25 per cent was assumed which appears to be realistic in view of the correlation of two sets of data.

The advantages of crystal detectors for flux measurement are its high efficiency and its rapid acquisition of data. The high efficiency

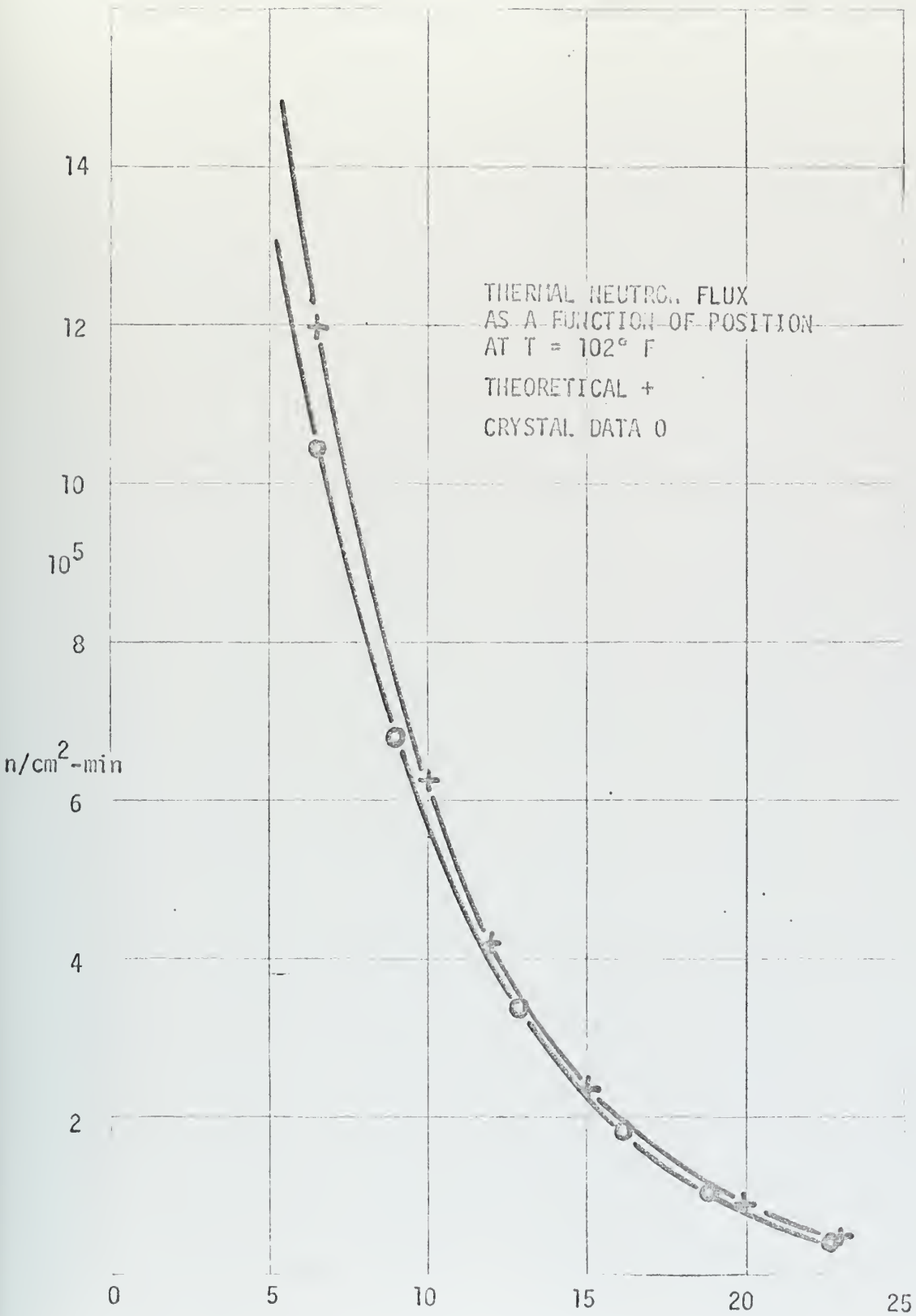
THERMAL NEUTRON FLUX
AS A FUNCTION OF POSITION
AT T = 102° F
THEORETICAL +
CRYSTAL DATA 0
14
12
10
10^5
8
n/cm^2-min
6
4
2
0
5
10
15
20
25
DISTANCE (cm)

FIGURE 41

of a crystal in a neutron detector permits the usage of a detector of a very small size which enhances the accessibility of the detector.

TABLE 10

THEORETICAL THERMAL FLUX AS A FUNCTION

OF DISTANCE, TEMPERATURE AND NON-INTEGER m

m = .281

Distance	Temperature (°F)				
(cm)	77	102	129	145	168
1	4694505	4714064	4714988	4707196	4681372
2	3686139	3720631	3742376	3746639	3743658
3	2905993	2947335	2980313	2991607	3002638
4	2300053	2343242	2381277	2396280	2415365
5	1827567	1869629	1908850	1925407	1948586
6	1457689	1496975	1535051	1551805	1576500
7	1167001	1202706	1238321	1254453	1279036
8	937659	969505	1002005	1017052	1040540
9	756021	784048	813197	826933	848776
10	611622	636046	661866	674214	694150
11	496402	517535	540197	551172	569121
12	404134	422321	442076	451750	467747
13	329988	345577	362708	371182	385333
14	270202	283526	298324	305712	318157
15	221839	232202	245949	252365	263262
16	182592	192270	203225	208783	218291
17	150649	158882	168284	173088	181363
18	124575	131576	139635	143781	150969
19	103234	109185	116089	119663	125896
20	85721	90779	96691	99770	105170
21	71314	75614	80675	83326	88000
22	59434	63091	67423	69705	73749
23	49616	52727	56437	58401	61898
24	41486	44134	47311	49001	52025
25	34740	36995	39717	41171	43785
26	29131	31053	33386	34638	36898

TABLE 10 (CONTINUED)

THEORETICAL THERMAL FLUX AS A FUNCTION

OF DISTANCE, TEMPERATURE AND NON-INTEGER m

Distance	Temperature (°F)				
(cm)	77	102	129	145	168
27	24461	26099	28099	29177	31132
28	20564	21962	23678	24607	26297
29	17309	18503	19975	20775	22237
30	14585	15605	16869	17559	18824
			m = .47		
1	4617565	4597102	4556127	4528439	4470656
2	3625726	3628318	3616285	3604360	3575150
3	2858366	2874208	2879898	2878000	3867485
4	2262357	2285103	2301046	2305280	2306645
5	1797614	1823241	1844536	1852290	1880877
6	1433799	1459833	1483331	1492875	1505539
7	1147875	1172865	1196599	1206815	1221464
8	922291	945450	968245	978430	993704
9	743631	764594	785798	795530	810571
10	601598	620265	639566	648611	662905
11	488266	504694	521996	530241	543504
12	397511	411842	427180	434594	446693
13	324580	337003	350487	357086	367989
14	265774	276491	288273	294102	303836
15	218203	227416	237662	242781	251412
16	179600	187499	196378	200854	208466
17	148180	154940	162614	166515	173200
18	122533	128311	134931	138321	144173
19	101542	10647	11217	115119	120230
20	84316	88527	93433	95981	100436
21	70145	73738	77957	80161	84039
22	58460	61525	65152	67058	70429

TABLE 10 (CONTINUED)

THEORETICAL THERMAL FLUX AS A FUNCTION

OF DISTANCE, TEMPERATURE AND NON-INTEGER m

Distance	Temperature (°F)				
(cm)	77	102	129	145	168
23	48803	51419	54536	56183	59112
24	40806	43039	45717	47140	49683
25	34170	36077	38378	39608	41815
26	28654	30283	32261	33322	35237
27	24060	25452	27152	28069	29731
28	20227	21418	22880	23672	25113
29	17025	18044	19302	19986	21236
30	14346	15218	16301	16892	17977

VI. CONCLUSIONS

The crystal and light pipe combination exhibit excellent potential for neutron flux determination as a function of position and temperature. The major advantages of the phosphor configuration used in this investigation were speed and flexibility. Data can be obtained rapidly and evaluated in a straightforward manner. In contrast, the Indium foil method was found to be extremely time consuming because of irradiation time requirements, foil counting time and extensive data analysis and calculations required prior to resolving the data.

The Indium foil technique will undoubtedly provide the most reliable data providing all possible sources of error are minimized; however, the crystal combination remains considerably simpler and much faster for data analysis. The crystal is adaptable to many different usages because of its size. In addition, the crystal would be suitable as a detector for isotopes with short half-lives.

The experimental phases of this investigation verified the trend of increasing flux with increasing temperature as predicted by theory. Since the cross section generally decreases with temperature, it is expected that the neutron reaction rates are almost insensitive to temperature.

APPENDIX A

COMPUTER PROGRAM NO 1A

```
C
C
C
C
C
C
C
C
C        THIS PROGRAM'S FUNCTION IS TO DETERMINE THE BEST FIT
C        TO REPRESENT THE SCATTERING CROSS SECTION OF WATER
C        AND IS BASED UPON FLANGE II ENERGY AND CROSS SECTION
C        DATA.  A TAYLOR SERIES EXPANSION IS USED AND THE SIMUL
C        TANEOUS LINEAR EQUATOONS ARE SOLVED FOR BY A SUB-
C        ROUTINE LLSQ.  AN ITERATION METHOD IS USED TO DETER-
C        MINE A SOLUTION TO THE DESIRED EXPRESSION...
C        THE DATA OBTAINED FROM THIS PROGRAM IS USED IN PROGRAM
C        DESIGNATED AS 1B.
C
C
C
// EXEC FORTCLG,PARM.FORT='MAP,LIST',REGION.GO=100K
//FORT.SYSIN DD
      REAL 8 E,SIG,F,D,C,NO,KO
      REAL 4 INDIA,IRA
      DIMENSION C(99),E(99),SIG(99),D(99),F(99),A(99,2),B(99
     1PEV(2),AUX(4,1)
      CALL CANCEL (2)
      READ(5,20) ((E(I),SIG(I)),I=1,99)
   20 FORMAT(2F9.0)
      WRITE(6,21) ((I,E(I),SIG(I)),I=1,99)
   21 FORMAT(I3,2D25.16)
C     TAYLOR SERIES EXPANSION ABOUT KO AND NO IN TERMS OF U
      KO=3.56D01
      NO=-2.0D-1
      EPS=1.0E-6
  111 DO 25 I=1,99
      F(I)=(E(I))  NO
      C(I)=(KO F(I)) DLOG(E(I))
      D(I)=KO F(I)-SIG(I)
   25 CONTINUE
      WRITE(6,12)((I,D(I),F(I),C(I)),I=1,99)
   12 FORMAT (I3,2X,D25.16,2X,D25.16,2X,D25.16)
      DO 100 I=1,99
      A(I,1)=-F(I)
  100 CONTINUE
      WRITE (6,26) (I,A(I,1),I=1,99)
   26 FORMAT (I3,E15.8)
      DO 110 I=1,99
      A(I,2)=-C(I)
  110 CONTINUE
      WRITE (6,27) (I,A(I,2),I=1,99)
   27 FORMAT (I3,E15.8)
      DO 120 I=1,99
      B(I,1)=D(I)
  120 CONTINUE
      WRITE (6,23) ((I,B(I,1),I=1,99))
   23 FORMAT (I3,D25.16)
      CALL LLSQ(A,B,99,2,1,X,IPEV,EPS,IER,AUX)
      WRITE(6,28) (I,X(I,1),I=1,2)
   28 FORMAT(I3,E15.8)
      KO=KO+X(1,1)
      NO=NO+X(2,1)
      WRITE(6,36) KO,NO
   36 FORMAT (2E15.8)
      INDIA=(X(1,1))  2.0
      IRA=SQRT(INDIA)
      IF(IRA.GT.0.005)GOTO111
      STOP
      END
//GO.SYSUDUMP DD SYSOUT=A
//GO.SYSIN DD
```

```
C                          APPENDIX A
CC
CC
CC                         COMPUTER PROGRAM NO 1B
CC
CC
CC       THE PURPOSE OF THIS PROGRAM IS TO PROVIDE TABULATED
CC       DATA ALONG WITH A GRAPHICAL PRESENTATION OF THE MICRO-
CC       SCOPIC CROSS SECTION AS DETERMINED FROMFLANGE II INPUT
CC       AND ALSO FOR THE BEST FIT FROM PROGRAM 1A TO  COM-
CC       PARE WITH THE EMPERICAL RELATION (THAT IS THE NON-
CC       INTEGER DESIGNATED AS M).............
CC       DESCRIPTION OF VARIABLES USED IS AS FOLLOWS.
CC       LAM(I) REPRESENTS THE EMPERICAL RELATION
CC       BEN(I) REPRESENTS THE SOLN OBTAINED FROM PROGRAM 1A
CC       SIG(I) REPRESENTS THE BEST AVAILABLE DATA ON THE CROSS
CC       SECTION AS A FUNCTION OF ENERGY IN THE THERMAL RANGE.
CC       EMPERICAL INPUT DATA ARE NL AND KL .  THE 1A INPUT
CC       CATA IS NB AND KB.
C
C
// EXEC FORTCLGP,PARM.FORT='MAP,LIST',REGION.GO=100K
//FORT.SYSIN DD *
      REAL KB,KL,NB,NL,E,EE,LAM,BEN,SIG
      REAL LABEL1/4HF-II/,LABEL2/4H.47 /,LABEL3/4H.255/.
      REAL 8 ITITLE (12)
      DIMENSION BEN(290),LAM(290),EE(290),E(81),SIG(81)
      INTEGER LAST
      CALL CANCEL (2)
      READ (5,20)((E(I),SIG(I)),I=1,81)
   20 FORMAT(2E9.0)
      READ (5,25)(ITITLE(I),I=1,12)
   25 FORMAT(6A8)
      NL=-4.7E-01
      KL=1.8294E01
C   THE NB & KB VALUES USED IN THIS PROGRAM WERE  DETERMINED
C     FROM COMPUTER PROGRAM 1A AND REFLECT THE ENERGY
C     INTERVAL OF THERMAL ENERGIES UP TO 1.45 EV
      NB=-2.55E-1
      KB=3.84E1
      DO 60 I=1,290
      EE(I)=0.005 I
      LAM(I)=KL*(EE(I)  NL)
      BEN(I)=KB*(EE(I)  NB)
   60 CONTINUE
      WRITE(6,30)((I,E(I),SIG(I)),I=1,81)
   30 FORMAT(' ',I3,2E15.8)
      WRITE(6,31)((I,EE(I),LAM(I),BEN(I)),I=1,290)
   31 FORMAT(' ',I3,3E15.8)
      CALL DRAW(81,E,SIG,1,0,LABEL1,ITITLE,0,0,0,0,0,0,6,9,1
     1,LAST)
      CALL DRAW(290,EE,LAM,2,0,LABEL2,ITITLE,0,0,0,0,0,0,6,9
     1,1,LAST)
      CALL DRAW(290,EE,BEN,3,0,LABEL3,ITITLE,0,0,0,0,0,0,6,9
     1,1,LAST)
      WRITE(6,32) LAST
   32 FORMAT(I3)
      STOP
      END
//GO.SYSUDUMP DD SYSOUT=A
//GO.SYSIN DD *
C
C      INPUT DATA
C
C ENERGY    CROSS SECTION
C   EV          BARNS
C
.005        152.428
.015        113.714
.025        104.3788
.035        93.6268
.045        85.6974
```

.055	79.8324
.065	75.489
.075	72.2118
.085	69.6338
.095	67.4992
.105	65.6648
.115	64.0558
.125	62.6264
.135	61.3444
.145	60.1798
.155	59.1072
.165	58.1108
.175	57.1828
.185	56.3234
.195	55.5406
.205	54.8346
.215	54.2002
.225	53.6218
.235	53.0856
.245	52.5736
.255	52.0946
.265	51.6204
.275	51.1852
.285	50.7594
.295	50.3516
.305	49.9604
.315	49.5850
.325	49.2236
.335	48.8744
.345	48.5372
.355	48.2106
.365	47.8942
.375	47.5878
.385	47.2916
.395	47.0056
.405	46.7302
.415	46.4672
.425	46.2176
.435	45.981
.445	45.758
.455	45.546
.465	45.3382
.475	45.1188
.485	44.8348
.495	44.3434
.545	43.849
.575	43.5592
.605	43.313
.635	43.0936
.665	42.9108
.695	42.7358
.725	42.7322
.755	42.5132
.785	42.3882
.815	42.2824
.845	42.184
.875	42.0918
.905	42.0046
.935	41.992
.965	41.8433
.995	41.7698
1.025	41.6542
1.055	41.621
1.085	41.5504
1.115	41.4808
1.145	41.414
1.175	41.3506
1.205	41.289
1.235	41.2294
1.265	41.173
1.295	41.1202
1.325	41.069

1.385	40.9726
1.355	41.0196
1.415	40.9292
1.45	40.8844

APPENDIX B

COMPUTER PROGRAM NO 2

THE PURPOSE OF THIS PROGRAM WAS TO DETERMIME THE THEORETICAL TEMPERATURE DEPENDENCE BY BOTH TABULATED DATA AND GRAPHICAL PRESENTATION OF THE FOLLOWING VARIABLES

VARIABLE	SYMBOL
DIFFUSION LENGTH	L/B
DIFFUSION COEFFIENT	D/C
AGE	TAU/TTA
MIGRATION AREA	M
SCATTERING CROSS SECTION	SIG/SAG
CONSTANTS	
LETHARGY	SQUIG
BOLTZMANNS CONSTANT	K
KELVIN REF TEMPERATURE	TO
NON-INTEGER CONSTANT	.47/.231

```
// EXEC FORTCLGP,REGION.GO=150K
//FORT.SYSIN DD
      REAL*8 L,D,SIG,TAU,T,B,C,SAG,TTA,TO,K,SQUIG,MIG
      REAL*8 ITITLE(12)
      REAL*4  LL,DD,SI,TA,LB,DC,SG,TT,TE,M
      REAL LABEL1/4H     /,LABEL2/4H     /
      DIMENSION L(200),LL(200),D(200),DD(200),TAU(200),TA(20
     1200),C(200),SAG(200),TTA(200),LB(200),DC(200),SG(200),
     1200),SI(200),TE(200),MIG(200),M(200)
      SQUIG=9.2D-1
      K=8.617065D-5
      TO=2.7361D02
      DO 10 I=1,200
      T(I)=1.0*I
      L(I)=2.64+0.0061*T(I)
      D(I)=0.1600*(1.0+T(I)/TO)**0.470
      TAU(I)=52.2*DEXP((1.8D-4)*T(I)+(1.04D-5)*((T(I)**2.0)
      SIG(I)=3.4560*DEXP(-((9.0D-5)*T(I)+(5.2D-6)*T(I)**2.0)
      MIG(I)=TAU(I)+L(I)**2.0
      TE(I)=T(I)
      LL(I)=L(I)
      DD(I)=D(I)
      SI(I)=SIG(I)
      TA(I)=TAU(I)
      M(I)=MIG(I)
   10 CONTINUE
      WRITE(6,42)
   42 FORMAT(' M=.470',2X,'TEMP DEG C',10X,'DIFFUSION LENGTH
     1SION COEFF',5X,'SCATT CROSS SECTION',8X,'AGE')
      WRITE(6,20)((T(I),L(I),D(I),SIG(I),TAU(I)),I=1,200)
   20 FORMAT(5D25.16)
      DO 11 I=1,200
      T(I)=1.0*I
      B(I)=2.64+0.0061*T(I)
      C(I)=0.1600*(1.0+T(I)/TO)**0.281
      TTA(I)=52.20*DEXP((1.8D-4)*T(I)+(1.04D-5)*((T(I)**2.0)
      SAG(I)=3.4560*DEXP(-((9.0D-5)*T(I)+(5.2D-6)*T(I)**2.0)
      TE(I)=T(I)
      LB(I)=B(I)
      DC(I)=C(I)
      SG(I)=SAG(I)
      TT(I)=TTA(I)
   11 CONTINUE
      WRITE(6,40)
   40 FORMAT(' M=.281',2X,'TEMP DEG C',10X,'DIFFUSION LENGTH
     1SION COEFF',5X,'SCATT CROSS SECTION',8X,'AGE')
      WRITE(6,21)((T(I),B(I),C(I),SAG(I),TTA(I)),I=1,200)
   21 FORMAT(5D25.16)
      READ(5,30)(ITITLE(I),I=1,12)
```

```
   30 FORMAT(6A8)
      CALL DRAW(200,TE,LL,1,0,LABEL1,ITITLE,0,0,0,0,0,0,6,9
     1,1,LAST)
      CALL DRAW(200,TE,LB,3,0,LABEL2,ITITLE,0,0,0,0,0,0,6,9
     1,1,LAST)
      READ(5,32)(ITITLE(I),I=1,12)
   32 FORMAT(6A8)
      CALL DRAW(200,TE,DD,1,0,LABEL1,ITITLE,0,0,0,0,0,0,6,9
     1,1,LAST)
      CALL DRAW(200,TE,DC,3,0,LABEL2,ITITLE,0,0,0,0,0,0,6,9
     1,1,LAST)
      READ(5,34)(ITITLE(I),I=1,12)
   34 FORMAT(6A8)
      CALL DRAW( 70,TE,SI,1,0,LABEL1,ITITLE,0,0,0,0,0,0,6,9
     1,1,LAST)
      CALL DRAW( 70,TE,SG,3,0,LABEL2,ITITLE,0,0,0,0,0,0,6,9
     1,1,LAST)
      READ(5,36)(ITITLE(I),I=1,12)
   36 FORMAT(6A8)
      CALL DRAW(70 ,TE,TA,1,0,LABEL1,ITITLE,0,0,0,0,0,0,6,9
     1,1,LAST)
      CALL DRAW( 70,TE,TT,3,0,LABEL2,ITITLE,0,0,0,0,0,0,6,9
     1,1,LAST)
      READ(5,55)(ITITLE(I),I=1,12)
   55 FORMAT(6A8)
      CALL DRAW(70,TE,LL,1,0,LABEL1,ITITLE,0,0,0,0,0,0,6,9,1
     1,LAST)
      CALL DRAW(70,TE, M,2,0,LABEL1,ITITLE,0,0,0,0,0,0,6,9,1
     1,LAST)
      CALL DRAW(70,TE,TA,3,0,LABEL1,ITITLE,0,0,0,0,0,0,6,9,1
     1,LAST)
      WRITE (6,31) LAST
   31 FORMAT(I3)
      STOP
      END
//GO.SYSIN DD
```

```
C                          APPENDIX C
C
C
C
C                  COMPUTER PROGRAM NO 3
C
C
C       THE PURPOSE OF THIS PROGRAM WAS TO TABULATE THEOR-
C       ETICAL DATA AND OBTAIN GRAPHICAL DATA BASED ON THE
C       THEORETACAL EXPRESSION FOR THERMAL FLUX AS DETERMINED
C       IN PART 1.  THE EXPRESSION TO BE EVALUATED IS AS
C       FOLLOWS.
C       FLUX(R,T)=SOURC L(T)**2 (EXP(-R/L(T)-EXP(R/TAU(T)  .5
C       DIVIDED BY 4 PI D(T) R (L(T)  2-TAU(T))
C       IDENTIFICATION OF VARIABLES IS AS FOLLOWS
C
C          VARIABLE                              SYMBOL
C       AGE                                       TAU
C       DIFFUSION LENGTH                          L
C       DIFFUSION COEFFICIENT                     D
C                        CONSTANTS
C       LETHARGY                                  SQUIG
C       PU-BE SOURCE STRENGTH                     SOURC
C       KELVIN REFERENCE TEMPERATURE              TO
C       BOLTZMANS CONSTANT                        K
C
C
// EXEC FORTCLGP,REGION.GO=100K
//FORT.SYSIN DD
      REAL*8 S,L,LL,SIG,SQUIG,D,TAU,TA,Q,T,SOURC,N,O,P,K,TO,
     1SIGS,NO,M
      REAL*8 ITITLE(12)
      REAL*4 NN,OO,PP,QQ,N1,O1,P1,Q1,MM,M1
      REAL LABEL1/4H     /,LABEL2/4H     /,LABEL3/4H     /,LABE
     1L4/4H     /
      DIMENSION L(5),LL(5),TAU(5),TA(5),D(5),SIG(5),T(5),Q(3
     10),R(30),N(30),O(30),P(30),NN(30),OO(30),PP(30),QQ(30)
     1,N1(30),O1(30),P1(30),Q1(30),M(30),MM(30),M1(30)
      INTEGER LAST,G
      DO77 G=1,2
      K=8.6170650-5
      TO=2.7361D2
      SIGS=3.443DO
      SOURC=3.24D8
      SQUIG=0.92
      READ(5,41)NO
   41 FORMAT(1F9.0)
      READ(5,20) (T(I),I=1,5)
   20 FORMAT(1F9.0)
      DO 18 I=1,5
      L(I)=2.64+0.0061*T(I)
      D(I)=0.16*(1.0+T(I)/TO)**NO
      TAU(I)=52.20*DEXP((1.80-4)*T(I)+(1.04D-5)*((T(I)**2.0)
      SIG(I)=3.456E4*DEXP(-((9.0D-5)*T(I)+(5.2D-6)*T(I)**2.0)
      LL(I)=L(I)**2.0
      TA(I)=TAU(I)**0.5
   18 CONTINUE
      WRITE(6,25)(I,L(I),D(I),SIG(I),TAU(I),I=1,5)
   25 FORMAT(I3,4D25.16)
      DO21 J=1,30
      I=1
      R(J)=1.0*J
      N(J)=SOURC*LL(I)/(12.58*R(J)*D(I)*(LL(I)-TAU(I)))*(DEX
     1P(-R(J)/L(I))-DEXP(-R(J)/TA(I)))
      N1(J)=N(J)
      NN(J)=DLOG(N(J))
   21 CONTINUE
      DO 22 J=1,30
      I=2
      R(J)=1.0*J
      O(J)=SOURC*LL(I)/(12.58*R(J)*D(I)*(LL(I)-TAU(I)))*(DEX
     1P(-R(J)/L(I))-DEXP(-R(J)/TA(I)))
```

```
      O1(J)=O(J)
      OO(J)=DLOG(O(J))
   22 CONTINUE
      DO 23 J=1,30
      I=3
      R(J)=1.0*J
      P(J)=SOURC*LL(I)/(12.58 R(J) D(I) (LL(I)-TAU(I))) (DEX
     1P(-R(J)/L(I))-DEXP(-R(J)/TA(I)))
      P1(J)=P(J)
      PP(J)=DLOG(P(J))
   23 CONTINUE
      DO 24 J=1,30
      I=4
      R(J)=1.0*J
      Q(J)=SOURC*LL(I)/(12.58 R(J) D(I) (LL(I)-TAU(I))) (DEX
     1P(-R(J)/L(I))-DEXP(-R(J)/TA(I)))
      Q1(J)=Q(J)
      QQ(J)=DLOG(Q(J))
   24 CONTINUE
      DO 26 J=1,30
      I=5
      R(J)=1.0*J
      M(J)=SOURC*LL(I)/(12.58 R(J) D(I) (LL(I)-TAU(I))) (DEX
     1P(-R(J)/L(I))-DEXP(-R(J)/TA(I)))
      M1(J)=M(J)
      MM(J)=DLOG(M(J))
   26 CONTINUE
      WRITE(6,31)((R(J),N(J)),J=1,30)
   31 FORMAT(2D25.16)
      WRITE(6,32)((R(J),O(J)),J=1,30)
   32 FORMAT(2D25.16)
      WRITE(6,33)((R(J),P(J)),J=1,30)
   33 FORMAT(2D25.16)
      WRITE(6,30)((R(J),Q(J)),J=1,30)
   30 FORMAT(2D25.16)
      WRITE(6,35)((R(J),M(J)),J=1,30)
   35 FORMAT(2D25.16)
      READ(5,17) (ITITLE(I),I=1,12)
   17 FORMAT(6A8)
      CALL DRAW(30,R,NN,1,0,LABEL1,ITITLE,0,0,0,0,0,0,6,9,1,
     1LAST)
      CALL DRAW(30,R,OO,2,0,LABEL2,ITITLE,0,0,0,0,0,0,6,9,1,
     1LAST)
      CALL DRAW(30,R,PP,2,0,LABEL3,ITITLE,0,0,0,0,0,0,6,9,1,
     1LAST)
      CALL DRAW(30,R,QQ,2,0,LABEL4,ITITLE,0,0,0,0,0,0,6,9,1,
     1LAST)
      CALL DRAW(30,R,MM,3,0,LABEL4,ITITLE,0,0,0,0,0,0,6,9,1,
     1LAST)
      READ(5,19) (ITITLE(I),I=1,12)
   19 FORMAT(6A8)
      CALL DRAW(30,R,N1,1,0,LABEL1,ITITLE,0,0,0,0,0,0,6,9,1,
     1LAST)
      CALL DRAW(30,R,O1,2,0,LABEL2,ITITLE,0,0,0,0,0,0,6,9,1,
     1LAST)
      CALL DRAW(30,R,P1,2,0,LABEL3,ITITLE,0,0,0,0,0,0,6,9,1,
     1LAST)
      CALL DRAW(30,R,Q1,2,0,LABEL4,ITITLE,0,0,0,0,0,0,6,9,1,
     1LAST)
      CALL DRAW(30,R,M1,3,0,LABEL4,ITITLE,0,0,0,0,0,0,6,9,1,
     1LAST)
      WRITE(6,39) LAST
   39 FORMAT(I3)
   77 CONTINUE
      STOP
      END
//GO.SYSIN DD *
C  INPUT NON INTEGER
0.281
C  INPUT TEMPERATURE IN DEG CENTIGRADE
25.0
38.9
```

```
54.4
62.2
75.5
C   INPUT NON INTEGER
0.47
C   INPUT TEMPERATURE IN DEG CENTIGRADE
25.0
38.9
54.4
62.2
75.5
```

```
C                          APPENDIX D
C
C
C                  COMPUTER PROGRAM NO 4
C
C       THE PURPOSE OF THIS PROGRAM IS TO DO THE FOLLOWING..
C
C       1.  READ IN DATA FROM SATURATED ACTIVITIES OF BARE AND
C         CADMIMUM COV'D FOILS.
C       2.  NORMALALIZE ALL FOIL WEIGTH'S TO FOIL NEAR SOURCE
C       3.  COMPUTE SATURATED COUNT RATE AS PER EQUATION (   )
C       4.  COMPUTE STANDARD DEVIATION DESIGNATED AS SIGMA
C       5.  COMPUTE SATURATED ACTIVITY TIMES DISTANCE SQUARED
C         AND ALSO TIMES DISTANCE TO THE FOURTH FOR BOTH
C         BARE FOILS AND CADMIMUM COV'D FOILS
C       6.  PROVIDE A GRAPHICAL PRESENTATION OF BOTH SETS OF
C         DATA AND A DUAL LOG PLOT
C       7.  DRAW AN EXPODENTIAL CURVE BASED ON PROGRAM 5 DATA
C         FOR EXTRAPOLATION  TO DETERMINE AREA
C
C
// EXEC FORTCLGP,REGION.GO=100K
//FORT.SYSIN DD *
      IMPLICIT REAL*8(A-H,O-Q,S-Z)
      REAL*4 ASRSQ,ASCDR,ASR,ACD,ASR4,ASCD4,R
      REAL BSSQ,BSCD,BS,BCD,BS4,BCD4
      REAL AC,AD,AA,BB,DISTA,DISTC
      REAL LABEL1/4H     /,LABEL2/4H B  /,LABEL3/4H   A/,LABE
     1L4/4H    /
      REAL*8 ITITLE(12)
      DIMENSION AC(25),AD(25),AA(25),BB(25),DISTA(25),DISTC(
     125),ASR4(25),ASCD4(25),ASRSQ(25),ASCDR(25),ASR(25),ACD
     1(25),R(25),BSSQ(25),BSCD(25),BS(25),BCD(25),BS4(25),BC
      WRITE(6,1)
    1 FORMAT(T5,'DISTANCE',T25,'SAT ACTIVITY',T56,'MEAN',
     1T87,'SIGMA'//)
C
C
C       RUN NUMBER ONE
C
C
      D=1.28D-2
      T=6.34D-7
      DO50 N=1,10
      READ(5,2) POS,C,X,Y,Z
    2 FORMAT(5F9.0)
      READ(5,6) W
    6 FORMAT(1F9.0)
      DIST=POS*0.254D01
      C=(9.166D-1)*C/((1.0D0-C*T)*W)
      ASAT=D*C/((1.0D0-DEXP(-D*X))*(DEXP(-D*Y)-DEXP(-D*Z)))
      SAT=ASAT
      AMEAN=C/5.0
      SIGMA=AMEAN**0.5D0
      F=1.11D0
      FSAT=F*SAT
      WRITE(6,4) DIST,FSAT,AMEAN,SIGMA
    4 FORMAT(T6,F5.2,6X,D25.16,6X,D25.16,6X,D25.16)
      A=FSAT*DIST**2.0D0
      B=FSAT*DIST**4.0D0
    8 FORMAT(/,T12,F5.2,6X,D25.16,6X,D25.16)
      WRITE(6,8) DIST,A,B
      DISTC(N)=DIST
      AC(N)=A
      AD(N)=B
   50 CONTINUE
      DO60 N=1,10
      READ(5,5) POS,C,X,Y,Z
    5 FORMAT(5F9.0)
      READ(5,7) W
```

```
    7 FORMAT(1F9.0)
      DIST=POS*0.254D01
      C=W*C/(1.0D0-C*T)
      ASAT=D*C/((1.0D0-DEXP(-D*X))*(DEXP(-D*Y)-DEXP(-D*Z)))
      SAT=ASAT
      AMEAN=C/5.0
      SIGMA=AMEAN*0.5D0
      WRITE(6,3) DIST,SAT,AMEAN,SIGMA
    3 FORMAT(T6,F5.2,6X,D25.16,6X,D25.16,6X,D25.16)
      A=SAT*DIST**2.0D0
      B=SAT*DIST**4.0D0
      WRITE(6,9) DIST,A,B
    9 FORMAT(/,T12,F5.2,6X,D25.16,6X,D25.16)
      DISTA(N)=DIST
      AA(N)=A
      BB(N)=B
   60 CONTINUE
      DO 77 I=1,15
      R(I)=15.0+I
      ASCDR(I)=EXP(1.270E1-(1.02E-1)*R(I))
      BSCD(I) =EXP(1.270E1-(1.02E-1)*R(I))
      ASRSQ(I)=EXP(1.513E1-(9.50E-2)*R(I))
      BSSQ(I) =EXP(1.513E1-(9.50E-2)*R(I))
      ASR(I)=ALOG(ASRSQ(I))
      ACD(I)=ALOG(ASCDR(I))
      BS(I)=ALOG(BSSQ(I))
      BCD(I)=ALOG(BSCD(I))
      ASCD4(I)=ASCDR(I)*R(I)**2.0
      ASR4(I)=ASRSQ(I)*R(I)**2.0
      BS4(I)=BSSQ(I)*R(I)**2.0
      BCD4(I)=BSCD(I)*R(I)**2.0
   77 CONTINUE
      READ (5,30) (ITITLE(I),I=1,12)
   30 FORMAT(6A8)
      CALL DRAW (10,DISTC,AC,1,3,LABEL1,ITITLE,0,0,0,0,0,0,6
     1,9,1,LAST)
      CALL DRAW (15,R,BSCD,2,0,  LABEL2,ITITLE,0,0,0,0,0,0,6
     1,9,1,LAST)
      CALL DRAW (15,R,ASCDR,3,0, LABEL3,ITITLE,0,0,0,0,0,0,6
     1,9,1,LAST)
      READ (5,32) (ITITLE(I),I=1,12)
   32 FORMAT(6A8)
      CALL DRAW (10,DISTA,AA,1,4,LABEL1,ITITLE,0,0,0,0,0,0,6
     1,9,1,LAST)
      CALL DRAW (15,R,BSSQ,2,0,  LABEL2,ITITLE,0,0,0,0,0,0,6
     1,9,1,LAST)
      CALL DRAW (15,R,ASRSQ ,3,0,LABEL3,ITITLE,0,0,0,0,0,0,6
     1,9,1,LAST)
      DO70 N=1,10
      AC(N)=ALOG(AC(N))
      AA(N)=ALOG(AA(N))
   70 CONTINUE
      READ (5,34) (ITITLE(I),I=1,12)
   34 FORMAT(6A8)
      CALL DRAW (10,DISTC,AC,1,3,LABEL1,ITITLE,0,0,0,0,0,0,6
     1,9,1,LAST)
      CALL DRAW (15,R,BS ,2,0,   LABEL2,ITITLE,0,0,0,0,0,0,6
     1,9,1,LAST)
      CALL DRAW (15,R,BCD,2,0,   LABEL2,ITITLE,0,0,0,0,0,0,6
     1,9,1,LAST)
      CALL DRAW (15,R,ASR,2,0,   LABEL3,ITITLE,0,0,0,0,0,0,6
     1,9,1,LAST)
      CALL DRAW (15,R,ACD,2,0,   LABEL3,ITITLE,0,0,0,0,0,0,6
     1,9,1,LAST)
      CALL DRAW (10,DISTA,AA,3,4,LABEL3,ITITLE,0,0,0,0,0,0,6
     1,9,1,LAST)
      STOP
      END
//GO.SYSIN DD *
1.343     21944.0   300.5     3.0         8.0
.9166
2.094     14598.0    306.0    3.0        8.0
```

.9194				
2.875	9147.0	311.5	3.0	8.0
.9232				
3.625	5307.0	317.0	3.0	8.0
.9254				
4.781	2480.0	322.5	3.0	8.0
.9265				
6.031	1163.0	328.0	3.0	8.0
.9273				
6.406	850.0	333.5	3.0	8.0
.9292				
7.594	500.0	339.0	3.0	8.0
.9306				
8.406	300.0	344.5	3.0	8.0
.9312				
9.219	150.0	350.0	3.0	8.0
.9312				
1.343	160750.0	245.0	3.5	8.5
.9156				
2.094	116000.0	251.0	3.0	8.0
.9402				
2.875	91300.0	256.5	3.0	8.0
.9233				
3.625	63091.0	262.0	3.0	8.0
.9388				
4.781	35271.0	267.5	3.0	8.0
.9500				
6.031	18896.0	273.0	3.0	8.0
.9484				
6.406	12308.0	284.0	3.0	8.0
.9333				
7.594	7851.0	289.5	3.0	8.0
.9422				
8.406	5219.0	295.0	3.0	8.0
.9444				
9.219	3176.0	240.0	3.0	8.0
.9393				

COMPUTER PROGRAM 4

COMPUTER DATA TABULATION FOR T = 77 F

CADMIUM COVERED FOILS

DISTANCE (CM)	SATURATED ACTIVITY	SAT ACTIVITY TIMES R^2	SAT ACTIVITY TIMES R^4	SIGMA
3.41	4906.4	57092.9	664357.4	63.5
5.32	3234.8	91510.3	2588755.4	51.6
7.30	2027.0	108095.2	5764343.3	40.8
9.21	1194.1	101240.3	858296.5	31.4
12.14	557.0	82147.4	12114324.8	21.4
15.32	260.9	61233.9	14369382.0	14.7
16.27	148.0	39173.5	10371327.6	11.1
19.29	94.5	35182.5	13089860.0	8.8
21.35	37.3	16990.6	7745612.6	5.6
23.42	10.1	5534.8	3034878.6	2.9
		BARE FOILS		
3.41	36797.1	428186.9	4982564.1	180.5
5.32	25955.1	734249.2	20771329.6	152.3
7.30	20042.5	1068801.5	56995454.3	134.0
9.21	13629.1	1155452.6	97957029.5	110.0
12.14	7467.5	1101239.4	162400252.8	82.0
15.32	3953.3	927711.5	217700297.1	59.7
16.27	2558.9	677475.1	179363748.2	48.1
19.29	1628.4	605875.5	225419784.6	38.4
21.35	1079.5	492141.2	224355093.7	31.3
23.42	674.6	369923.1	202836703.6	24.4

COMPUTER PROGRAM 4

COMPUTER DATA TABULATION FOR T = 102 F

CADMIUM COVERED FOILS

DISTANCE (CM)	SATURATED ACTIVITY	SAT ACTIVITY TIMES R	SAT ACTIVITY TIMES R	SIGMA
3.41	5291.5	61574.0	716502.0	66.3
5.32	3426.8	96942.0	2742415.0	53.3
7.30	2226.7	118743.0	6332184.0	43.0
9.21	1308.7	110952.0	9406343.0	33.0
12.14	651.8	96121.0	14175146.0	23.3
15.32	350.0	82138.0	19274899.0	17.1
16.27	237.3	62835.0	16636030.0	14.0
19.29	159.6	59401.0	22100702.0	11.5
21.35	108.1	49301.0	22475521.0	9.5
23.42	81.4	44625.0	24469018.0	8.2
		BARE FOILS		
3.41	35251.6	410202.0	4773284.0	180.0
5.32	27716.3	784073.0	22180810.0	159.5
7.30	18558.1	989639.0	52774019.0	130.5
9.21	13789.4	1169042.0	99109141.0	112.6
12.14	7734.3	1145076.0	168201320.0	84.3
15.32	2535.0	594875.0	139595585.0	61.7
16.27	2661.0	704522.0	186524496.0	49.5
19.29	1735.3	645615.0	240205144.0	40.0
21.35	1130.3	515264.0	234896353.0	32.2
23.42	726.7	398469.0	218489421.0	25.9

COMPUTER PROGRAM 4

COMPUTER DATA TABULATION FOR T = 129° F

CADMIUM COVERED FOILS

DISTANCE (CM)	SATURATED ACTIVITY	SAT ACTIVITY TIMES R^2	SAT ACTIVITY TIMES R^4	SIGMA
3.41	4863.3	56592.0	658531.0	62.3
5.32	3382.8	95697.0	2707200.0	52.0
7.30	2169.1	115671.0	6168340.0	41.7
9.21	1326.8	112487.0	9536457.0	32.7
12.14	627.8	96109.0	14711868.0	22.5
15.32	345.0	80975.0	19001931.0	16.7
16.27	223.9	59285.0	15696075.0	13.4
19.29	155.8	57964.0	21566024.0	11.2
21.35	111.4	50805.0	23161133.0	9.5
23.42	72.2	39599.0	21713226.0	7.7

BARE FOILS

3.41	23266.0	270739.0	3150436.0	139.8
5.32	19733.0	558234.0	15792022.0	129.1
7.30	14367.0	766164.0	40856899.0	110.5
9.21	10248.0	868831.0	73657854.0	93.7
12.14	6669.2	983524.0	145040767.0	75.8
15.32	3462.2	812457.0	190654446.0	54.8
16.27	2401.8	635891.0	168354317.0	45.6
19.29	1482.2	551478.0	205181020.0	36.0
21.35	1055.5	481211.0	219372322.0	30.5
23.42	705.2	386668.0	212018442.0	25.0

COMPUTER PROGRAM 4

COMPUTER DATA TABULATION FOR T = 145° F

CADMIUM COVERED FOILS

DISTANCE (CM)	SATURATED ACTIVITY	SAT ACTIVITY TIMES R^2	SAT ACTIVITY TIMES R^4	SIGMA
3.41	4221.2	66444.4	1045895.0	58.0
5.32	3005.0	85011.0	2404911.0	49.1
7.30	1860.0	99215.0	5290837.0	38.7
9.21	1126.0	95473.0	8094066.0	30.2
12.14	582.9	85959.0	12676428.0	21.7
15.32	285.4	66972.0	15716010.0	15.2
16.27	210.2	55664.0	14737173.0	13.1
19.29	130.8	48660.0	18104442.0	10.3
21.35	106.6	48604.0	22157503.0	9.3
23.42	75.9	41625.0	22823907.0	7.8
		BARE FOILS		
3.41	33306.0	387569.0	4509927.0	167.2
5.32	28044.0	793358.0	22443495.0	153.9
7.30	19035.0	1015102.0	54131865.0	127.3
9.21	13978.0	1185087.0	100469387.0	109.4
12.14	8179.0	1206265.0	177888526.0	83.9
15.32	4217.0	989632.0	232230875.0	60.0
16.27	2694.0	713491.0	188898183.0	48.1
19.29	1880.0	699465.0	260240362.0	40.3
21.35	1164.0	530635.0	241903860.0	31.9
23.42	791.0	433836.0	27881691.0	26.3

```
C                          APPENDIX E
C
C
C                  COMPUTER PROGRAM NO 5
C
C       THE PURPOSE OF THIS PROGRAM IS TO DETERMINE THE FOLLOW
C        ING.
C
C       1.  BASED ON SIMPSONS RULE INTEGRATE THE AREA UNDER
C         THE CURVE WITH DATA DETERMINED FROM APPENDIX E WHICH
C         IS COMPRISED OF THE SATURATED ACTIVITY TIMES DISTANC
C         SQUARED AT EQUAL INTERVALS..  THE EXTRAPOLATED
C         PORTION OF THE CURVE IS BASED ON THE RELAXATION
C         LENGTH.
C
C         THE COMPUTER SOLUTION IS SET UP TO PROVIDE VALUES
C         OF AGE, MIGRATION LENGTH, AND DIFFUSION LENGTH.
C         THE DETERMINATION OF AGE IS BASED UPON EQUATION (  )
C         THE SOLUTION FOR THE DETERMINATION OF MIGRATION
C         LENGTH IS BASED UPON EQUATION (  ).
C         THE DIFFUSION LENGTH IS BASED UPON EQUATION(  ).
C
C
C
//  EXEC FORTCLG,REGION.GO=150K
//FORT.SYSIN DD
      REAL*8 H,SUM2,SUM4,SCD2,S4, SCD4,A2,ACD2,AS2,AS4,ASCD2
     1S2,Y,YCD,C2,R,CD2,B,BCD,Y1,YC1,C22,CD22
      DIMENSION Y(100),YCD(100),R(100),Y1(14),YC1(24)
C
C   RUN WITH TEMPERATURE = 75 DEG F
C   THIS DATA IS FOR COMPARISON OF AREAS WITH LENGTH
C
C
C      COMPUTING SATURATED ACTIVITY TIMES DISTANCE SQUARED AR
C
      READ(5,10) (Y1(I),I=1,14)
   10 FORMAT(1F10.0)
      READ (5,50) (YC1(I),I=1,24)
   50 FORMAT(1F10.0)
C
C      COMPUTING AREAS UNDER LINEAR PORTION OF CURVES
C  THIS DATA BASED ON CURVE FOR MIG AREA
      DO 500 K=1,5
      DO 505 L=1,5
      C2=DEXP(1.520D1-(5.0D-2) L)
      B=1.06D1-(2.0D-2) K
      C22=DLOG(C2)
      WRITE(6,501) B,C2,C22
  501 FORMAT(3D25.16)
      DO 11 I=1,14
      Y(I)=Y1(I)
   11 CONTINUE
      N=79
      DO 160 I=15,80
      R(I)=1.0 (I)
      Y(I)=C2 DEXP(-R(I)/B)
  160 CONTINUE
      H=1.0
      SUM2=0.0D0
      SUM4=0.0D0
      M=N-1
      DO20 I=3,N,2
      SUM2=SUM2+Y(I)
   20 CONTINUE
      DO30 I=2,M,2
      SUM4=SUM4+Y(I)
   30 CONTINUE
      S2=H/.3D1 (Y(I)+.4D1 SUM4+.2D1 SUM2+Y(N+1))
      WRITE(6,40) S2
```

```
   40 FORMAT(T19,'SIMPSONS APPROXIMATION',D25.16///)
C
C       AS(CD) R **2
C
        DO555 J=1,5
C THIS DATA IS BASED ON CURVE  FOR DETERMONATION OF TAU
        CD2=DEXP(1.2850I+(1.0D-2)*L)
        BCD=9.7D0
        CD22=DLOG(CD2)
        WRITE(6,551) BCD,CD2,CD22
  551   FORMAT(3D25.16)
        DO 12 I=1,24
        YCD(I)=YC1(I)
   12   CONTINUE
        N=79
C
C        AS(CD) R** 2
C
        DO 230 I=25,80
        R(I)=1.0 (I)
        YCD(I)=CD2 DEXP(-R(I)/BCD)
  230   CONTINUE
        H=1.0
        SUM2=0.0D0
        SUM4=0.0D0
        M=N-1
        DO60 I=3,N,2
        SUM2=SUM2+YCD(I)
   60   CONTINUE
        DO70 I=2,M,2
        SUM4=SUM4+YCD(I)
   70   CONTINUE
        SCD2=H/.3D1 (YCD(I)+.4D1 SUM4+.2D1 SUM2+YCD(N+1))
        WRITE(6,80) SCD2
   80   FORMAT(T19,'SIMPSONS APPROXIMATION',D25.16///)
C
C       COMPUTING SATURATED ACTIVITY DISTANCE TO THE FOURTH AR
C
        DO 90 I=1,14
        R(I)=1.0 (I)
        Y(I)=Y1(I)
        Y(I)=Y(I)*R(I)** 2.0
   90   CONTINUE
        H=1.0
C
C         EXPODENTIAL PORTION
C
        DO 200 I=15,80
        R(I)=1.0 (I)
        Y(I)=C2 DEXP(-R(I)/B)*R(I)  2.0
  200   CONTINUE
        SUM2=0.0D0
        SUM4=0.0D0
        N=79
        M=N-1
        DO100 I=3,N,2
        SUM2=SUM2+Y(I)
  100   CONTINUE
        DO110 I=2,M,2
        SUM4=SUM4+Y(I)
  110   CONTINUE
        S4=H/.3D1 (Y(I)+.4D1 SUM4+.2D1 SUM2+Y(N+1))
        WRITE(6,120) S4
  120   FORMAT(T19,'SIMPSONS APPROXIMATION',D25.16///)
C
C    AS(CD) R **4
C
        H=1.0
        N=79
        DO 130 I=1,24
        R(I)=1.0 (I)
        YCD(I)=YC1(I)
```

```
      YCD(I)=YCD(I)*R(I)  2.0
  130 CONTINUE
C
C       EXPODENTIAL PORTION
      DO 260 I=25,80
      R(I)=1.0*(I)
C
      YCD(I)=CD2 DEXP(-R(I)/BCD) R(I)  2.0
  260 CONTINUE
      SUM2=0.0D0
      SUM4=0.0D0
      M=N-1
      DO140 I=3,N,2
      SUM2=SUM2+YCD(I)
  140 CONTINUE
      DO145 I=2,M,2
      SUM4=SUM4+YCD(I)
  145 CONTINUE
      SCD4=H/.3D1 (YCD(I)+.4D1 SUM4+.2D1 SUM2+YCD(N+1))
      WRITE(6,150) SCD4
  150 FORMAT(T19,'SIMPSONS APPROXIMATION',D25.16///)
C
C     COMPUTING DIFFUSION LENGTH
C
      AS2=S2
      AS4=S4
      ASCD2=SCD2
      ASCD4=SCD4
      MIG=AS4/(AS2 6.0)
      WRITE(6,290) MIG
  290 FORMAT(T19,'MIGRATION AREA=',D25.16///)
      AGE=ASCD4/(ASCD2 6.0)
      WRITE(6,300) AGE
  300 FORMAT(T19,'AGE=',D25.16///)
      DL=(MIG-(AGE+1.8))  .5
      WRITE(6,310) DL
  310 FORMAT(T19,'DIFFUSION LENGTH=',D25.16///)
  555 CONTINUE
  505 CONTINUE
  500 CONTINUE
      STOP
      END
//GO.SYSIN DD *
C    SAT ACTIVITY TIMES DISTANCE SQUARED
C    BARE FOILS
50000.0
125000.0
220000.0
335000.0
440000.0
555000.0
630000.0
690000.0
745000.0
765000.0
745000.0
690000.0
645000.0
600000.0
C    SAT ACTIVITY TIMES DISTANCE SQUARED
C  CADMIMUM COV'D FOILS
14000.0
33000.0
50000.0
68000.0
84000.0
102000.0
113000.0
119500.0
117300.0
113000.0
108000.0
```

101000.0
94000.0
87000.0
81000.0
74000.0
68000.
60000.0
55000.0
50000.0
44000.0
40000.0
36000.0
32000.0

```
C                             APPENDIX F
C
C
C
C
C               COMPUTER PROGRAM NO 6
C
C
C        THE PURPOSE OF THIS PROGRAM WAS TO OBTAIN A GRAPHICAL
C        SET OF CURVES REFLECTING THE FLUX VERSUS DISTANCE AS A
C        FUNCTION OF TEMPERATURE
C        THIS SET OF CURVES WAS BASED ON THE EXPERIMENTAL
C        DATA FROM THE INDIUM FOILS.
C        THE CURVES CONSISTED OF TOTAL FLUX, FAST FLUX AND ALSO
C        THERMAL FLUX FROM THE DIFFERENCE OF THE OTHER TWO.
C        CONSTANTS USED FOR THIS PROGRAM ARE AS FOLLOWS.
C        SIGA IS THE MACROSCOPIC CROSS SECTION OF WATER
C        THE SOURCE WAS DETERMINED TO BE 4.55E6 NEUTRONS PER
C        CM-SQUARED MINUTE
C        THE CONSTANT FOR THE FOILS WAS DETERMINED FROM
C        EQUATION (    ).
C
C
C
C
C
//  EXEC FORTCLGP,REGION.GO=100K
//FORT.SYSIN DD
      REAL 8 ITITLE (12)
      REAL 4 QT,QF,R,QT77,QF77,QT7,QF7,Q77,QT102,QF102,QT02,
     1QF02,Q102,QT129,QF129,QT29,QF29,Q129,QT145,QF145,QT45,
     1QF45,Q145   ,SOURC,SIGA,CONST,AT77,AF77,AT102,AF102,AT1
     129,AF129,AT145,AF145,CT77,CF77,CT102,CF102,CT129,CF129
     1,CT145,CF145,PI,RR
      REAL LABEL1/4H1   /,LABEL2/4H 2  /,LABEL3/4H  3 /,LABE
     1L4/4H    4/
      DIMENSION QT77(10),QF77(10),R(10),QT102(10),QF102(10),
     1QT129(10),QF129(10),QT145(10).QF145(10),QT7(10),QF7(10
     1),QT02(10),QF02(10),QT29(10),QF29(10),QT45(10),QF45(10
     1),Q77(10),Q102(10),Q129(10),Q145(10)
      SIGA=2.22E-2
      PI=3.14159E0
      SOURC=3.24E8
      CONST=SOURC/(4.0 PI SIGA)
C
C
C
      AT102=2.172E7
      AT77=AT102
      AF77=AT102
      AF102=AT102
      AT129=AT102
      AF129=AT102
      AT145=AT102
      AF145=AT102
C
      CT77=CONST/AT77
      CF77=CONST/AF77
      CT102=CONST/AT102
      CF102=CONST/AF102
      CT129=CONST/AT129
      CF129=CONST/AF129
      CT145=CONST/AT145
      CF145=CONST/AF145
      DO20 I=1,10
      READ(5,21) QT,QF,RR
   21 FORMAT(3F9.0)
      R(I)=RR
      QT77(I)=QT
      QF77(I)=QF
      QT7(I)=QT77(I) CT77
      QF7(I)=QF77(I) CF77
      Q77(I)=QT7(I)-QF7(I)
```

```
20 CONTINUE
   DO30 I=1,10
   READ(5,31) QT,QF
31 FORMAT(2F9.0)
   QT102(I)=QT
   QF102(I)=QF
   QT02(I)=QT102(I) CT102
   QF02(I)=QF102(I) CF102
   Q102(I)=QT02(I)-QF02(I)
30 CONTINUE
   DO40 I=1,10
   READ(5,41) QT,QF
41 FORMAT(2F9.0)
   QT129(I)=QT
   QF129(I)=QF
   QT29(I)=QT129(I) CT129
   QF29(I)=QF129(I) CF129
   Q129(I)=QT29(I)-QF29(I)
40 CONTINUE
   DO50 I=1,10
   READ(5,51) QT,QF
51 FORMAT(2F9.0)
   QT145(I)=QT
   QF145(I)=QF
   QT45(I)=QT145(I) CT145
   QF45(I)=QF145(I) CF145
   Q145(I)=QT45(I)-QF45(I)
50 CONTINUE
   WRITE(6,61)
61 FORMAT(8X,'FLUX AND SATURATED ACTIVITY CONSTANTS')
   WRITE(6,62)
62 FORMAT(2X,'F L U X',5X,'FAST',5X,'T=77,102,129,145 DEG
   WRITE(6,85) CT77,CF77
85 FORMAT(' ',2E15.8)
   WRITE(6,86) CT102,CF102
86 FORMAT(' ',2E15.8)
   WRITE(6,87)CT129,CF129
87 FORMAT(' ',2E15.8)
   WRITE(6,88)CT145,CF145
88 FORMAT(' ',2E15.8)
   WRITE(6,34)
34 FORMAT(2X,'DISTANCE',6X,'  FLUX  T=77F',3X,'FAST T=77F
  1X T=102F',3X,'FAST T=102F')
   WRITE(6,35)(R(I),QT7(I),QF7(I),QT02(I),QF02(I),I=1,10)
35 FORMAT(' ',5E15.8)
   WRITE(6,36)
36 FORMAT(2X,'DISTANCE',6X,'F L U X T=129F',3X,'FAST T=12
  1U X T=145F',3X,'FAST T=145F')
   WRITE(6,37)(R(I),QT29(I),QF29(I),QT45(I),QF45(I),I=1,1
  10)
37 FORMAT(' ',5E15.8)
   WRITE(6,63)
63 FORMAT(2X,'DISTANCE(CM)',2X,'FLUX T=77F',6X,'FLUX T=10
  1 T=129F',6X,'FLUX T=145F')
   WRITE(6,75)(R(I),Q77(I),Q102(I),Q129(I),Q145(I),I=1,10
75 FORMAT(' ',5E15.8)
   READ(5,99)(ITITLE(I),I=1,12)
99 FORMAT(6A8)
   CALL DRAW(10,R,Q77 ,1,0,LABEL1,ITITLE,0,0,0,0,0,0,6,9,
  11,LAST)
   CALL DRAW(10,R,Q102,2,0,LABEL2,ITITLE,0,0,0,0,0,0,6,9,
  11,LAST)
   CALL DRAW(10,R,Q129,2,0,LABEL3,ITITLE,0,0,0,0,0,0,6,9,
  11,LAST)
   CALL DRAW(10,R,Q145,3,0,LABEL4,ITITLE,0,0,0,0,0,0,6,9,
  11,LAST)
   READ(5,97)(ITITLE(I),I=1,12)
97 FORMAT(6A8)
   CALL DRAW(10,R, QT7,1,0,LABEL1,ITITLE,0,0,0,0,0,0,6,9,
  11,LAST)
   CALL DRAW(10,R,QT02,2,0,LABEL2,ITITLE,0,0,0,0,0,0,6,9,
  11,LAST)
```

```
      CALL DRAW(10,R,QT29,2,0,LABEL3,ITITLE,0,0,0,0,0,0,6,9,
     11,LAST)
      CALL DRAW(10,R,QT45,3,0,LABEL4,ITITLE,0,0,0,0,0,0,6,9,
     11,LAST)
      READ(5,98)(ITITLE(I),I=1,12)
   98 FORMAT(6A8)
      CALL DRAW(10,R, QF7,1,0,LABEL1,ITITLE,0,0,0,0,0,0,6,9,
     11,LAST)
      CALL DRAW(10,R,QF02,2,0,LABEL2,ITITLE,0,0,0,0,0,0,6,9,
     11,LAST)
      CALL DRAW(10,R,QF29,2,0,LABEL3,ITITLE,0,0,0,0,0,0,6,9,
     11,LAST)
      CALL DRAW(10,R,QF45,3,0,LABEL4,ITITLE,0,0,0,0,0,0,6,9,
     11,LAST)
      STOP
      END
//GO.SYSIN DD *
C   THE INPUT DATA IS LISTED IN THREE COLUMS'S WITH DISTANCE
C   READ IN FOR THE FIRST SET OF FOILS ONLY
C   THE FIRST COLUMN IS THE SATURATED ACTIVITY FOR THE BARE
C   FOILS, THE SECOND COLUMN IS THE CADMIMUN COVERED FOIL
C   DATA AND THE THIRD COLUMN IS THE DISTANCE FROM SOURCE
36797.0   4906.0    3.41
25955.0   3235.0    5.32
20043.0   2027.0    7.30
13629.0    1194.0    9.21
7468.0     557.0    12.14
3953.0      261.0     15.32
2559.0      148.0     16.27
1629.0      95.0     19.29
1080.0      37.0       21.35
675.0        10.0       23.42
35252.0    5291.0
27716.0   3427.0
18558.0   2227.0
13789.0    1339.0
7734.0    652.0
2535.0    350.0
2661.0      237.0
1735.0      160.0
1130.0      108.0
727.0       81.0
23267.0    4863.0
19733.0    3383.0
14367.0    2169.0
10248.0     1327.0
6665.0      628.0
3462.0      345.0
2402.0      224.0
1482.0      156.0
1056.0      111.0
705.0      72.0
33307.0    4221.0
28045.0    3005.0
19036.0    1860.0
13979.0    1126.0
8180.0      583.0
4217.0      285.0
2695.0      210.0
1880.0      131.0
1164.0      107.0
791.0       76.0
```

```
C                              APPENDIX G
C
C
C
C                   COMPUTER PROGRAM NO 7
C
C
C          THIS PROGRAM PROVIDES A GRAPHICAL PRESENTATION OF THE
C          CRYSTAL DATA FOR TOTAL, FAST AND ALSO THE THERMAL REL-
C          ATIVE FLUX PLOTS, WITH CORRECTIONS FOR EFFICIENCY
C
C
C
C
C
// EXEC FORTCLGP,REGION.GO=100K
//FORT.SYSIN DD
      REAL 8ITITLE(12)
      REAL DISTT,DIST,C84,C102,C145,CD84,CD102,CD145.LC84,LC
     1102,LC145,LD84,LD102,LD145,SIG84,SIG02,SIG45,SAG84,SAG
     102,SAG45,F84,F102,F145,FL84,FL102,FL145,C168,CD168,LC1
     168,LD168.SIG68,SAG68,F168,FL168
      REAL C129,CD129,LC129,LD129,SIG29,SAG29,F129,FL129
      REAL LABEL1/4H    /,LABEL2/4H    /,LABEL3/4H    /
      DIMENSION  DISTT(16),C84(16),C102(16),C145(16),CD84(16
     1),CD102(16),CD145(16),LC84(16),LC102(16),LC145(16),LD8
     1),LD102(16),LD145(16),SIG84(16),SIG02(16),SIG45(16),SA
     1G84(16),SAG02(16),SAG45(16), F84(16),F102(16),F145(16)
     1,FL84(16),FL102(16),FL145(16),C129(16),CD129(16),LC129
     1LD129(16),SIG29(16),SAG29(16),F129(16),FL129(16),C168(
     1,CD168(16),LC168(16),LD168(16),SIG68(16),SAG68(16),F16
     1(16),FL168(16)
C   NEUTRON FLUX RELATIVE MEASUREMENTS
      DO 50 I=1,16
      READ(5,2)POS,CA,CB,CC,CD,CE
    2 FORMAT(6F9.0)
      DISTT(I)=POS 2.54D0
      C84(I)=4.0 CA
      C102(I)=4.0 CB
      C129(I)=4.0 CC
      C145(I)=4.0 CD
      C168(I)=4.0 CE
      SIG84(I)=SQRT(C84(I))
      SIG02(I)=SQRT(C102(I))
      SIG29(I)=SQRT(C129(I))
      SIG45(I)=SQRT(C145(I))
      SIG68(I)=SQRT(C168(I))
      LC84(I)=ALOG(C84(I))
      LC102(I)=ALOG(C102(I))
      LC129(I)=ALOG(C129(I))
      LC145(I)=ALOG(C145(I))
      LC168(I)=ALOG(C168(I))
   50 CONTINUE
      WRITE(6,64)
   64 FORMAT(5X,'DISTANCE(CM)',2X,'FLUX T=84F',2X,'SIGMA',6X
     1X')
      WRITE(6,65)(DISTT(I),C84(I),SIG84(I),LC84(I),I=1,16)
   65 FORMAT(' ',4E15.8)
      WRITE(6,66)
   66 FORMAT(5X,'DISTANCE(CM)',2X,'FLUX T=102F',2X,'SIGMA',6
     1UX')
      WRITE (6,67)(DISTT(I),C102(I), SIG02(I),LC102(I),I=1,1
   67 FORMAT(' ',4E15.8)
      WRITE(6,40)
   40 FORMAT(5X,'DISTANCE(CM)',2X,'FLUX T=129F',2X,'SIGMA',6
     1UX')
      WRITE (6,88)(DISTT(I),C129(I), SIG29(I),LC129(I),I=1,1
   88 FORMAT(' ',4E15.8)
      WRITE (6,68)
   68 FORMAT(5X,'DISTANCE(CM)',2X,'FLUX T=145F',2X,'SIGMA',6
     1UX')
      WRITE (6,69)(DISTT(I),C145(I), SIG45(I),LC145(I),I=1,1
   69 FORMAT(' ',4E15.8)
```

```
      WRITE(6,4)
    4 FORMAT(5X,'DISTANCE(CM)',2X,'FLUXT=168F',2X,'SIGMA',6X
     1X')
      WRITE(6,5)(DISTT(I),C168(I),SIG68(I),LC168(I),I=1,16)
    5 FORMAT(' ',4E15.8)
C   CADMIUM COVERED FLUX MEASUREMENTS
      DO 52 I=1,16
      READ(5,3)POS,CDA,CDB,CDC,CDD,CDE
    3 FORMAT(6F9.0)
      DISTT(I)=POS*2.54D0
      CD84(I)=4.0*CDA
      CD102(I)=4.0*CDB
      CD129(I)=4.0*CDC
      CD145(I)=4.0*CDD
      CD168(I)=4.0*CDE
      SAG84(I)=SQRT(CD84(I))
      SAG02(I)=SQRT(CD102(I))
      SAG29(I)=SQRT(CD129(I))
      SAG45(I)=SQRT(CD145(I))
      SAG68(I)=SQRT(CD168(I))
      LD84(I)=ALOG(CD84(I))
      LD102(I)=ALOG(CD102(I))
      LD129(I)=ALOG(CD129(I))
      LD145(I)=ALOG(CD145(I))
      LD168(I)=ALOG(CD168(I))
   52 CONTINUE
      WRITE(6,42)
   42 FORMAT(5X,'DISTANCE(CM)',2X,'FAST T=84 F',2X,'SIGMA',6
     1FLUX')
      WRITE(6,91)(DISTT(I),CD84(I),SAG84(I),LD84(I),I=1,16)
   91 FORMAT(' ',4E15.8)
      WRITE(6,41)
   41 FORMAT(5X,'DISTANCE(CM)',2X,'FAST T=102F',2X,'SIGMA',6
     1FLUX')
      WRITE(6,92)(DISTT(I),CD102(I),SAG02(I),LD102(I),I=1,16
   92 FORMAT(' ',4E15.8)
      WRITE(6,43)
   43 FORMAT(5X,'DISTANCE(CM)',2X,'FAST T=129F',2X,'SIGMA',6
     1FLUX')
      WRITE(6,11)(DISTT(I),CD129(I),SAG29(I),LD129(I),I=1,16
   11 FORMAT(' ',4E15.8)
      WRITE(6,44)
   44 FORMAT(5X,'DISTANCE(CM)',2X,'FAST T=145F',2X,'SIGMA',6
     1FLUX')
      WRITE(6,93)(DISTT(I),CD145(I),SAG45(I),LD145(I),I=1,16
   93 FORMAT(' ',4E15.8)
      WRITE(6,7)
    7 FORMAT(5X,'DISTANCE(CM)',2X,'FAST T=168F',2X,'SIGMA',6
     1FLUX')
      WRITE(6,8 )(DISTT(I),CD168(I),SAG68(I),LD168(I),I=1,16
    8 FORMAT(' ',4E15.8)
C THERMAL FLUX =NEUTRON FLUX -FAST FLUX
      DO 53 I=1,16
      F84(I)=C84(I)-CD84(I)
      F102(I)=C102(I)-CD102(I)
      F129(I)=C129(I)-CD129(I)
      F145(I)=C145(I)-CD145(I)
      F168(I)=C168(I)-CD168(I)
      FL84(I)=ALOG(F84(I))
      FL102(I)=ALOG(F102(I))
      FL129(I)=ALOG(F129(I))
      FL145(I)=ALOG(F145(I))
      FL168(I)=ALOG(F168(I))
   53 CONTINUE
      WRITE(6,48)
   48 FORMAT(5X,'DISTANCE(CM)',2X,'THERM =84 F',2X,'LOG OF T
      WRITE(6,80)(DISTT(I),F84(I),FL84(I),I=1,16)
   80 FORMAT(' ',3E15.8)
      WRITE(6,47)
   47 FORMAT(5X,'DISTANCE(CM)',2X,'THERM =102F',2X,'LOG OF T
      WRITE(6,81)(DISTT(I),F102(I),FL102(I),I=1,16)
   81 FORMAT(' ',3E15.8)
```

```
      WRITE(6,46)
   46 FORMAT(5X,'DISTANCE(CM)',2X,'THERM =129F',2X,'LOG OF T
      WRITE(6,83)(DISTT(I),F129(I),FL129(I),I=1,16)
   83 FORMAT(' ',3E15.8)
      WRITE(6,45)
   45 FORMAT(5X,'DISTANCE(CM)',2X,'THERM =145F',2X,'LOG OF T
      WRITE(6,82)(DISTT(I),F145(I),FL145(I),I=1,16)
   82 FORMAT(' ',3E15.8)
      WRITE(6,9)
    9 FORMAT(5X,'DISTANCE(CM)',2X,'THERM=168 F',2X,'LOG OF T
      WRITE(6,10)(DISTT(I),F168(I),FL168(I),I=1,16)
   10 FORMAT(' ',3E15.8)
      READ(5,90)(ITITLE(I),I=1,12)
   90 FORMAT(6A8)
      CALL DRAW(16,DISTT,C84 ,1,1,LABEL1,ITITLE,0,0,0,0,0,0,
     16,9,1,LAST)
      CALL DRAW(16,DISTT,C102,2,2,LABEL1,ITITLE,0,0,0,0,0,0,
     16,9,1,LAST)
      CALL DRAW(16,DISTT,C129,2,3,LABEL1,ITITLE,0,0,0,0,0,0,
     16,9,1,LAST)
      CALL DRAW(16,DISTT,C168,2,5,LABEL1,ITITLE,0,0,0,0,0,0,
     16,9,1,LAST)
      CALL DRAW(16,DISTT,C145,3,4,LABEL1,ITITLE,0,0,0,0,0,0,
     16,9,1,LAST)
      READ(5,22)(ITITLE(I),I=1,12)
   22 FORMAT(6A8)
      CALL DRAW(16,DISTT,CD84 ,1,1,LABEL2,ITITLE,0,0,0,0,0,0
     1,6,9,1,LAST)
      CALL DRAW(16,DISTT,CD102,2,2,LABEL2,ITITLE,0,0,0,0,0,0
     1,6,9,1,LAST)
      CALL DRAW(16,DISTT,CD129,2,3,LABEL2,ITITLE,0,0,0,0,0,0
     1,6,9,1,LAST)
      CALL DRAW(16,DISTT,CD168,2,5,LABEL2,ITITLE,0,0,0,0,0,0
     1,6,9,1,LAST)
      CALL DRAW(16,DISTT,CD145,3,4,LABEL2,ITITLE,0,0,0,0,0,0
     1,6,9,1,LAST)
      READ(5,23)(ITITLE(I),I=1,12)
   23 FORMAT(6A8)
      CALL DRAW(16,DISTT, F84 ,1,1,LABEL3,ITITLE,0,0,0,0,0,0
     1,6,9,1,LAST)
      CALL DRAW(16,DISTT, F102,2,2,LABEL3,ITITLE,0,0,0,0,0,0
     1,6,9,1,LAST)
      CALL DRAW(16,DISTT, F129,2,3,LABEL3,ITITLE,0,0,0,0,0,0
     1,6,9,1,LAST)
      CALL DRAW(16,DISTT, F168,2,5,LABEL3,ITITLE,0,0,0,0,0,0
     1,6,9,1,LAST)
      CALL DRAW(16,DISTT, F145,3,4,LABEL3,ITITLE,0,0,0,0,0,0
     1,6,9,1,LAST)
      STOP
      END
//GO.SYSIN DD *
2.5       286000.0 298446.0 304331.0   304526.0   308636.
3.0       211020.0 238571.0 250689.0   257125.0264672.0
3.5       170437.0  194947.0210380.0   206885.0 218133.0
4.0       125252.0  157924.0165014.0   163323.0174308.0
4.5       107430.0 121938.0 127491.0   130007.0139286.0
5.0        73602.0   97301.0  99014.0   101831.0109333.0
5.5        67413.0   72725.0 77283.0    79350.0  84545.0
6.0        50353.0   54764.0   56832.0   61414.0  64731.0
6.5        42305.0   42625.0   44264.0    48344.051227.0
7.0        31785.0   32223.0   33433.0    37399.0   39509.0
7.5        22070.0   24868.0   25664.0    29334.0 31651.0
8.0        16985.0    19805.0   20489.0   22987.0   24080.0
8.5        14543.0    15123.0  15482.0    17900.0   18640.0
9.0        11477.0    12139.012797.0     14122.0   15045.0
9.5         8890.0   10051.0   10082.0    11380.0   11891.0
10.0        6962.0    7770.0    7382.0     9009.0    9266.0
2.5        42120.0   42500.0   48047.0    49418.0   51678.0
3.0        32922.0   35100.0   36670.0    38106.0   41314.0
3.5        25465.0   24760.0   28599.0    32006.0   33215.0
4.0        19332.0   19393.0   21624.0   24030.0    25314.0
4.5        12662.0   14926.0   16400.0    19019.0   20101.0
```

5.0	11976.0	11038.0	13258.0	14521.0	15515.0
5.5	8207.0	9473.0	10125.0	11393.0	12106.0
6.0	7127.0	7141.0	8101.0	8724.0	9375.0
6.5	5507.0	5500.0	6086.0	6811.0	7582.0
7.0	3765.0	4200.0	5008.0	5144.0	5908.0
7.5	3424.0	3193.0	3821.0	4185.0	4769.0
8.0	2395.0	2567.0	3013.0	3288.0	3687.0
8.5	2265.0	1968.0	2388.0	2566.0	3125.0
9.0	1671.0	1559.0	1910.0	2167.0	2364.0
9.5	1373.0	1290.0	1625.0	1765.0	1814.0
10.0	1074.0	1020.0	1204.0	1313.0	1427.0

BIBLIOGRAPHY

1. Harshaw Chemical Company, Harshaw Scintillation Phosphors, Second Edition, 1969.

2. Price, W. J., Nuclear Radiation Detection, McGraw-Hill Book Company, 1964.

3. Murray, R. B., "LiI(Eu) Crystal As a Fast Neutron Scintillation Detector," Nuclear Instruments, 84, 2, 1958.

4. Lamarsh, J. R., Introduction to Nuclear Reactor Theory, Addison-Wesley, 1966.

5. United States Energy Commission, ANL-5800, Reactor Physics Constants, 1963.

6. United States Atomic Energy Commission Report, GA-6824, Description of Flange Code, 1964.

7. United States Atomic Energy Commission, BNL-235, Neutron Cross Sections, 1955.

8. Etherington, H., Nuclear Engineering Handbook, McGraw-Hill Book Company, 1958.

9. Valente, A. V., A Manual of Experiments in Reactor Physics, The MacMillan Company, 1963.

10. Furuta, Y., Kinbara, S., and Kaieda, K., "Spectrum Measurements of Intermediate Energy Neutrons by an Organic Scintillator," Nuclear Instruments and Methods, 87, 269-274, 15 July 1970.

INITIAL DISTRIBUTION LIST

		No. Copies
1.	Defense Documentation Center Cameron Station Alexandria, Virginia 22314	2
2.	Library, Code 0212 Naval Postgraduate School Monterey, California 93940	2
3.	Asst Professor D. Nguyen, Code 59 Ng (thesis advisor) Department of Mechanical Engineering Naval Postgraduate School Monterey, California 93940	1
4.	Professor T. Sarpkaya, Code 59 Sl Chairman, Department of Mechanical Engineering Naval Postgraduate School Monterey, California 93940	2
5.	LCDR Robert Gordon BENNETT, USN (student) 38 Mystic Street Methuen, Massachusetts 01618	1
6.	Naval Ship Systems Command Code 2052 Via Code 031 Department of the Navy Washington, D. C. 20360	1

UNCLASSIFIED

Security Classification

DOCUMENT CONTROL DATA - R & D

(Security classification of title, body of abstract and indexing annotation must be entered when the overall report is classified)

1 ORIGINATING ACTIVITY (Corporate author)

Naval Postgraduate School
Monterey, California 93940

2a. REPORT SECURITY CLASSIFICATION

Unclassified

2b. GROUP

3 REPORT TITLE

The Measurement of Temperature Dependent Thermal Neutrons in Water Using a Crystal Detector

4 DESCRIPTIVE NOTES (Type of report and inclusive dates)

Master's Thesis (December 1970)

5 AUTHOR(S) (First name, middle initial, last name)

Robert G. Bennett

6. REPORT DATE	7a. TOTAL NO. OF PAGES	7b. NO. OF REFS
December 1970	121	10

8a. CONTRACT OR GRANT NO.	9a. ORIGINATOR'S REPORT NUMBER(S)
b. PROJECT NO	
c.	9b. OTHER REPORT NO(S) (Any other numbers that may be assigned this report)
d.	

10 DISTRIBUTION STATEMENT

This document has been approved for public release and sale; its distribution is unlimited.

11. SUPPLEMENTARY NOTES	12. SPONSORING MILITARY ACTIVITY
	Naval Postgraduate School Monterey, California 93940

13 ABSTRACT

This research was concerned with the temperature dependence of thermal neutron flux. In view of the excellent neutron detection capability exhibited by the Lithium Iodide Europium enriched crystal this phosphor was utilized for the investigation. A miniature crystal (4mm x 4mm) and a flexible light pipe combination was used to determine the neutron spatial distribution as a function of temperature using a Pu-Be source in a light-water medium.

A separate experimental investigation, with Indium foils and activation analysis, was used to determine the temperature dependence of thermal neutron flux under the same experimental conditions as the crystal.

A theoretical analysis was also conducted using Two-Group theory to obtain an expression for thermal flux with spatial and temperature dependent parameters.

The results of the research indicate that the thermal neutron flux is temperature dependent in the region investigated (77° - 168° F). The experimental results verify the increasing trend of flux magnitude with increasing temperature, as predicted by the Two-Group solution.

DD FORM 1 NOV 65 1473 (PAGE 1)

S/N 0101-807-6811

UNCLASSIFIED

Security Classification

A-31408

14 KEY WORDS	LINK A		LINK B		LINK C	
	ROLE	WT	ROLE	WT	ROLE	WT
Scintillator						
Phosphor						
LiI(Eu) Crystal						
Temperature-dependent flux						
Light-pipe						
Flux-mapping						

Thesis
B377
c.1

125502

Bennett
The measurement of temperature dependent thermal neutrons in water using a crystal detector.

Thesis
B377
c.1

125502

Bennett
The measurement of temperature dependent thermal neutrons in water using a crystal detector.

thesB377
The measurement of temperature dependent
3 2768 002 13707 7
DUDLEY KNOX LIBRARY